-AN ABSTRACT OF THE DISSERTATION OF

Adam L. Campbell for the degree of Doctor of Philosophy in Pharmacy, presented on May 31, 2012

Title: The Role of the Homeodomain Transcription Factor Pitx2 in Regulating Skeletal Muscle Precursor Migration and Higher Order Muscle Assembly

Abstract approved:

Chrissa Kioussi

Cells of the ventrolateral dermomyotome delaminate and migrate into the limb buds where they give rise to all muscles of the limbs. The migratory cells proliferate and form myoblasts, which withdraw from the cell cycle to become terminally differentiated myocytes. The regulatory mechanisms that control the later steps of this myogenic program are not well understood. The homeodomain transcription factor Pitx2 is expressed specifically in the muscle lineage from the migration of precursors to adult muscle. Ablation of Pitx2 results in distortion, rather than loss, of limb muscle anlagen, suggesting that its function becomes critical during the colonization of, and/or fiber assembly in, the anlagen. Microarrays were used to identify changes in gene expression in flow-sorted migratory muscle precursors from Wild type and Pitx2 null mice. Changes in gene expression were observed in genes encoding cytoskeletal, adhesion and fusion proteins which play a role in cell motility and myoblast fusion. We observed decreased cellular motility, disrupted cytoskeleton organization and focal adhesion distribution, decreased fusion of mononucleated myoblasts into multinucleated myotubes and decreased proliferation in presence of Ptix2. These studies suggest that Pitx2 plays a critical role in regulating the timing of myoblast filling the limb anlagen which may have detrimental consequences for higher order muscle architecture.

The Role of the Homeodomain Transcription Factor Pitx2 in Regulating Skeletal Muscle Precursor Migration and Higher Order Muscle Assembly

by

Adam L. Campbell

A THESIS

Submitted to

Oregon State University

In partial fulfillment of

the requirements for the

degree of

Doctor of Philosophy

Presented May 31, 2012

Commencement June 2013

Doctor of Philosophy dissertation of Adam L. Campbell presented on May 31, 2012.

APPROVED:

Major Professor, representing Pharmacy

Dean of the College of Pharmacy

Dean of the Graduate School

I understand that my dissertation will become part of the permanent collection of Oregon State University libraries. My signature below authorizes the release of my dissertation to any reader upon request.

Adam L. Campbell, Author

CONTRIBUTION OF AUTHORS

Chrissa Kioussi designed research, data analysis, and writing and editing, contributed reagents; Adam Campbell performed research, data analysis, and writing; Michael K. Gross contributed reagents, data analysis, analytic tools; Hung Ping Shih provided data; Jun Xu contributed editing and data analysis; Diana Eng performed data analysis, provided analytical tools, and editing.

TABLE OF CONTENTS

TABLE OF CONTENTS (Continued)

LIST OF FIGURES

LIST OF TABLES

From Myoblast to Myotube to Muscle, An Introduction to Skeletal Myogenesis

Chapter 1

Adam Campbell and Chrissa Kioussi

From Mesoderm to Myoblast

The limb skeletal muscle is derived from cells of the dermomyotome, which originates from the somites. The somites are transient anatomical structures, which form due to segmentation of the presomitic mesoderm, and flank the neural tube and run parallel to the body axis. The somites provide the source for a number of progenitor cells that give rise to various tissues of the body such as cartilage, endothelial cells, tendon, connective tissue, dermis, and skeletal muscles [1,2]. The ventral region of the somite, called the sclerotome, provides cells, which will form the axial skeleton. The dorsal region of the somite, called the dermomyotome (DM), provides cells, which form limb and trunk muscles. The DM is further subdivided into the epaxial DM, giving rise to the deep back muscles, and the hypaxial DM, giving rise to the limb and trunk muscles. The surrounding embryonic structures (neural tube, notochord, lateral mesoderm, and ectoderm) secrete diffusible signaling molecules (Shh, Wnt1, Wnt7a, Wnt6, and Bmp4) each establishing their own gradients along the DM, influencing the commitment of the progenitor cells to different myogenic programs depending on their location within the DM [3,4,5,6]. Within somites that are located at limb level cells along the ventrolateral lip (VLL) of the DM undergo an epithelial to mesenchymal transition (EMT), delaminate as single cells, and undergo long distance migration into the developing limb bud to areas where the presumptive muscle groups will form (Fig 1).

The hierarchal expression of genes has been identified as regulators for development and migration of hypaxial muscle precursors into the forelimb. Among the genes identified as being expressed earliest (E9.0) during myogenic progression are *Pax3*, Paired domain transcription factor, *Met*, Met proto-oncogene, and *Lbx1*, Ladybird homeobox homolog 1, due to the observation that they are expressed prior to expression of known muscle regulatory factors (MRFs) and ablation of any of these

genes leads to a loss of migratory precursors and failure for forelimb muscles to form [7,8,9,10,11,12]. The MRFs are a family of transcription factors consisting of 4 members; *Myod1*, Myogenic differentiation 1; *Myf5*, Myogenic factor 5; *Myog*, Myogenin, and *Mrf4*, Myogenic factor 4. The expression of MRFs was identified as the marker for the onset of muscle development due to the observation that ectopic expression can induce cultured cells to initiate the myogenic program [13].

At E9.5-9.75 $Lbx1^{+}/Pax3^{+}$ migratory muscle precursors (MMP) delaminate from the VLL of the DM and migrate laterally into the limb bud. At E10.5 the dorsal and ventral muscle anlagen of the limb buds consists of numerous $Lbx1^{+}/Pax3^{+}$ muscle progenitor MPs cells and persist until at least E12.5 [11]. During the period of E11-12.5 the MP cells continuously proliferate and the muscle anlagen enlarge in size and position themselves within the limb with respect to the developing bone anlagen. The expression of MRFs *Myf5* and *Myod1* are observed in proliferative myoblasts, while expression of *Myog* and *Mrf4* are observed in terminally differentiated myotubes [14,15,16]. The MRFs work cooperatively to control the expression of downstream skeletal muscle genes, such as growth, cell cycle, and contractile proteins [17]. The regulation of downstream skeletal muscle genes is accomplished through interactions between muscle specific transcription factors and chromatin remodeling enzymes, histone acetyltransferases (HATs) and histone deacetylases (HDACs) [18].

Myoblast Motility

Efficient migration of the myoblasts to their intended destinations requires the internal cellular machinery to become highly polarized, locally segregated, tightly regulated and rapidly adaptable entity that can be assembled and disassembled in a orchestrated

manner. External signals such as growth factors, cytokines, mechanical forces and extracellular matrix (ECM) proteins lead to polarization and polymerization of actin fibers which elongate and protrude the cell membrane as either broad lamellapodia or spike like filopodia in the direction of movement. Attachment of the protrusions to the substratum requires a variety of adhesion proteins (integrins, syndecans, cadherins and cell adhesion molecules [CAMs]) which provide both points of traction and sites of regulatory signals to control adhesion dynamics and stabilize protrusion of the cell membrane [19]. Attachment to the substratum induces conformational changes in the adhesion proteins, This results in the unmasking of intracellular regions which allows the cross-linking of the adhesion proteins to the cytoskeleton through interactions with multiprotein complexes [20,21,22,23]. In the central and rear regions of the migrating cell the actin filaments organize themselves into thick bundles called stress fibers which terminate at both ends at the focal adhesions connected to the extracellular matrix ECM [24]. Inward movement of the cell trailing edge accompanied by dispersal of the adhesion structure allows the cell membrane to roll forward achieving cellular motion. This process must be well coordinated in order to maintain the appropriate amount of cell–cell contacts between migratory muscle progenitor cells. These cell-cell contacts work to control the growth and architecture of individual muscle; influencing the ultimate shape, size and physiological function of the muscle organ system.

Myoblast Fusion

Cell-cell fusion is an essential and coordinated event that occurs during development. This process forms and shapes the developing tissues and organs, while promoting tissue homeostasis. The majority of cells in the body remain single mononucleated cells, suggesting that fusion must be under tight control as aberrant cell fusion is implicated in

carcinogenesis [25]. Muscle development and repair are dependent on fusion of myoblasts into large bundles of multinucleated fibers in order to produce the muscle groups required for force generation. The molecular mechanisms that regulate this process are not clearly understood. Further knowledge of this process will help us develop new treatments in muscle wasting diseases, combat atrophy, and help mitigate the aging process.

Most of our knowledge of the process of myoblast fusion comes from studies of myoblast fusion in *Drosophila melanogaster*. To briefly describe the process of myoblast fusion during *Drosophila* development 30 somatic muscle fibers are present in each abdominal hemisegment. Each somatic muscle fiber is unique in size, shape, orientation, number of nuclei and innervations, and attachment sites of tendons [26,27]. Each hemisegment muscle fiber is the result of a single myoblast called the founder cell (FC), fusing with several fusion competent myoblasts (FCMs) each cell type arising from the somatic mesoderm. The size of each muscle is determined by the number of FCMs, ranging from 2-24, that migrate and fuse to the FC in temporal phases over a 5.5 hour period during late embryogenesis [28,29].

Critical genes that have been identified in regulating migration in *Drosophila* myogenesis are Dumbfounded/Kirre (Duf) and Roughest/Irrec (Rst), which encode for a FC-specific Immunoglobulin (Ig) domain containing transmembrane protein which acts as an attractant for FCMs [30,31]. FCMs recognize these attractants expressed on the surface of the FCs, migrate toward and adhere to FCs or growing myotubes. Adherence is mediated by the FCM-specific Ig domain-containing transmembrane protein Sticks and Stones (SNS) and Hibris (Hbs) [32,33,34]. Interactions between Duf, Rst, Sns and Hbs result in the formation of a ring-like fusion-restricted myogenic-adhesive structure,

termed FuRMAS. This structure serves as a signaling center allowing the recruitment of the fusion machinery to the membrane [35,36,37,38].

The FuRMAS provides a platform for many scaffolding and adaptor proteins to transmit signal cascades leading to the formation of an actin ring structure inside the FuRMAS called the “focus” cross linking the actin cytoskeleton to adhesion proteins Duf, Sns, Hbs, and Rst [38]. At sites where the FuRMAS and the focus occur, electron dense vesicles align along the apposed membranes and form pores in the membranes. The formation of pores along with contraction of the actin structures between the opposing cells is believed to lead to union of the membranes into a continuous multinucleated cell [39].

A similar process plays out in vertebrate myogenesis with skeletal muscles arising from precursors cells within the somites. Precursor cells from the VLL of the DM undergo EMT and separate from a continuous sheet to become single cells and migrate into the forelimb. Once they reach their destination the MP cells must undergo homophilic cell sorting through surface receptors and adhere to one another to undergo fusion. The mouse encodes orthologues for Drosophila proteins: Duf/Kirre/Rst and Sns/Hbs [40,41,42], but the exact mechanisms these orthologues play in unclear. The Sns orthologue in mice and humans is Nephrin which is expressed in developing mouse skeletal muscle. In Nephrin$^{-/-}$ mice myoblasts do show an impairment in fusion with each other, while not required for myoblasts to fuse to established myotubes [40]. Knockout analysis of the remaining orthologues has not been done to date. A variety of other adhesion molecules and surface receptors have been identified as playing a role in myoblast fusion such as cadherins, integrins, mannose receptors, chemokine receptors, etc.; suggesting that combinatorial interactions mediate the recognition and adhesion of myoblasts [43,44,45,46].

Although vertebrates lack the appearance of the FuRMAS and “focus” structures at cell-cell contact points. The activation of Rho Family GTPases can be observed which leads to the polymerization and accumulation of actin filaments at these contact points along the cell membrane [47,48]. These cell-cell contact points of actin enrichment recruit the ferlin family protein, Myoferlin along with the eps15 homology domain protein, EHD2 to presumably target endocytic vesicles and begin thinning of the opposing cell membranes allowing for fusion [49,50,51].

Pitx2 in Myogenesis

The homeodomain transcription factor *Pitx2* is expressed in the lateral plate mesoderm and in muscle anlagen in all stages of myogenic progression [52,53]. *Pitx2* contributes to the establishment of network kernels that specify pre-myogenic progenitors for extraocular and mastication muscles [54]. Ablation of *Pitx2* causes lethality in the mouse at E10.5-E14.5 with axial malformations, open body wall, heart defects, and arrest of organ development [55,56,57,58]. Ablation of Pitx2 resulted in distortion or absence of hypaxial derived muscles (i.e. latissmus dorsi and acromiotrapezius). When present the muscles where smaller in size with thick, clumpy muscle fibers. In addition to axial malformation, open body wall, defects in left-right asymmetry, heart defects, arrest of organ development, and lethality of embryos (E10-E14) (Kioussi et al. 1999; Shih, Gross et al. 2007). *Pitx2* is positioned downstream of both Wnt and growth factor signaling pathways in skeletal myogenesis and promotes muscle progenitor proliferation by direct regulation of the expression of a number of cyclin-dependent kinases [59].

In the study presented in chapter 2, we identified genes that are regulated by Pitx2 in the $Lbx1^{EGFP}$ myogenic cells by gene expression arrays in flow-sorted cells. We identify

several genes involved in microtubule stabilization, actin cross-linking, tubulin related, adhesion, and intermediate filament as target genes of Ptix2. We present evidence that Pitx2 influences myogenic cell migration through regulation of target genes involved in cellular polarization of the cytoskeleton and cell shape by restricting microtubule dynamic instability and membrane associated proteins needed for forward protrusion, myoblast fusion and muscle formation. In chapter 3, we identified several genes known to regulate myoblast recognition, adhesion and fusion, using information from microarray data of $Lbx1^{EGFP}$ muscle precursors isolated from wild type and Pitx2 ablated mice. We generated stable over expressed Pitx2 in C2C12 cells and used them as our model system to study myoblast behavior. We observed decreased myoblast proliferation, improved migration, increased number of nuclei in myofibers and enhanced alignment of myotubes into parallel arrays in the presence of Pitx2. These data identify Pitx2 as a key regulator for the formation and arrangement of myofibers important for skeletal muscle development, growth and regeneration. For chapter 4, we utilized the information from microarray data of $Lbx1^{EGFP}$ muscle precursors isolated from wild type and Pitx2 ablated mice in combination with online gene ontology databases and in house scripts to predict the presence of *Cis*-Regulatory Modules (CRM). A total of 557 individual genes were placed into a total of 175 bins based on putative functional annotations using the DAVID Bioinformatics Functional Annotation Tool [60,61]. The first 10 bins had similar enrichment scores reported and an even number of bins contained GOTERMs referring to cytoskeletal or transcription factor functions. These genes were analyzed for predicted Pitx2 binding sites within the genomic gene sequence and -20kb upstream region. The top 2 genes from each bin that contained Pitx2 binding site conserved in at least 4 species with a representative pool of 20 genes. A predicted network model was constructed using BioTapestry version 5.0.2 to visually link Pitx2 with its target genes. Finally for chapter 5, we make general conclusions of how Pitx2 interacts with the genes

identified from microarray data to promote myoblast proliferation, promote migration, grow myofibers and enhance the alignment of myotubes.

Chapter 1-Figure 1

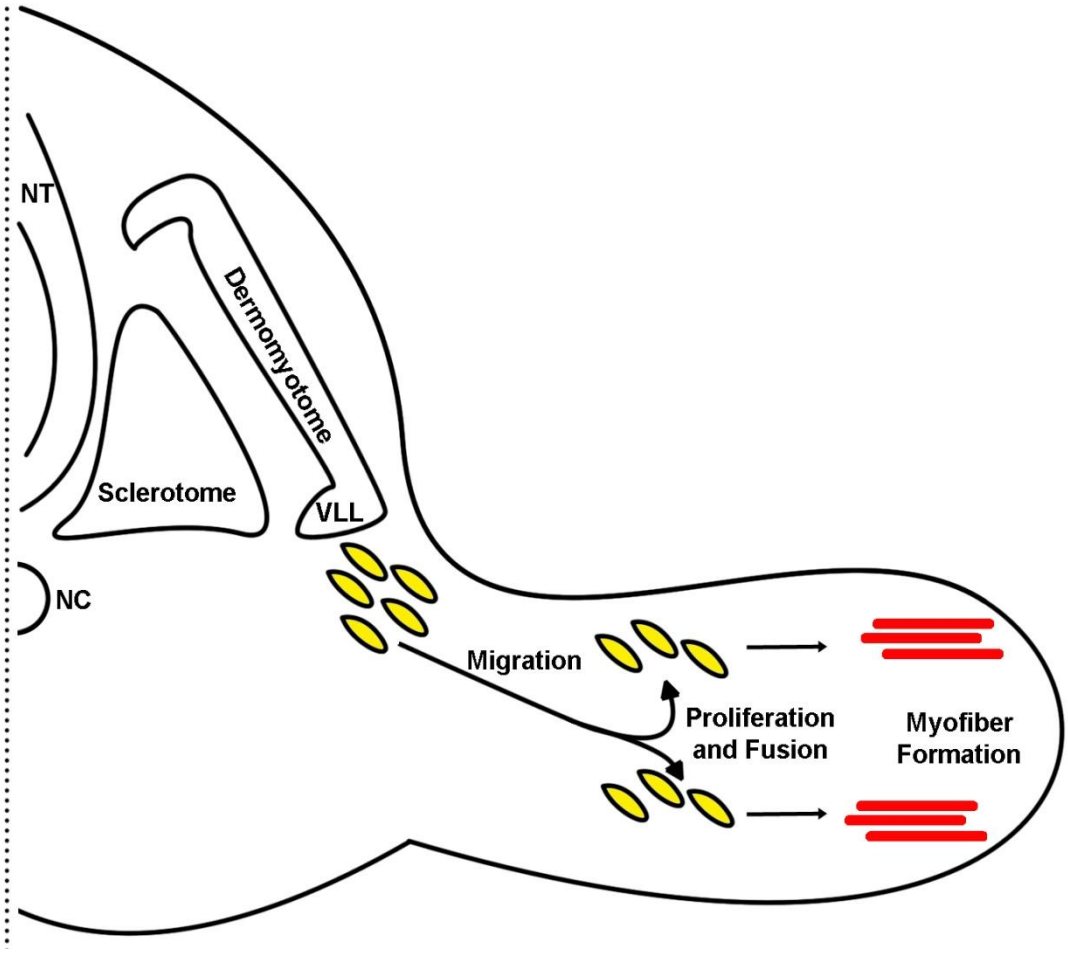

Figure 1. Diagram of Forelimb Myogenesis. Skeletal muscle precursors delaminate from the VLL of the DM to migrate as single cells at approximately early E9.25. These cells enter the limb about a day later (E10.5) and populate prepatterned areas where the muscle groups will form. Once there the muscle precursors proliferate, undergo differentiation, and fuse to form parallel arrays of myotubes. These parallel arrays will grow and form bundles to become the myofibers of the skeletal muscles.

References

1. Gossler A, Hrabe de Angelis M (1998) Somitogenesis. Curr Top Dev Biol 38: 225-287.
2. Kalcheim C, Ben-Yair R (2005) Cell rearrangements during development of the somite and its derivatives. Curr Opin Genet Dev 15: 371-380.
3. Borycki AG, Emerson CP, Jr. (2000) Multiple tissue interactions and signal transduction pathways control somite myogenesis. Curr Top Dev Biol 48: 165-224.
4. Munsterberg AE, Kitajewski J, Bumcrot DA, McMahon AP, Lassar AB (1995) Combinatorial signaling by Sonic hedgehog and Wnt family members induces myogenic bHLH gene expression in the somite. Genes Dev 9: 2911-2922.
5. Pourquie O, Fan CM, Coltey M, Hirsinger E, Watanabe Y, et al. (1996) Lateral and axial signals involved in avian somite patterning: a role for BMP4. Cell 84: 461-471.
6. Tajbakhsh S, Borello U, Vivarelli E, Kelly R, Papkoff J, et al. (1998) Differential activation of Myf5 and MyoD by different Wnts in explants of mouse paraxial mesoderm and the later activation of myogenesis in the absence of Myf5. Development 125: 4155-4162.
7. Goulding M, Lumsden A, Paquette AJ (1994) Regulation of Pax-3 expression in the dermomyotome and its role in muscle development. Development 120: 957-971.
8. Bober E, Franz T, Arnold HH, Gruss P, Tremblay P (1994) Pax-3 is required for the development of limb muscles: a possible role for the migration of dermomyotomal muscle progenitor cells. Development 120: 603-612.
9. Mennerich D, Schafer K, Braun T (1998) Pax-3 is necessary but not sufficient for lbx1 expression in myogenic precursor cells of the limb. Mech Dev 73: 147-158.
10. Schafer K, Braun T (1999) Early specification of limb muscle precursor cells by the homeobox gene Lbx1h. Nature Genetics 23: 213-216.
11. Gross MK, Moran-Rivard L, Velasquez T, Nakatsu MN, Jagla K, et al. (2000) Lbx1 is required for muscle precursor migration along a lateral pathway into the limb. Development 127: 413-424.
12. Dietrich S, Abou-Rebyeh F, Brohmann H, Bladt F, Sonnenberg-Riethmacher E, et al. (1999) The role of SF/HGF and c-Met in the development of skeletal muscle. Development 126: 1621-1629.
13. Weintraub H, Dwarki VJ, Verma I, Davis R, Hollenberg S, et al. (1991) Muscle-specific transcriptional activation by MyoD. Genes Dev 5: 1377-1386.
14. Emerson CP (1990) Myogenesis and developmental control genes. Curr Opin Cell Biol 2: 1065-1075.
15. Wright WE, Sassoon DA, Lin VK (1989) Myogenin, a factor regulating myogenesis, has a domain homologous to MyoD. Cell 56: 607-617.
16. Edmondson DG, Olson EN (1989) A gene with homology to the myc similarity region of MyoD1 is expressed during myogenesis and is sufficient to activate the muscle differentiation program. Genes Dev 3: 628-640.
17. Charbonnier F, Gaspera BD, Armand AS, Van der Laarse WJ, Launay T, et al. (2002) Two myogenin-related genes are differentially expressed in Xenopus laevis myogenesis and differ in their ability to transactivate muscle structural genes. J Biol Chem 277: 1139-1147.
18. McKinsey TA, Zhang CL, Olson EN (2001) Identification of a signal-responsive nuclear export sequence in class II histone deacetylases. Molecular and Cellular Biology 21: 6312-6321.

19. Hynes RO (2002) Integrins: bidirectional, allosteric signaling machines. Cell 110: 673-687.
20. Zaidel-Bar R, Milo R, Kam Z, Geiger B (2007) A paxillin tyrosine phosphorylation switch regulates the assembly and form of cell-matrix adhesions. J Cell Sci 120: 137-148.
21. Campbell ID, Ginsberg MH (2004) The talin-tail interaction places integrin activation on FERM ground. Trends Biochem Sci 29: 429-435.
22. Otey CA, Carpen O (2004) Alpha-actinin revisited: a fresh look at an old player. Cell Motil Cytoskeleton 58: 104-111.
23. Ziegler WH, Liddington RC, Critchley DR (2006) The structure and regulation of vinculin. Trends Cell Biol 16: 453-460.
24. Amano M, Chihara K, Kimura K, Fukata Y, Nakamura N, et al. (1997) Formation of actin stress fibers and focal adhesions enhanced by Rho-kinase. Science 275: 1308-1311.
25. Duelli D, Lazebnik Y (2007) Cell-to-cell fusion as a link between viruses and cancer. Nat Rev Cancer 7: 968-976.
26. Baylies MK, Bate M, Ruiz Gomez M (1998) Myogenesis: a view from Drosophila. Cell 93: 921-927.
27. Frasch M (1999) Controls in patterning and diversification of somatic muscles during Drosophila embryogenesis. Curr Opin Genet Dev 9: 522-529.
28. Bate M (1990) The embryonic development of larval muscles in Drosophila. Development 110: 791-804.
29. Beckett K, Baylies MK (2006) The development of the Drosophila larval body wall muscles. Int Rev Neurobiol 75: 55-70.
30. Ruiz-Gomez M, Coutts N, Suster ML, Landgraf M, Bate M (2002) myoblasts incompetent encodes a zinc finger transcription factor required to specify fusion-competent myoblasts in Drosophila. Development 129: 133-141.
31. Strunkelnberg M, Bonengel B, Moda LM, Hertenstein A, de Couet HG, et al. (2001) rst and its paralogue kirre act redundantly during embryonic muscle development in Drosophila. Development 128: 4229-4239.
32. Artero RD, Castanon I, Baylies MK (2001) The immunoglobulin-like protein Hibris functions as a dose-dependent regulator of myoblast fusion and is differentially controlled by Ras and Notch signaling. Development 128: 4251-4264.
33. Bour BA, Chakravarti M, West JM, Abmayr SM (2000) Drosophila SNS, a member of the immunoglobulin superfamily that is essential for myoblast fusion. Genes Dev 14: 1498-1511.
34. Dworak HA, Charles MA, Pellerano LB, Sink H (2001) Characterization of Drosophila hibris, a gene related to human nephrin. Development 128: 4265-4276.
35. Kesper DA, Stute C, Buttgereit D, Kreiskother N, Vishnu S, et al. (2007) Myoblast fusion in Drosophila melanogaster is mediated through a fusion-restricted myogenic-adhesive structure (FuRMAS). Dev Dyn 236: 404-415.
36. Onel SF, Renkawitz-Pohl R (2009) FuRMAS: triggering myoblast fusion in Drosophila. Dev Dyn 238: 1513-1525.
37. Kim S, Shilagardi K, Zhang S, Hong SN, Sens KL, et al. (2007) A critical function for the actin cytoskeleton in targeted exocytosis of prefusion vesicles during myoblast fusion. Dev Cell 12: 571-586.
38. Richardson BE, Beckett K, Nowak SJ, Baylies MK (2007) SCAR/WAVE and Arp2/3 are crucial for cytoskeletal remodeling at the site of myoblast fusion. Development 134: 4357-4367.

39. Doberstein SK, Fetter RD, Mehta AY, Goodman CS (1997) Genetic analysis of myoblast fusion: blown fuse is required for progression beyond the prefusion complex. Journal of Cell Biology 136: 1249-1261.
40. Sohn RL, Huang P, Kawahara G, Mitchell M, Guyon J, et al. (2009) A role for nephrin, a renal protein, in vertebrate skeletal muscle cell fusion. Proc Natl Acad Sci U S A 106: 9274-9279.
41. Sellin L, Huber TB, Gerke P, Quack I, Pavenstadt H, et al. (2003) NEPH1 defines a novel family of podocin interacting proteins. FASEB J 17: 115-117.
42. Ueno H, Sakita-Ishikawa M, Morikawa Y, Nakano T, Kitamura T, et al. (2003) A stromal cell-derived membrane protein that supports hematopoietic stem cells. Nat Immunol 4: 457-463.
43. George-Weinstein M, Gerhart J, Blitz J, Simak E, Knudsen KA (1997) N-cadherin promotes the commitment and differentiation of skeletal muscle precursor cells. Dev Biol 185: 14-24.
44. Horsley V, Jansen KM, Mills ST, Pavlath GK (2003) IL-4 acts as a myoblast recruitment factor during mammalian muscle growth. Cell 113: 483-494.
45. Rosen GD, Sanes JR, LaChance R, Cunningham JM, Roman J, et al. (1992) Roles for the integrin VLA-4 and its counter receptor VCAM-1 in myogenesis. Cell 69: 1107-1119.
46. Donalies M, Cramer M, Ringwald M, Starzinski-Powitz A (1991) Expression of M-cadherin, a member of the cadherin multigene family, correlates with differentiation of skeletal muscle cells. Proc Natl Acad Sci U S A 88: 8024-8028.
47. Charrasse S, Meriane M, Comunale F, Blangy A, Gauthier-Rouviere C (2002) N-cadherin-dependent cell-cell contact regulates Rho GTPases and beta-catenin localization in mouse C2C12 myoblasts. Journal of Cell Biology 158: 953-965.
48. Vasyutina E, Martarelli B, Brakebusch C, Wende H, Birchmeier C (2009) The small G-proteins Rac1 and Cdc42 are essential for myoblast fusion in the mouse. Proc Natl Acad Sci U S A 106: 8935-8940.
49. Davis DB, Doherty KR, Delmonte AJ, McNally EM (2002) Calcium-sensitive phospholipid binding properties of normal and mutant ferlin C2 domains. J Biol Chem 277: 22883-22888.
50. Doherty KR, Cave A, Davis DB, Delmonte AJ, Posey A, et al. (2005) Normal myoblast fusion requires myoferlin. Development 132: 5565-5575.
51. Doherty KR, Demonbreun AR, Wallace GQ, Cave A, Posey AD, et al. (2008) The endocytic recycling protein EHD2 interacts with myoferlin to regulate myoblast fusion. J Biol Chem 283: 20252-20260.
52. Shih HP, Gross MK, Kioussi C (2007) Cranial muscle defects of Pitx2 mutants result from specification defects in the first branchial arch. Proc Natl Acad Sci U S A 104: 5907-5912.
53. Shih HP, Gross MK, Kioussi C (2007) Expression pattern of the homeodomain transcription factor Pitx2 during muscle development. Gene Expr Patterns 7: 441-451.
54. Shih HP, Gross MK, Kioussi C (2008) Muscle development: forming the head and trunk muscles. Acta Histochem 110: 97-108.
55. Lu MF, Pressman C, Dyer R, Johnson RL, Martin JF (1999) Function of Rieger syndrome gene in left-right asymmetry and craniofacial development. Nature 401: 276-278.
56. Lin CR, Kioussi C, O'Connell S, Briata P, Szeto D, et al. (1999) Pitx2 regulates lung asymmetry, cardiac positioning and pituitary and tooth morphogenesis. Nature 401: 279-282.

57. Gage PJ, Suh H, Camper SA (1999) Dosage requirement of Pitx2 for development of multiple organs. Development 126: 4643-4651.
58. Kitamura K, Miura H, Miyagawa-Tomita S, Yanazawa M, Katoh-Fukui Y, et al. (1999) Mouse Pitx2 deficiency leads to anomalies of the ventral body wall, heart, extra- and periocular mesoderm and right pulmonary isomerism. Development 126: 5749-5758.
59. Kioussi C, Briata P, Baek SH, Rose DW, Hamblet NS, et al. (2002) Identification of a Wnt/Dvl/beta-Catenin --> Pitx2 pathway mediating cell-type-specific proliferation during development. Cell 111: 673-685.
60. Dennis G, Jr., Sherman BT, Hosack DA, Yang J, Gao W, et al. (2003) DAVID: Database for Annotation, Visualization, and Integrated Discovery. Genome Biol 4: P3.
61. Huang da W, Sherman BT, Lempicki RA (2009) Systematic and integrative analysis of large gene lists using DAVID bioinformatics resources. Nat Protoc 4: 44-57.

Regulation of Motility of Myogenic Cells in Filling Limb Muscle Anlagen by Pitx2

Chapter 2

Adam L Campbell, Hung-Ping Shih, Jun Xu, Michael K Gross and Chrissa Kioussi

PLoS ONE
Published April 27, 2012
PLoS ONE 7(4): e35822
Doi:10.1371/journal.pone.003582

Abstract

Cells of the ventrolateral dermomyotome delaminate and migrate into the limb buds where they give rise to all muscles of the limbs. The migratory cells proliferate and form myoblasts, which withdraw from the cell cycle to become terminally differentiated myocytes. The myogenic lineage colonizes pre-patterned regions to form muscle anlagen as muscle fibers are assembled. The regulatory mechanisms that control the later steps of this myogenic program are not well understood. The homeodomain transcription factor Pitx2 is expressed specifically in the muscle lineage from the migration of precursors to adult muscle. Ablation of Pitx2 results in distortion, rather than loss, of limb muscle anlagen, suggesting that its function becomes critical during the colonization of, and/or fiber assembly in, the anlagen. Microarrays were used to identify changes in gene expression in flow-sorted migratory muscle precursors, labeled by $Lbx1^{EGFP/+}$, which resulted from the loss of *Pitx2*. Very few genes showed changes in expression. Many small-fold, yet significant, changes were observed in genes encoding cytoskeletal and adhesion proteins which play a role in cell motility. Myogenic cells from genetically-tagged mice were cultured and subjected to live cell-tracking analysis using time-lapse imaging. Myogenic cells lacking Pitx2 were smaller, more symmetrical, and had more actin bundling. They also migrated about half of the total distance and velocity. Decreased motility may prevent myogenic cells from filling pre-patterned regions of the limb bud in a timely manner. Altered shape may prevent proper assembly of higher-order fibers within anlagen. *Pitx2* therefore appears to regulate muscle anlagen development by appropriately balancing expression of cytoskeletal and adhesion molecules.

Introduction

During embryogenesis the paraxial mesoderm along the dorsal-ventral axis undergoes segmentation giving rise to the somites. These somites further differentiate to give rise to the dermomyotome and the sclerotome. The dermomyotome is subdivided into the epaxial and hypaxial dermomyotomes, and is the source of muscle progenitor cells that will form the deep back and lateral trunk musculature. Cells of the hypaxial dermomyotome delaminate and migrate to the regions of presumptive muscle group in the developing limbs. Formation of limb migratory muscle progenitor (MMP) cells begins when inductive cues from the lateral mesoderm and surface ectoderm synergistically induce the expression of Lbx1 within the ventrolateral Pax3 expression domain of dermomyotomes at limb levels [1]. The lateral mesoderm also provides signals that repress myogenesis in limb level dermomyotomes [2], and promote their delamination [3,4] and migration [5] into the limb bud. Lbx1 expression in mice begins in the dermomyotome lips at E9.25 at forelimb levels, and is required for lateral migration. The dorsal and ventral muscle masses of E10.5 mouse limb buds consist of $Lbx1^{+}/Pax3^{+}$ limb muscle progenitor (MP) cells [6]. Numerous $Lbx1^{+}/Pax3^{+}$ myogenic cells persist in all limb muscle anlagen until at least E12.5. In the period between E11 and E12.5 the muscle masses enlarge, split and ultimately become the muscle anlagen, which resemble the adult muscles in shape and position with respect to bone anlagen. MP cells proliferate, undergo withdrawal from the cell cycle and become terminally differentiated myocytes Pax3 and Lbx1 have generally been placed at the beginning of myogenic progression and activation of the Muscle Regulatory Factors (MRFs) in the embryonic limb because they are expressed earlier and their mutation leads to a loss of migratory precursors before MRFs are normally expressed [6,7,8,9,10]. These myocytes fuse with each other to form multinucleated myotubes and muscle fibers. The precise

regulatory mechanisms that control each step of the myogenic program are not well understood to date.

MP cells must maintain adhesion throughout morphogenesis in order to develop into terminally differentiated muscle [11]. In order to migrate efficiently, the migrating cell must orientate the internal cellular machinery to a highly polarized, locally segregated, tightly regulated, and rapidly adaptable entity that can be rearranged in a coordinated manner. Migration occurs in a cyclical process, beginning with an external signal such as a growth factors, chemokines, mechanical forces, and ECM proteins. This leads to polarization and protrusion of the cell membrane with actin rich structures such as the broad lamellapodia or spike like filopodia, in the direction of movement. These protrusions are stabilized with a variety of adhesion proteins (integrins, syndecans, cadherins, and cell adhesion molecules) attaching the protrusion to the substratum. Adhesions serve as points of traction and of regulatory signaling to control adhesion dynamics and protrusion of the cell membrane [12]. The successful attachment to the substratum unmasks intracellular regions of the adhesion molecules to allow multiprotein complexes, termed the adhesome, to cross-link the adhesion molecule to the cytoskeleton [13]. There are several cross-linking proteins such as talin, vinculin, and alpha-actinin [14,15,16]. In the central and rear regions of the migrating cell the actin filaments organize themselves into thick bundles called stress fibers which terminate at both ends at the focal adhesions connected to the extracellular matrix ECM [17]. Disassembly of the adhesions is accompanied by inward movement of the cell edge and dispersal of the adhesion structures. This well orchestrated process maintains the appropriate cell–cell contacts between migratory muscle progenitor cells, controls the architecture of individual muscles and influences the ultimate shape, size and physiological function of the muscle organ system.

The bicoid–related homeobox gene Pitx2 is expressed in the lateral plate mesoderm and in muscle anlagen in all stages of myogenic progression [18,19]. Pitx2 contributes to the establishment of network kernels that specify pre-myogenic progenitors for extraocular and mastication muscles [20]. Ablation of Pitx2 causes lethality in the mouse at E10.5-E14.5 with axial malformations, open body wall, heart defects, and arrest of organ development [21,22,23,24]. Pitx2 is positioned downstream of both Wnt and growth factor signaling pathways in skeletal myogenesis and promotes muscle progenitor proliferation by direct regulation of the expression of a number of cyclin-dependent kinases [25]. Alternatively, Pitx2 represses T-box genes by recruiting corepressors and HDACs [26] and activates Hox genes during abdominal wall development (Eng et al., unpublished data).

The exact source, timing, and migration patterns of the muscle progenitors have recently been described using classic lineage tracing techniques in embryos. In this study, we identified genes that are regulated by Pitx2 in the Lbx1^{EGFP} myogenic cells by gene expression arrays in flow-sorted cells. Several genes involved in cell migration, adhesion and motility have been identified as Pitx2 targets, including microtubule stabilization, actin cross-linking, and tubulin related and intermediate filament associated genes. Data from these studies suggest that myogenic cells have large single protrusions with a highly directed migration by continuous remodeling of their cytoskeleton and stabilization of their adhesion to the ECM. Pitx2 can regulate myogenic cell migration by influencing their polarity and shape by restricting the microtubule growth and providing membrane and associated proteins needed for forward protrusion, fusion and muscle formation.

Results

Deformed and Reduced Appendicular Muscle Anlagen in Pitx2 Mutants

Analysis of E10.5 - E14.5 X-gal stained Pitx2 HET embryos revealed many patches of localized blue staining in regions between the skin and bone. These patches have the pattern of muscles in the forelimbs suggesting that Pitx2 is normally expressed in muscle anlagen (Fig 1A-H). Intense X-gal staining was observed in scattered spots throughout each anlage with a more diffuse low-level stain permeating the entire anlagen. A fibrous muscle-like texture was observed in the larger stained anlagen and regions between the anlagen were not stained. The tight spatial restriction of Pitx2 expression to the muscle anlagen suggests that Pitx2 plays a role in muscle development, differentiation, and/or mature function.

The limb muscle anlagen of $Pitx2^{LacZ/+}$ (HET) were compared with those of $Pitx2^{LacZ/LacZ}$ (MUT) at stages E10.5 – E14.5 (Fig 1), E14.5 being the latest stage possible, as MUT do not live past E14.5 due to failure of the body wall to close. At this crude level of analysis, it appeared that most, if not all, limb muscle anlagen had formed. Thus, Pitx2 was therefore not essential for the gross patterning of limb muscle anlagen. The right forelimb was the least distorted of all limbs in MUT, being only slightly pronated. Although all the appropriate muscle anlagen appeared to be present in this limb (Fig 1D,H), careful inspection revealed some differences in the shape of muscle anlagen. They appeared to be either fatter or thinner, and less finely fibered than corresponding anlagen in HET. The differences were not linked in an obvious way to the slight overall distortion of the limb in this area.

Using flow sorting we isolated $EGFP^{+}$ cells from $Pax3^{Cre}|ROSA^{EGFP}|Pitx2^{LacZ/+}$ (HET) and $Pax3^{Cre}|ROSA^{EGFP}|Pitx2^{LacZ/LacZ}$ (MUT) embryos at E12.5 forelimb tissue dissociated into single cell suspensions. From forelimb tissue collected the mean (± SEM) percentage of

EGFP$^+$ cells was 17 ± 0.6% in HET (n = 8) and 11 ± 1% in MUT (n = 7) tissue mean (Fig 1I). The mean percentage of EGFP$^+$ cells present in MUT tissue was reduced by 26% compared to HET and this reduction was determined significant using unpaired t-test (p = 0.0001), (Fig S1). The reduced number of cells at E12.5 may have been due to altered cell cycle in the cells isolated from MUT forelimb tissue. These EGFP$^+$ cells were stained with propidium iodide (PI) and the distribution of the cells in the cell cycle showed that MUT cells had an increase in G1- phase (74 ± 0.009%) of the cell cycle compared to those isolated from HET (69 ± 0.007%) forelimb tissue this difference was determined significant using unpaired t-test (p = 0.0102) (Fig 1J,K), suggesting that Pitx2 regulates exit from the cell cycle. Pitx2 therefore appeared to influence the shape of limb muscle anlagen and the hypothesis was advanced that Pitx2 played a role in the proper differentiation or growth of appendicular muscle.

Pitx2 Target Genes in the Lbx1 Myogenic Cell Lineage

To better understand the Pitx2 dependent mechanisms involved in muscle development, identification of Pitx2 target genes in forelimb muscle was initiated. During mouse embryonic development *Pax3* is expressed in the dermomyotome, whereas *Lbx1* is coexpressed with *Pax3* specifically in migratory hypaxial muscle precursors that undergo long-range migration to the limb buds and diaphragm [4,6,9]. We isolated the *Lbx1* population from forelimb tissue at E12.5 using Lbx1^{EGFP} mouse line. The Lbx1^{EGFP} mouse line [6] provides a robust system for developing genome-wide analyses of epistatic interactions in mammalian embryos. At E12.5, muscle progenitors in the limb have been segregated into distinct populations that mark the developing muscle anlagen. Lbx1$^+$ marks and regulates MMP forelimb cells [6] (Fig 2A). The Lbx1 fluorescent cells from E12.5 embryos are also expressing Pitx2 [19]. The ratio of green to white cells accurately reflected the EGFP expression observed by

immunohistochemistry (Fig 2B). Thus, fluorescence activated cell sorting (FACS) was used to purify the $EGFP^{+}$ (G) and $EGFP^{-}$ (W) cells from pools of 3-4 sets of forelimbs of MUT, HET and WT mice at E12.5 (Fig 2C). Total RNA from three biological replicates of each of the four conditions, HET green (hG), HET white (hW), MUT green (mG) and MUT white (mW), was used to probe Affymetrix Mouse 430 arrays (Fig 2D). Data from all twelve arrays were normalized using GC robust multi-array averaging in GeneSpring software (Fig 2E-J). The analysis focused on probe sets corresponding to genes involved in cell adhesion and motility. These annotated genes used in this analysis include: 18 adhesion, 9 microtubule, 9 cytoskeleton or cytoskeleton binding proteins and 2 signaling related functions. These 38 genes were collectively monitored by 102 probe sets. Genes with the greatest fold change in expression are involved in actin cytoskeleton, microtubule dynamics, cellular adhesion and contraction, extracellular matrix and signaling (Table 1).

Cytoskeletal Defects in Myogenic Cells in Pitx2 Mutants

The expression of numerous genes encoding for cytoskeletal components or proteins regulating the dynamic assembly and disassembly of cytoskeletal components were altered in Pitx2 MUT myogenic cells. To investigate if these alterations in gene expression resulted in cytoskeletal defects immunohistochemistry on E12.5 limbs and on primary cultured limb myogenic cells were performed in series of double labeling experiments. Phalloidin was used to visualize the actin filaments (F-actin) and beta-Gal to visualize the expression of $Pitx2^{LaZ}$. Special care was given to positioning both HET and MUT forelimbs for cross sectioning of the forelimbs. Actin filaments were equally distributed represented with a round shape in the HET forelimb muscle tissue (Fig 3A) while they were clustered together forming long fibers in the MUT (Fig 3B). Cultured myogenic cells were characterized with a smooth flat shape with several protrusions with

filaments at the border of the cell (Fig 3C, arrow) while MUT cells were smaller, less developed with increased actin filaments along their body (Fig 3D, arrow). The muscle specific actin binding protein tropomyosin (Tpm) had very similar expression pattern (Fig 3E, F). Forelimb muscle sections from HET tissue indicated that cells were surrounded by orderly Tpm fibers (3E, arrows), while in MUT cells were surrounded by thicker denser looking fibers with Tpm forming a ring around them (3F, arrow). Cultured HET cells had an elongated shape with thin smooth fibers throughout the entire body and able to come together for further fusion (Fig 3G, arrow), compared to the MUT cells which exhibited a more round appearance with shorter thicker fibers (Fig 3H, arrow). The muscle specific intermediate filament protein desmin was not significantly mis-regulated in the gene expression arrays. However, its distribution did change in the forelimb tissue of the MUT, with desmin positive muscle cells not tightly connected and positioned without a distinct anatomical formation (Fig 3I, J). Cultured HET cells were more finely fibered and had an elongated shape (Fig 3K). In contrast, the MUT cells had shorter and thicker filaments (Fig 3L).

A similar approach was used to investigate if genes that encode for microtubule components, organization, or regulate dynamics resulted in defects. Microtubule Associated protein Tau (Microtubules) had a lighter more diffuse staining throughout the cell body in HET (Fig 3M) compared to the strong dense levels in MUT (Fig 3N). Myogenic HET isolated cultured cells had elongated cell shape (Fig 3O, arrow), in contrast to the MUT cells with a smaller rounder appearance and increased Tau levels (Fig 3P, arrow). Stathmin 2 (stmn) immunostaining was light and diffused in the cell body of HET muscle forelimb cells (Fig 3Q) while it was highly expressed in the segregated MUT cell bodies in a disorganized manner forming a web like structure (Fig 3R). Similarly, stmn expression was elevated in the body of the MUT stumpy looking cultured

cells (Fig 3T). Tubulin expression was highly detected in MUT tissue (Fig 3V) and isolated cells (Fig 3X). Myogenic MUT cells maintained round separated and failed to elongate and contact with each other to form multinucleated myofibers (Fig 3D, H, L, P, T, X). Thus, Pitx2 might act as a balance factor for (1) the formation of cytoskeleton by regulating the molecular ratio of thin and intermediate filaments and (2) the cell motion by regulating microtubules.

Defected Focal Adhesions in Myogenic Cells in Pitx2 Mutants

The directional migration of cells is initiated by extracellular cues. Initiation of migration occurs by polarizing and extending a protrusion, containing the broad lamellapodia and spiky filopodia, of the cell membrane towards the cue. Both of these structures are driven by polymerization of actin filaments, which then stabilized by adhering the actin cytoskeleton to the ECM. Signals from the newly formed, more stable and mature adhesions influence cytoskeletal organization, which in turn influences the formation and disassembly of the adhesions. This feedback loop coordinates spatial dynamics and mechanical stresses that lead to directional cell movement. Cells express cell surface adhesion receptors integrins that anchor them to extracellular matrices and alter their function by activating intracellular signaling pathways after ligand binding. The integrin-actin linkage is mediated by several proteins. Talin is an actin-binding protein that binds integrin tails and transitions integrin to an active state.

The expression of numerous genes involved in adhesion and in actin cytoskeleton has been altered in the Pitx2 mutants, suggesting that the formation of nascent adhesions in this cell population should be malformed. Forelimb cultured myogenic cells from HET and MUT mice were subject to triple labeling immunostaining for beta-Gal (Pitx2), talin to detect the focal adhesions and Phalloidin to detect the F-actin stress fibers (Fig 4). Talin and actin were coexpressed along the cell body, identifying the focal points (Fig 4 A, C,

E). Talin and actin coexpression was weakly detected in very few locations of the cells with small cytoplasm, suggesting that the focal points were limited in the MUT cells (Fig 4 B, D, F). As cells migrate through their environment the cytoskeleton stresses and contracts forming a leading and a trailing edge respectively. The nucleus moves towards the trailing edge allowing space for the cell to extend its cytoplasm (Fig 4A), while in the MUT cells the nucleus occupied the most of the body (Fig 4B). Focal adhesion points stained for both talin and Phalloidin were identified and counted in both HET and MUT cells. HET cells characterized with distinct trailing stress fibers and a smooth leading (Fig 4C) and trailing edge (Fig 4E) and similar number of focal adhesion points (Fig 4G). In MUT cells trailing and leading edges were not distinct with reduced number of focal adhesion points by 36% in leading and 25% in trailing edge (Fig 4G). However, the size of focal adhesion points was increased in MUT cells by 25% compared to HET cells (Fig 4H).

The observed phenotype of the myogenic cultured cells (Fig 3 and 4) was in accord with the phenotype observed in limb muscle groups (Fig 1). The clumpy, disorganized and truncated cells resulted to the formation of a dense and sort in length muscle. The leading edge, the more dynamic end of the cell, changes rapidly in order for the cell to sample its environment. Disruption of microtubules using pharmacological agents results in loss of cell polarity, increase in focal adhesion size, and formation of actin stress fibers [27]. At the leading edge of the cell, formation of many nascent adhesions to anchor the cell to the substratum occurs. Nascent adhesions are small (<1.0 micrometer) transient structures. These nascent adhesions rapidly assemble and disassemble allowing for sampling of the environment prior to formation of more stable or mature contacts. The maturation of focal adhesions are accompanied by an increase in size (2-10 micrometer) and the formation of actin stress fibers that terminate at the focal adhesion, presumably

to allow for contraction of the cell body to propel the cell forward. Disruption of the microtubule dynamics leads to the formation of larger focal adhesions, loss of cell polarity, and increased formation of actin stress fibers [27]. Thus, we suggest that adhesion irregularities of myogenic cells delay their ability to move fast and populate their muscle anlagen.

Impaired Motility of Myogenic Cells in Pitx2 Mutants

The hypocellularity and distortion of forelimb muscle groups observed in Pitx2 MUT mice (Fig. 1) might be the result of impaired migration of MMP cells to the distal forelimb. Live imaging of primary cultures of E12.5 forelimb MMP cells from $Lbx1^{EGFP/+}|Pitx2^{+/+}$ (WT), $Lbx1^{EGFP/+}|Pitx2^{LacZ/+}$ (HET) and $Lbx1^{EGFP/+}|Pitx2^{LacZ/LacZ}$ (MUT) (Fig 5) and proliferating MP cells from $Pax3^{Cre/+}|ROSA^{EGFP}|Pitx2^{+/+}$ (WT), $Pax3^{Cre/+}|ROSA^{EGFP}|Pitx2^{LacZ/+}$ (HET) and $Pax3^{Cre/+}|ROSA^{EGFP}|Pitx2^{LacZ/LacZ}$ (MUT) (Fig S2) was performed. Individual cells were visualized by EGFP expression and changes in position were recorded every 5 min for a period of 2 hrs. MMP WT cells migrated in a random fashion with cells frequently moving and several changes in direction (Fig 5A). MMP HET cells migrated in a similar fashion with cells frequently moving but with fewer changes in direction (Fig 5B). MMP MUT cells migrated much differently with cells spending more time paused and with fewer changes in direction (Fig 5C). MUT cells traveled half the distance of WT and almost 1/3 of the HET (Fig 5D). Velocity was also decreased in MMP MUT (0.2 ± 0.02 micrometer/min) compared to HET (0.6 ± 0.1 micrometer/min) and WT (0.5 ± 0.1 micrometer/min cells), (Fig 5E). Migratory behavior of MMP cells was also altered. MUT cells spent more time paused (66 ± 14 min) than moving (59 ±14 min), while WT (92 ± 16 min moving, 32 ± 17 min paused) and HET (101 ± 7 min moving, 24 ± 7 min paused) cells were moving more and spent only 1/3 or 1/4 of their time paused respectively (Fig 5F). All differences were determined statistically significant using a Dunnett's ANOVA

using WT as the control group, followed by an unpaired T-test between WT and MT determined significance values for distance traveled (p=0.0001), velocity (p=0.0001), time moving (p=0.0089) and time paused (p=0.0082). To quantify differences in migration patterns, the ratios of the shortest direct distance from the starting point of each recording to the end point (D), to the total track distance of the cell (T) was compared [28]. The ratio D/T to a value of 1 using data collected from MMP WT cells was normalized. MMP MUT cells showed an increased ratio of 127%, while HET showed reduced ratio of 63%, compared to WT cells (Fig 5G). The random vs. directional cell motility, was measured by a mean square displacement assay [29]. The mean square displacement of total pathway distance traveled (T^2) measured every 20 min was calculated and plotted against time. If movement is purely random, the linear regression line would pass through the origin. The x-intercept for HET cells was as close to the origin, as the intercept for MUT cells exhibited migration behaviors, (Fig 5H).

Similar analysis was performed in proliferating MP cells (Fig S2). WT and HET cells migrated in a random fashion similar to MMP cells with the exception that MP cells tended to persist in a single direction longer before changing.

Data from these studies suggest that myogenic cells take longer time to populate the limb anlagen in Pitx2 mutants due to their random movement and reduced velocity. As they proliferate they continue to migrate in a slower pace. This delay to reach their final destination does not follow the general growth limb program and the forming muscle is distorted and disorganized in the Pitx2 mutants.

Discussion

In this report we identified a cadre of Pitx2 target genes that function as components of or act in the assembly, organization and regulation of the cytoskeleton in forelimb myogenic cells (Table 1, Fig 6). In order to migrate efficiently the cell must respond to both intracellular and extracellular cues that reorganize the cytoskeleton. This constant reorganization influences the cell morphology and ultimately cell fate. The leading edge of the migrating cell is dominated by actin based structures lamellapodia and filopodia. Actin based cell motility is highly dynamic, conserved across eukaryotes and a fundamental process driving tissue development [30]. A network of proteins link the internal cytoskeleton of the cell to the external environment through adhesion molecules, allowing for the generation of force needed for cell movement [31].

The actin isoform actin alpha 1 (*Acta1*) is expressed in skeletal muscle tissue [32] and its expression was inhibited by Pitx2 (Table 1, Fig 6). In the initial stages of elongation *Acta1* expression levels increase in multinucleated myotubes while it localizes with the sarcomeric thin filaments [33]. Overexpression of *Acta1* reduces the ability of cell spreading and elicit the expression of a subset of muscle differentiation genes in the absence of normal muscle differentiation without withdrawal from the cell cycle [34]. The muscle specific alpha-actinin-3 (*Actn3*) acts as scaffolding protein that cross-links actin stress fibers to focal adhesion proteins providing anchor points, regulates the activity of a number of cell surface receptors, and acts as a scaffolding protein to connect the cytoskeleton to signaling pathways [14]. The cysteine and glycine-rich proteins (CRPs) are a subset of LIM domain protein family. *Csrp1* is ubiquitously expressed in striated and smooth muscle [35] and its expression, was promoted by Pitx2 (Table 1). *Csrp1* binds to alpha-actinin, which binds and bundles actin filaments into stress fibers and is responsible for maintaining proper tissue homeostasis [36]. The isoform Pitx2a has been

previously shown in regulating actin cytoskeleton dynamics indirectly through Rho GTPases in HeLa cells [37]. However, in our microarrays in forelimb migratory muscle precursor cells no mis-regulation of genes involved in Rho GTPase signaling was detected.

A downstream target of Rho GTPase signaling pathway is the cyclic-nucleotide-dependent kinase PKA which act to phosphorylate Ena/VASP proteins and promote their dissociation from the focal adhesion terminating actin fiber formation and negatively regulating lamellapodia formation [38]. The mammalian homolog of *Drosophila* enabled (*Enah*) *Mena* is a member of the enabled/vasodilator-stimulated phosphoprotein (*Ena/VASP*) family of actin regulatory proteins that act as critical regulators of actin assembly and cell motility with increased levels in heart failure [39,40]. Ena/VASP proteins bind to the focal adhesion proteins zyxin and vinculin, and to the actin nucleation protein profilin where it prevents capping and branching of the growing actin filament by the Arp2/3 complex. This complex promotes growth and formation of actin stress fibers allowing for protrusion of the cell membrane forming lamellapodia. The Ena/VASP proteins are also substrates for the cyclic-nucleotide-dependent kinases PKA and PKG, which act to phosphorylate Ena/VASP proteins and promote their dissociation from the focal adhesion terminating actin fiber formation and negatively regulating lamellapodia formation [41]. Pitx2 acted as an inhibitor of Enah in myogenic cells (Table 1, Fig 6).

Another gene family that was affected in Pitx2 MUT myogenic cells was the microtubule related gene family (Table 1). Microtubules are an active constituent during cell migration. They are organized with the growing end toward the leading edge that extends to the base of the lamellipodium. The constant growth and shrinkage (dynamic instability) of the microtubules is required for cell migration. Pharmacological agents that

either promote stabilization or depolymerization microtubules result in reduction of migration [42]. Tau binds to the outside surface of the microtubule and stabilizes the microtubule promoting growth [43]. Rho GTPase signaling influences microtubule dynamics through activation of Cdc42 and Rac. The activation of these two proteins leads to the phosphorylation of the microtubule destabilization protein stathmin [44]. The phosphorylation of stathmin leads to the inhibition of its ability to form ternary complexes with tubulin dimers preventing their incorporation into growing microtubules and promoting shrinkage of the microtubules [45]. Stathmins form ternary complexes with tubulin dimers preventing their incorporation into growing microtubules and promoting shrinkage of the microtubules [45]. During migration microtubules undergo dynamic instability to explore the intracellular environment. Growing microtubules are stabilized to focal adhesion complexes [38]. During myogenic differentiation the transition from myoblast to myotube is accompanied by extensive changes in morphology and reorganization of the cytoskeleton [46]. During myotubes formation the individual myoblasts' eliminate their microtubule organizing centers (MTOC) and align themselves into stabilized linear arrays along the multinucleated myotubes.

The expression profile of adhesion related genes was altered in the Pitx2 MUT forelimb myogenic cells (Table 1). Myozenin 2 (*Myoz2*) binds to alpha-actinin and γ-filamin and colocalized with alpha-actinin and gamma-filamin along the Z-Disc of striated muscle where it organizes and spaces the actin thin filament [47].

Integrins are transmembrane receptors that mediate attachment between the cell and the surrounding environment via cell-cell contacts or to the extracellular matrix (ECM). They provide anchoring points for the cytoskeleton and transduce environmental information to inside the cell thereby regulating cell shape, motility, differentiation, and the cell cycle [48]. Integrins consist of two transmembrane subunits, the alpha controls

selective binding to substrate, and the beta controls signal transduction into the cell [49]. Integrins are clustered at focal adhesions along with other phosphorylated adhesion proteins: paxillin, talin and focal adhesion kinase (FAK) which initiate signaling cascades that lead to activation of protein kinase C (PKC) that promote muscle cell survival, spreading and migration [50,51].

Syndecans are type 1 transmembrane heparin sulfate proteoglycans (HSPGs) that contain a short cytoplasmic domain, a transmembrane domain, and a long intracellular domain [52]. *Sdc4* is colocalized to focal adhesions containing talin, vinculin, alpha-actinin, paxillin, and FAK while its overexpression results in excessive focal adhesion formation and reduced cell migration [53]. After focal adhesions have formed, *Sdc4* modulates focal adhesion strength through recruitment of the GTP•RhoA protein, which acts to strengthen and cap focal adhesions preventing further actin stress fiber formation, and Rac1, which acts to weaken focal adhesions allowing for increased stress fiber formation and protrusion of lamellapodia [54,55].

The protein kinase cAMP regulatory subunit II beta (*Prkar2b*), a key enzyme for the regulation of the protein kinase A (PKA), was also regulated by Pitx2. PKA is a positive and negative regulator of cell migration and is spatially enriched at the leading edge of the cell [56]. At the leading edge PKA is required for the activation of Rac and Cdc42 proteins promoting actin filament assembly; conversely it inhibits the proteins Rho and PAK, as well as VASP proteins [57,58].

The 3-phosphoinositide dependent protein kinase 1 (*Pdpk1*) is recognized as a master kinase of the cell required for the activation of many signaling pathways. The Pdpk1 protein is phosphorylated by 3-phosphoinositide kinase (PI3K) protein. Phosphatidylinositol (PI) signaling is complex and crucial for migration. In general signaling through PKA and the G-proteins (Rac, Rho and Cdc42) at the leading edge

leads to increased PI levels due to activation of type 1 phosphatidylinositol kinases (PIPK1) resulting in an increase in actin polymerization [59]. At the trailing edge, the protein Calpain acts to begin disassembly of focal adhesions using PIs as a substrate to dissociate integrins from the cytoskeleton [60].

Pitx2 affects muscle specification in the jaw but appears to disrupt higher-order muscle assembly in virtually all skeletal muscles. In limb muscle, it does so without affecting muscle specification or cellular muscle differentiation. Despite all of this apparent normality, the muscle anlagen become oddly distorted and granular 1-2 days after being colonized, suggesting that Pitx2 function becomes critical between colonization and myofibril assembly. Our results indicate that anlagen volume and proliferative indices differ in mutant anlagen, and suggest that there is a defect in the mechanism that maintains correct progenitor pool size as muscles enlarge and engage in higher-order assembly. Many cytoskeletal proteins with established roles in cellular motility and adhesion in other systems have significantly altered expression levels in myogenic cells. Embryos use transcriptional network states during pattern formation to specify where and when muscle progenitor cells will form in the developing body plan (Fig 6). These muscle progenitor cells proliferate, express MRFs, and colonize particular regions of the body to form muscle anlagen. The anlagen assemble on a pre-pattern that is also set up by pattern formation processes. Once myoblasts arrive at their anlage they begin to pull out of the cell cycle and engage in higher-order assembly of muscle. Higher-order assembly is likely to happen in a similar way at all anatomical positions, but still needs to be understood at the molecular level to help understand how myopathies form and can be cured.

Materials and Methods

Mice. ICR Pitx2$^{LacZ/+}$ mouse embryos (HET) [22], Lbx1$^{EGFP/+}$ [6], Pax3$^{Cre/+}$ [61] and Rosa$^{EGFP/+}$ [62] were used. Pitx2$^{LacZ/+}$ mice were bred with Pitx2$^{LacZ/+}$, Lbx1$^{EGFP/+}$ and Pax3$^{Cre/+}$|Rosa$^{EGFP/+}$ to generate Lbx1$^{EGFP/+}$|Pitx2$^{LacZ/LacZ}$, Lbx1$^{EGFP/+}$|Pitx2$^{LacZ/+}$, Lbx1$^{EGFP/+}$|Pitx2$^{+/+}$, Pax3$^{Cre/+}$|Rosa$^{EGFP/+}$|Pitx2$^{LacZ/LacZ}$, Pax3$^{Cre/+}$|Rosa$^{EGFP/+}$|Pitx2$^{LacZ/+}$, Pax3$^{Cre/+}$|Rosa$^{EGFP/+}$|Pitx2$^{+/+}$ mice. Genomic DNA was extracted from tail and used for PCR genotyping [6,22]. For cell flow sorting, embryos were rapidly genotyped under a fluorescent microscope to identify Lbx1 HET mice. To identify the Pitx2 genotypes, only Lbx1 HET embryos were subjected to X-gal staining.

X-Gal Staining. Mouse embryos at E12.5 were washed with PBS and incubated with 1 mg/ml X-Gal in 2 mM $MgCl_2$, 0.02% NP40, 5 mM $K_3F_4(CN)_6$, 5 mM $K_4F_3(CN)_6$ in PBS. For whole body staining embryos were incubated at 37^{o}C O/N and for quick genotyping dissected heads were incubated for at least 0.5h. Samples were washed with PBS and clarified with glycerol for analysis and photography.

Flow-Sorting EGFP$^+$ Forelimb Myogenic Cells: Synchronous Lbx1$^{EGFP/+}$ containing litters were removed at E12.5 and rapidly genotyped under a fluorescent microscope to identify Lbx1$^{EGFP/+}$ HET embryos and X-gal staining to identify Pitx2 MUT and HET. Limb buds and ventral body wall compartments between the caudal edge of the shoulder and lumbar region were dissected. For enzymatic dissociation, 40 limb buds were incubated in 1 ml of dissociation buffer (HBSS without HEPES [Hyclone; Rockford, IL USA], 1 mg/ml Type I Collagenase [Worthington Biochem; Lakewood, NJ USA]) for 3 min at 37^o C. Large tissue was disrupted by 10 times repetitive pipetting through a 1 ml tip with an additional pipetting followed by 1 ml quench buffer (DMEM/F12 with 15 mM HEPES and 2.5 mM Glutamine [Hyclone; Rockford, IL USA], 25 microgram/ml BSA Fraction V [Sigma; St. Louis, MO USA], 0.5 M EDTA, 100 mM EGTA, 50 U/ml Pen/Strep [Cellgro;

Manassas, VA USA], 0.25 microgram/ml Fungizone [Invitrogen; Carlsbad, CA USA]). Cells were filtered through 30 micrometer^2 Nitex filter, centrifuged and flow sorted using MoFlo high-performance cell sorter [Dako Colorado Inc.; Carpinteria, CA USA].

Propidium Iodide Staining and Cell Cycle Analysis. Flow sorted PAX3^{CRE}|ROSA^{EGFP} cells were collected in 5 ml culture tubes containing PBS. These cells were centrifuged at 300 x g for 5 min, supernatant was discarded and pellet resuspended in PBS. Cells were centrifuged and supernatant was discarded and the pellet resuspended in 0.5 ml PBS + 0.1% Triton-X 100 in addition to 10 microliter of RNase A (10 microgram/ml; [Invitrogen; Carlsbad, CA USA]) and 10 microliter Propidium Iodide (1 mg/ml; [Sigma-Aldrich, St. Louis, MO USA]). Cells were incubated for 30 min at room temp prior to cell cycle using FC500 flow cytometer [Beckman Coulter; Brea, CA USA].

Extraction of Total RNA. Flow sorted EGFP$^+$ cells (green, G) and EGFP$^-$ cells (white, W) were lysed with RLT buffer [Qiagen; Valencia, CA USA], (2x10^6 cells/350 microliter). For extraction of total RNA RNAeasy Micro Kits [Qiagen; Valencia, CA USA] were used according to manufacture protocols

RNA Preparation and Microarray Analysis. Lbx1^{EGFP} forelimb cells were enriched from three pools of WT (Lbx1^{EGFP}|Pitx2$^{+/+}$), HET (Lbx1^{EGFP}|Pitx2$^{LacZ/+}$), and MUT (Lbx1^{EGFP}|Pitx2$^{LacZ/LacZ}$) embryos by cell sorting using MoFlo high-performance cell sorter [Dako Colorado Inc.; Carpinteria, CA USA] on basis of EGFP signal. Total RNA was prepared from forelimbs and probes prepared from these RNA were applied to nine Mouse Genome 430 2.0 microarrays [63]. The results from all nine arrays were normalized by RMA. The mean expression value obtained from three biological replicates was compared between genotypes. The data discussed in this publication have been deposited in NCBI's Gene Expression Omnibus [64] and are accessible

through GEO Series accession number GSE31945 (http://www.ncbi.nlm.nih.gov/geo/query/acc.cgi?acc=GSE31945).

Myogenic Cell Cultures. Forelimbs from E12.5 $Pitx2^{LacZ}$ HET and MUT mice were dissected and dissociated into single cells in dissociation buffer (HBSS without HEPES [Hyclone; Rockford, IL USA], 1 mg/ml Type I Collagenase [Worthington Biochem; Lakewood, NJ USA]) for 3 min at 37^{o} C. Cells were plated in growth media (DMEM/F12 [Gibco; Carlsbad, CA USA], 2.5 mM Glutamine [Hyclone; Rockford, IL USA], 15% horse serum, 50 U/ml Pen/Strep [Cellgro; Manassas, VA USA], 0.25 microgram/ml Fungizone [Invitrogen; Carlsbad, CA USA] and 2 ng/ml bFgf [Upstate/ Millipore; Billerica, MA USA] with 20,000 cells/well in 24-well tissue culture plate [Costar; Corning, NY USA] containing type 1 collagen [Sigma; St. Louis, MO USA] coated coverslips for immunocytochemistry or in 35 mm glass bottom culture dish [MatTek; Ashland, MA USA] coated with type 1 collagen for cell tracking assay. Cells were allowed to attach for 1 hr before switching to serum free media containing phenol red free DMEM [Cellgro; Manassas, VA USA], 50 U/ml Pen/Strep [Cellgro; Manassas, VA USA], 0.25 microg/ml Fungizone [Invitrogen; Carlsbad, CA USA], 2.5 mM L-glutamine, 25 mM HEPES, 1 mM Na-pyruvate [Cellgro; Manassas, VA USA].

Live Cell Tracking Assays. Glass bottom culture dishes containing attached myogenic cells from MMP ($Lbx1^{EGFP}|Pitx2^{+/+}$, $Lbx1^{EGFP}|Pitx2^{LacZ/+}$, $Lbx1^{EGFP}|Pitx2^{LacZ/LacZ}$) and MP ($Pax3^{Cre}|Rosa^{EGFP}|Pitx2^{+/+}$, $Pax3^{Cre}|Rosa^{EGFP}|Pitx2^{LacZ/+}$, $Pax3^{Cre}|Rosa^{EGFP}|Pitx2^{LacZ/LacZ}$) cells were taken immediately after switching to serum free media for imaging that persisted for approximately 40 hrs. Culture dishes were placed inside live cell chamber incubator set at 37°C and 5% CO_2. Single cells were imaged under Zeiss Confocal Microscope LSM 510 Meta [Zeiss; Oberkochen Germany] using EGFP signal as a tracer. The position of individual cells was recorded every 5 min for a total of 2 hrs.

Immunohistochemistry/Immunocytochemistry. Cryosectioning of fixed E12.5 embryo blocks were cut at 12 microm thickness or myogenic cell culture coverslips were harvested and fixed in 4% Paraformaldehyde containing 0.1% Triton X-100 for 5 min. Samples were washed 3 times with PBS and blocked for 1 hr at room temperature with 3SB blocking buffer (5% Fetal Calf Serum, 5% Goat Serum, 1% Calf Serum, 0.3% Boehringer Blocker, 0.1% Triton X-100, PBS). Primary antibodies anti-mouse Talin (1:1000, [Sigma; St. Louis, MO USA]), anti-mouse Tropomyosin (undiluted, [DSHB; Iowa City, IA USA]), anti-mouse beta-gal (1:1000, [Cappel; Cochranville PA USA]), anti-mouse Tau (1:100, [Santa Cruz; Santa Cruz, CA USA]), anti-mouse alpha-tubulin (1:1000, [Sigma; St. Louis, MO USA]), anti-rabbit Stmn2 (1:100, [Abcam; San Francisco, CA USA]), anti-rat BrdU (1:50 [Accurate Chemical and Scientific West Bury, NY USA] and anti-rabbit desmin (1:20, [Sigma; St. Louis, MO USA]) added to samples, and samples were incubated overnight at 4° C. Samples were washed 3 times with PBST (PBS + 0.1% Triton X-100) for 10 min. Fluorescent conjugated secondary antibodies [1:500, Jackson Immuno.; West Grove, PA USA] and Alexa Fluor 488 conjugated or Rhodamine conjugated Phalloidin [1:100, Invitrogen; Carlsbad, CA USA] were added and samples were incubated at room temperature for 2 hrs, followed by 3 times wash with PBST for 10 min. Samples were dehydrated and mounted with DPX mounting media. Single cells were imaged under Zeiss Confocal Microscope LSM 510 Meta [Zeiss; Oberkochen Germany] at 63x magnification. While tissue sections were imaged under Zeiss Imager.Z1 Microscope [Zeiss; Oberkochen Germany] at 63x magnification.

Visualization of Predicted Gene Network. Cytoscape 2.6.3 was utilized for composing visualizations of microarray gene expression data [65]. The top ten genes were clustered based on fold change, from Table 1 in the families of actin, microtubule, and adhesion. Connections between the nodes are displayed as solid lines for direct interactions and

dashed lines for possible interactions. Direct or indirect, not yet determined, was based on current literature search.

Acknowledgments

We thank Anne-Marie Girard for microarray processing, Sam Bradford for flow sorting, Diana Eng and Hsiao-Yen Ma for colony maintenance, the College of Pharmacy, the Center for Genome Research and Bioinformatics, and the Environmental and Health Sciences Center (P30ES000210 NIEHS-NIH) in OSU for infrastructural support.

References

1. Tremblay P, Dietrich S, Mericskay M, Schubert FR, Li Z, et al. (1998) A crucial role for Pax3 in the development of the hypaxial musculature and the long-range migration of muscle precursors. Dev Biol 203: 49-61.
2. Venters SJ, Argent RE, Deegan FM, Perez-Baron G, Wong TS, et al. (2004) Precocious terminal differentiation of premigratory limb muscle precursor cells requires positive signalling. Dev Dyn 229: 591-599.
3. Bladt F, Riethmacher D, Isenmann S, Aguzzi A, Birchmeier C (1995) Essential role for the c-met receptor in the migration of myogenic precursor cells into the limb bud. Nature 376: 768-771.
4. Dietrich S, Abou-Rebyeh F, Brohmann H, Bladt F, Sonnenberg-Riethmacher E, et al. (1999) The role of SF/HGF and c-Met in the development of skeletal muscle. Development 126: 1621-1629.
5. Hayashi K, Ozawa E (1995) Myogenic cell migration from somites is induced by tissue contact with medial region of the presumptive limb mesoderm in chick embryos. Development 121: 661-669.
6. Gross MK, Moran-Rivard L, Velasquez T, Nakatsu MN, Jagla K, et al. (2000) Lbx1 is required for muscle precursor migration along a lateral pathway into the limb. Development 127: 413-424.
7. Goulding M, Lumsden A, Paquette AJ (1994) Regulation of Pax-3 expression in the dermomyotome and its role in muscle development. Development 120: 957-971.
8. Bober E, Franz T, Arnold HH, Gruss P, Tremblay P (1994) Pax-3 is required for the development of limb muscles: a possible role for the migration of dermomyotomal muscle progenitor cells. Development 120: 603-612.
9. Mennerich D, Schafer K, Braun T (1998) Pax-3 is necessary but not sufficient for lbx1 expression in myogenic precursor cells of the limb. Mech Dev 73: 147-158.
10. Schafer K, Braun T (1999) Early specification of limb muscle precursor cells by the homeobox gene Lbx1h. Nature Genetics 23: 213-216.
11. Gurdon JB (1988) A community effect in animal development. Nature 336: 772-774.
12. Hynes RO (2002) Integrins: bidirectional, allosteric signaling machines. Cell 110: 673-687.
13. Zaidel-Bar R, Milo R, Kam Z, Geiger B (2007) A paxillin tyrosine phosphorylation switch regulates the assembly and form of cell-matrix adhesions. J Cell Sci 120: 137-148.
14. Otey CA, Carpen O (2004) Alpha-actinin revisited: a fresh look at an old player. Cell Motil Cytoskeleton 58: 104-111.
15. Campbell ID, Ginsberg MH (2004) The talin-tail interaction places integrin activation on FERM ground. Trends Biochem Sci 29: 429-435.
16. Ziegler WH, Liddington RC, Critchley DR (2006) The structure and regulation of vinculin. Trends Cell Biol 16: 453-460.
17. Amano M, Chihara K, Kimura K, Fukata Y, Nakamura N, et al. (1997) Formation of actin stress fibers and focal adhesions enhanced by Rho-kinase. Science 275: 1308-1311.
18. Shih HP, Gross MK, Kioussi C (2007) Cranial muscle defects of Pitx2 mutants result from specification defects in the first branchial arch. Proc Natl Acad Sci U S A 104: 5907-5912.
19. Shih HP, Gross MK, Kioussi C (2007) Expression pattern of the homeodomain transcription factor Pitx2 during muscle development. Gene Expr Patterns 7: 441-451.

20. Shih HP, Gross MK, Kioussi C (2008) Muscle development: forming the head and trunk muscles. Acta Histochem 110: 97-108.
21. Lu MF, Pressman C, Dyer R, Johnson RL, Martin JF (1999) Function of Rieger syndrome gene in left-right asymmetry and craniofacial development. Nature 401: 276-278.
22. Lin CR, Kioussi C, O'Connell S, Briata P, Szeto D, et al. (1999) Pitx2 regulates lung asymmetry, cardiac positioning and pituitary and tooth morphogenesis. Nature 401: 279-282.
23. Gage PJ, Suh H, Camper SA (1999) Dosage requirement of Pitx2 for development of multiple organs. Development 126: 4643-4651.
24. Kitamura K, Miura H, Miyagawa-Tomita S, Yanazawa M, Katoh-Fukui Y, et al. (1999) Mouse Pitx2 deficiency leads to anomalies of the ventral body wall, heart, extra- and periocular mesoderm and right pulmonary isomerism. Development 126: 5749-5758.
25. Kioussi C, Briata P, Baek SH, Rose DW, Hamblet NS, et al. (2002) Identification of a Wnt/Dvl/beta-Catenin --> Pitx2 pathway mediating cell-type-specific proliferation during development. Cell 111: 673-685.
26. Hilton T, Gross MK, Kioussi C (2010) Pitx2-dependent occupancy by histone deacetylases is associated with T-box gene regulation in mammalian abdominal tissue. J Biol Chem 285: 11129-11142.
27. Bershadsky A, Chausovsky A, Becker E, Lyubimova A, Geiger B (1996) Involvement of microtubules in the control of adhesion-dependent signal transduction. Curr Biol 6: 1279-1289.
28. Gu J, Tamura M, Pankov R, Danen EH, Takino T, et al. (1999) Shc and FAK differentially regulate cell motility and directionality modulated by PTEN. Journal of Cell Biology 146: 389-403.
29. Gail M (1973) Time lapse studies on the motility of fibroblasts in tissue culture. Ciba Found Symp 14: 287-310.
30. Locascio A, Nieto MA (2001) Cell movements during vertebrate development: integrated tissue behaviour versus individual cell migration. Curr Opin Genet Dev 11: 464-469.
31. Carlier MF, Le Clainche C, Wiesner S, Pantaloni D (2003) Actin-based motility: from molecules to movement. Bioessays 25: 336-345.
32. Bandman E (1992) Contractile protein isoforms in muscle development. Dev Biol 154: 273-283.
33. Hayward LJ, Zhu YY, Schwartz RJ (1988) Cellular localization of muscle and nonmuscle actin mRNAs in chicken primary myogenic cultures: the induction of alpha-skeletal actin mRNA is regulated independently of alpha-cardiac actin gene expression. Journal of Cell Biology 106: 2077-2086.
34. Gunning PW, Ferguson V, Brennan KJ, Hardeman EC (2001) Alpha-skeletal actin induces a subset of muscle genes independently of muscle differentiation and withdrawal from the cell cycle. J Cell Sci 114: 513-524.
35. Jain MK, Kashiki S, Hsieh CM, Layne MD, Yet SF, et al. (1998) Embryonic expression suggests an important role for CRP2/SmLIM in the developing cardiovascular system. Circ Res 83: 980-985.
36. Lilly B, Clark KA, Yoshigi M, Pronovost S, Wu ML, et al. (2010) Loss of the serum response factor cofactor, cysteine-rich protein 1, attenuates neointima formation in the mouse. Arterioscler Thromb Vasc Biol 30: 694-701.
37. Wei Q, Adelstein RS (2002) Pitx2a expression alters actin-myosin cytoskeleton and migration of HeLa cells through Rho GTPase signaling. Molecular Biology of the Cell 13: 683-697.

38. Small JV, Geiger B, Kaverina I, Bershadsky A (2002) How do microtubules guide migrating cells? Nat Rev Mol Cell Biol 3: 957-964.
39. Blaxall BC, Spang R, Rockman HA, Koch WJ (2003) Differential myocardial gene expression in the development and rescue of murine heart failure. Physiol Genomics 15: 105-114.
40. Gertler FB, Niebuhr K, Reinhard M, Wehland J, Soriano P (1996) Mena, a relative of VASP and Drosophila Enabled, is implicated in the control of microfilament dynamics. Cell 87: 227-239.
41. Barzik M, Kotova TI, Higgs HN, Hazelwood L, Hanein D, et al. (2005) Ena/VASP proteins enhance actin polymerization in the presence of barbed end capping proteins. J Biol Chem 280: 28653-28662.
42. Mikhailov A, Gundersen GG (1998) Relationship between microtubule dynamics and lamellipodium formation revealed by direct imaging of microtubules in cells treated with nocodazole or taxol. Cell Motil Cytoskeleton 41: 325-340.
43. Al-Bassam J, Ozer RS, Safer D, Halpain S, Milligan RA (2002) MAP2 and tau bind longitudinally along the outer ridges of microtubule protofilaments. Journal of Cell Biology 157: 1187-1196.
44. Daub H, Gevaert K, Vandekerckhove J, Sobel A, Hall A (2001) Rac/Cdc42 and p65PAK regulate the microtubule-destabilizing protein stathmin through phosphorylation at serine 16. J Biol Chem 276: 1677-1680.
45. Jourdain L, Curmi P, Sobel A, Pantaloni D, Carlier MF (1997) Stathmin: a tubulin-sequestering protein which forms a ternary T2S complex with two tubulin molecules. Biochemistry 36: 10817-10821.
46. Bugnard E, Zaal KJ, Ralston E (2005) Reorganization of microtubule nucleation during muscle differentiation. Cell Motil Cytoskeleton 60: 1-13.
47. Takada F, Vander Woude DL, Tong HQ, Thompson TG, Watkins SC, et al. (2001) Myozenin: an alpha-actinin- and gamma-filamin-binding protein of skeletal muscle Z lines. Proc Natl Acad Sci U S A 98: 1595-1600.
48. Cox D, Brennan M, Moran N (2010) Integrins as therapeutic targets: lessons and opportunities. Nat Rev Drug Discov 9: 804-820.
49. Hynes RO (1992) Integrins: versatility, modulation, and signaling in cell adhesion. Cell 69: 11-25.
50. Disatnik MH, Rando TA (1999) Integrin-mediated muscle cell spreading. The role of protein kinase c in outside-in and inside-out signaling and evidence of integrin cross-talk. J Biol Chem 274: 32486-32492.
51. Kornberg L, Earp HS, Parsons JT, Schaller M, Juliano RL (1992) Cell adhesion or integrin clustering increases phosphorylation of a focal adhesion-associated tyrosine kinase. J Biol Chem 267: 23439-23442.
52. Kim CW, Goldberger OA, Gallo RL, Bernfield M (1994) Members of the syndecan family of heparan sulfate proteoglycans are expressed in distinct cell-, tissue-, and development-specific patterns. Molecular Biology of the Cell 5: 797-805.
53. Couchman JR (2003) Syndecans: proteoglycan regulators of cell-surface microdomains? Nat Rev Mol Cell Biol 4: 926-937.
54. Dovas A, Yoneda A, Couchman JR (2006) PKCbeta-dependent activation of RhoA by syndecan-4 during focal adhesion formation. J Cell Sci 119: 2837-2846.
55. Bass MD, Roach KA, Morgan MR, Mostafavi-Pour Z, Schoen T, et al. (2007) Syndecan-4-dependent Rac1 regulation determines directional migration in response to the extracellular matrix. Journal of Cell Biology 177: 527-538.
56. Howe AK, Baldor LC, Hogan BP (2005) Spatial regulation of the cAMP-dependent protein kinase during chemotactic cell migration. Proc Natl Acad Sci U S A 102: 14320-14325.

57. Feoktistov I, Goldstein AE, Biaggioni I (2000) Cyclic AMP and protein kinase A stimulate Cdc42: role of A(2) adenosine receptors in human mast cells. Mol Pharmacol 58: 903-910.
58. Arthur WT, Noren NK, Burridge K (2002) Regulation of Rho family GTPases by cell-cell and cell-matrix adhesion. Biol Res 35: 239-246.
59. Oude Weernink PA, Schmidt M, Jakobs KH (2004) Regulation and cellular roles of phosphoinositide 5-kinases. Eur J Pharmacol 500: 87-99.
60. Franco SJ, Huttenlocher A (2005) Regulating cell migration: calpains make the cut. J Cell Sci 118: 3829-3838.
61. Engleka KA, Gitler AD, Zhang M, Zhou DD, High FA, et al. (2005) Insertion of Cre into the Pax3 locus creates a new allele of Splotch and identifies unexpected Pax3 derivatives. Dev Biol 280: 396-406.
62. Mao X, Fujiwara Y, Chapdelaine A, Yang H, Orkin SH (2001) Activation of EGFP expression by Cre-mediated excision in a new ROSA26 reporter mouse strain. Blood 97: 324-326.
63. Kioussi C, Gross MK (2008) How to build transcriptional network models of mammalian pattern formation. PLoS One 3: e2179.
64. Edgar R, Domrachev M, Lash AE (2002) Gene Expression Omnibus: NCBI gene expression and hybridization array data repository. Nucleic Acids Res 30: 207-210.
65. Shannon P, Markiel A, Ozier O, Baliga NS, Wang JT, et al. (2003) Cytoscape: a software environment for integrated models of biomolecular interaction networks. Genome Res 13: 2498-2504.
66. Sassoon DA, Garner I, Buckingham M (1988) Transcripts of alpha-cardiac and alpha-skeletal actins are early markers for myogenesis in the mouse embryo. Development 104: 155-164.
67. Reinhard M, Jarchau T, Walter U (2001) Actin-based motility: stop and go with Ena/VASP proteins. Trends Biochem Sci 26: 243-249.
68. Kim E, Waters SH, Hake LE, Hecht NB (1989) Identification and developmental expression of a smooth-muscle gamma-actin in postmeiotic male germ cells of mice. Molecular and Cellular Biology 9: 1875-1881.
69. Jin L, Gan Q, Zieba BJ, Goicoechea SM, Owens GK, et al. (2010) The actin associated protein palladin is important for the early smooth muscle cell differentiation. PLoS One 5: e12823.
70. Dixson JD, Forstner MJ, Garcia DM (2003) The alpha-actinin gene family: a revised classification. J Mol Evol 56: 1-10.
71. Miyasaka KY, Kida YS, Sato T, Minami M, Ogura T (2007) Csrp1 regulates dynamic cell movements of the mesendoderm and cardiac mesoderm through interactions with Dishevelled and Diversin. Proc Natl Acad Sci U S A 104: 11274-11279.
72. Wang S, Yu WM, Zhang W, McCrae KR, Neel BG, et al. (2009) Noonan syndrome/leukemia-associated gain-of-function mutations in SHP-2 phosphatase (PTPN11) enhance cell migration and angiogenesis. J Biol Chem 284: 913-920.
73. Schevzov G, Fath T, Vrhovski B, Vlahovich N, Rajan S, et al. (2008) Divergent regulation of the sarcomere and the cytoskeleton. J Biol Chem 283: 275-283.
74. Hubberstey AV, Mottillo EP (2002) Cyclase-associated proteins: CAPacity for linking signal transduction and actin polymerization. FASEB J 16: 487-499.
75. Schmetsdorf S, Arnold E, Holzer M, Arendt T, Gartner U (2009) A putative role for cell cycle-related proteins in microtubule-based neuroplasticity. Eur J Neurosci 29: 1096-1107.
76. Kamath K, Oroudjev E, Jordan MA (2010) Determination of microtubule dynamic instability in living cells. Methods Cell Biol 97: 1-14.

77. Lee C, Scherr HM, Wallingford JB (2007) Shroom family proteins regulate gamma-tubulin distribution and microtubule architecture during epithelial cell shape change. Development 134: 1431-1441.
78. Lewis SA, Lee MG, Cowan NJ (1985) Five mouse tubulin isotypes and their regulated expression during development. Journal of Cell Biology 101: 852-861.
79. Wang D, Villasante A, Lewis SA, Cowan NJ (1986) The mammalian beta-tubulin repertoire: hematopoietic expression of a novel, heterologous beta-tubulin isotype. Journal of Cell Biology 103: 1903-1910.
80. Tachikawa K, Sasaki S, Maeda T, Nakajima K (2008) Identification of molecules preferentially expressed beneath the marginal zone in the developing cerebral cortex. Neurosci Res 60: 135-146.
81. Zilberman Y, Ballestrem C, Carramusa L, Mazitschek R, Khochbin S, et al. (2009) Regulation of microtubule dynamics by inhibition of the tubulin deacetylase HDAC6. J Cell Sci 122: 3531-3541.
82. Frey N, Richardson JA, Olson EN (2000) Calsarcins, a novel family of sarcomeric calcineurin-binding proteins. Proc Natl Acad Sci U S A 97: 14632-14637.
83. Leu SJ, Liu Y, Chen N, Chen CC, Lam SC, et al. (2003) Identification of a novel integrin alpha 6 beta 1 binding site in the angiogenic inducer CCN1 (CYR61). J Biol Chem 278: 33801-33808.
84. Jungers KA, Le Goff C, Somerville RP, Apte SS (2005) Adamts9 is widely expressed during mouse embryo development. Gene Expr Patterns 5: 609-617.
85. Hu M, Sun XJ, Zhang YL, Kuang Y, Hu CQ, et al. (2010) Histone H3 lysine 36 methyltransferase Hypb/Setd2 is required for embryonic vascular remodeling. Proc Natl Acad Sci U S A 107: 2956-2961.
86. Zhang HY, Timpl R, Sasaki T, Chu ML, Ekblom P (1996) Fibulin-1 and fibulin-2 expression during organogenesis in the developing mouse embryo. Dev Dyn 205: 348-364.
87. Gersdorff N, Muller M, Schall A, Miosge N (2006) Secreted modular calcium-binding protein-1 localization during mouse embryogenesis. Histochem Cell Biol 126: 705-712.
88. Nelson WJ, Lazarides E (1985) Posttranslational control of membrane-skeleton (ankyrin and alpha beta-spectrin) assembly in early myogenesis. Journal of Cell Biology 100: 1726-1735.
89. Nagae S, Tanoue T, Takeichi M (2007) Temporal and spatial expression profiles of the Fat3 protein, a giant cadherin molecule, during mouse development. Dev Dyn 236: 534-543.
90. Kawai J, Shinagawa A, Shibata K, Yoshino M, Itoh M, et al. (2001) Functional annotation of a full-length mouse cDNA collection. Nature 409: 685-690.
91. Sutherland AE, Sanderson RD, Mayes M, Seibert M, Calarco PG, et al. (1991) Expression of syndecan, a putative low affinity fibroblast growth factor receptor, in the early mouse embryo. Development 113: 339-351.
92. David G, Bai XM, Van der Schueren B, Marynen P, Cassiman JJ, et al. (1993) Spatial and temporal changes in the expression of fibroglycan (syndecan-2) during mouse embryonic development. Development 119: 841-854.
93. Yagami-Hiromasa T, Sato T, Kurisaki T, Kamijo K, Nabeshima Y, et al. (1995) A metalloprotease-disintegrin participating in myoblast fusion. Nature 377: 652-656.
94. Abreu JG, Ketpura NI, Reversade B, De Robertis EM (2002) Connective-tissue growth factor (CTGF) modulates cell signalling by BMP and TGF-beta. Nat Cell Biol 4: 599-604.
95. Saba JD, Hla T (2004) Point-counterpoint of sphingosine 1-phosphate metabolism. Circ Res 94: 724-734.

96. Mandicourt G, Iden S, Ebnet K, Aurrand-Lions M, Imhof BA (2007) JAM-C regulates tight junctions and integrin-mediated cell adhesion and migration. J Biol Chem 282: 1830-1837.
97. Holaska JM, Rais-Bahrami S, Wilson KL (2006) Lmo7 is an emerin-binding protein that regulates the transcription of emerin and many other muscle-relevant genes. Hum Mol Genet 15: 3459-3472.
98. Ruan K, Bao S, Ouyang G (2009) The multifaceted role of periostin in tumorigenesis. Cell Mol Life Sci 66: 2219-2230.
99. Garcia-Espana A, Chung PJ, Sarkar IN, Stiner E, Sun TT, et al. (2008) Appearance of new tetraspanin genes during vertebrate evolution. Genomics 91: 326-334.
100. Singh IS, Luo ZJ, Eng A, Erlichman J (1991) Molecular cloning and characterization of the promoter region of the mouse regulatory subunit RII beta of type II cAMP-dependent protein kinase. Biochem Biophys Res Commun 178: 221-226.
101. Dong LQ, Zhang RB, Langlais P, He H, Clark M, et al. (1999) Primary structure, tissue distribution, and expression of mouse phosphoinositide-dependent protein kinase-1, a protein kinase that phosphorylates and activates protein kinase Czeta. J Biol Chem 274: 8117-8122.

Chapter 2-Figure 1

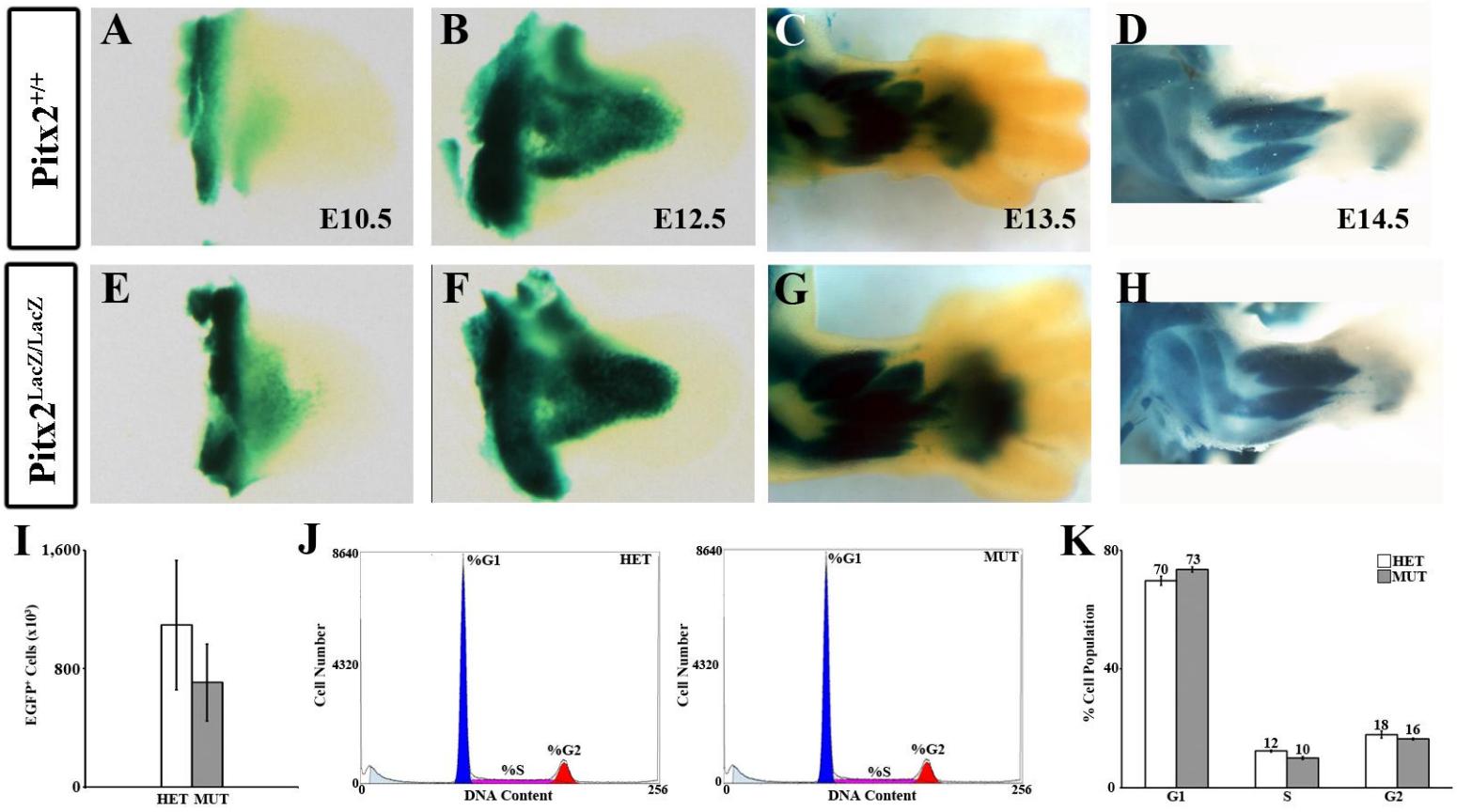

Figure 1. Regulation of Shape and Size of Limb Muscle Anlagen by Pitx2. (A-H) Whole mount X-gal staining of $Pitx2^{LacZ/+}$ and $Pitx2^{LacZ/LacZ}$ knock-in mice from E10.5 – E14.5. Pitx2 was expressed throughout muscle anlagen but not in epidermis, mesenchyme or bone anlagen. Most distal limb muscle anlagen were mildly deformed. Muscle groups are outlined. **(I)** Percentage of $EGFP^{+}$ cells collected from $Pax3^{Cre}|ROSA^{EGFP}|Pitx2^{LacZ/+}$ (HET) and $Pax3^{Cre}|ROSA^{EGFP}|Pitx2^{LacZ/LacZ}$ (MUT) embryos at E12.5 forelimb tissue dissociated into single cell suspension. The percentage of $EGFP^{+}$ cells had a mean ± standard error of the mean (SEM) of 17 ± 0.6% for HET (n = 8) and 11 ± 1% for MUT (n = 7). This 26% reduction in $EGFP^{+}$ cells in the MUT forelimb was considered to be significant using unpaired t-test with a p-value = 0.0001. **(J)** Example histograms of propidium iodide (PI) staining of HET and MUT $EGFP^{+}$ cells isolated from forelimb tissue at E12.5. **(K)** Results of cell cycle analysis using PI staining showing distribution (mean ± SEM) of the $EGFP^{+}$ cell population between HET (n = 5) and MUT (n = 4) during G1 (69 ± 0.007% HET, 74 ± 0.009% MUT); S (18 ± 0.005% HET, 17 ± 0.006% MUT); and G2 (13 ± 0.003% HET, 9 ± 0.015%MUT) phases. The increase in MUT cells during G1 phase was determined to be significant using unpaired t-test with a p-value = 0.0102.

Chapter 2-Figure 2

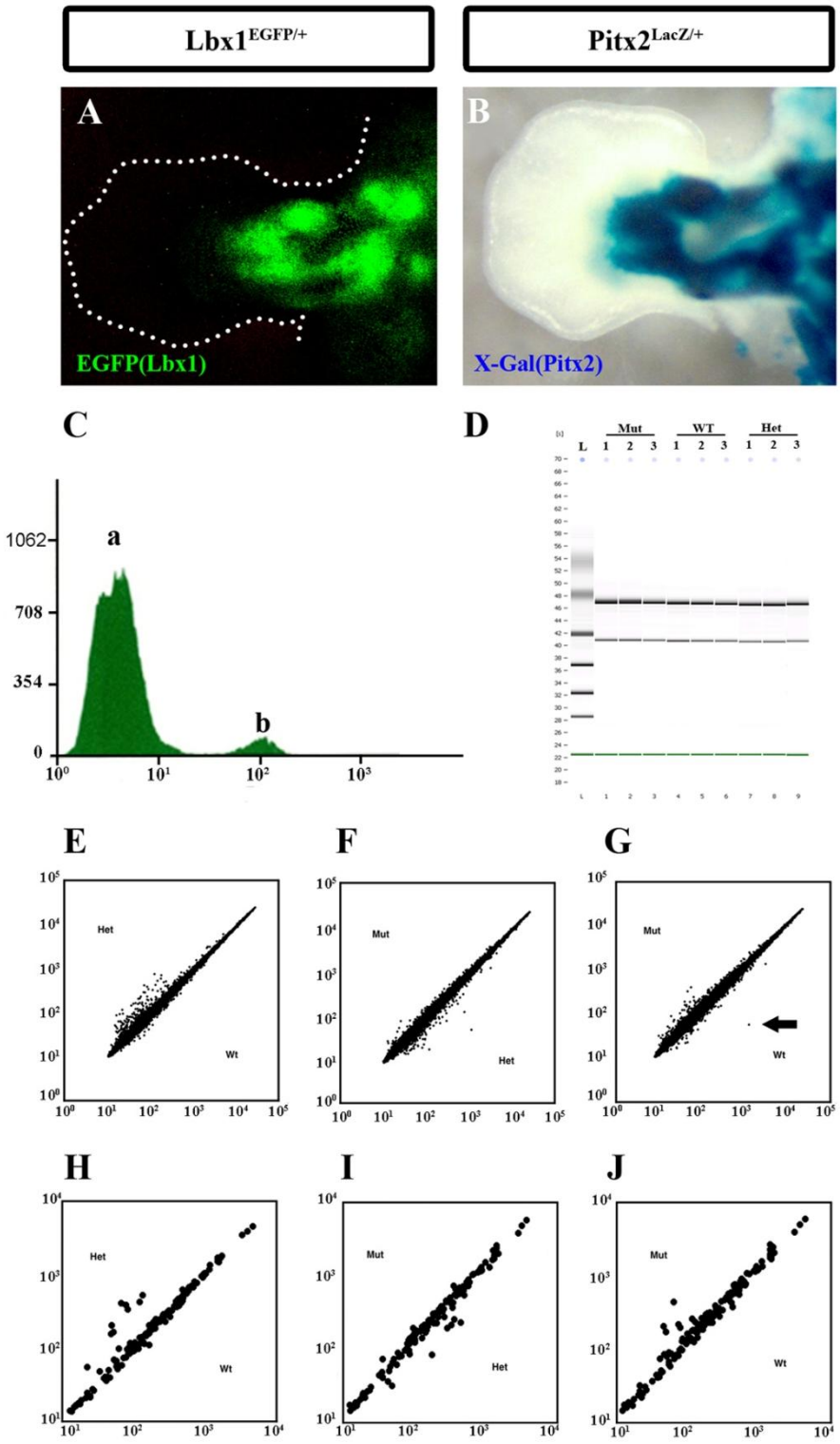

Figure 2. Flow-Sorting EGFP^{+} MMP Cells from Forelimbs. (A) EGFP indicating Lbx1 expression in Lbx1$^{EGFP/+}$ E12.5 mouse. **(B)** Immunohistochemistry of cross-sectioned Lbx1$^{EGFP/+}$|Pitx2$^{LacZ/+}$ E12.5 mouse forelimb. beta-Gal(Pitx2) and Lbx1(EGFP) are co-localized in the flexor and extensor muscle groups. **(C)** FACS analysis of sorted Lbx1$^{EGFP/+}$ cells. The automated multiwell plating function on the MoFlo was used to test a variety of substrate and media at systematically controlled plating densities. Cells were sorted at a rate of 10,000 cells/sec with a purity of 95-99+%, depending on the stringency of gating. Cell number (Y axis, log scale) vs. florescence intensity (X axis, FL1) plot. The “a” peak represented EGFP^{-} cell population, and the “b” peak represented the GFP^{+} cell population. The GFP^{+} population represents 5-7% of the total limb bud cellular pool. **(D)** RNA samples were quantified and ran on an Agilent Bioanalyser 2100 to assess RNA quality prior to microarray analysis. **(E)** Comparison of expression of total RNA from HET (y axis) vs. WT (y axis). Each dot in both axes represents relative RNA expression levels for an individual gene in WT vs. HET respectively. If a dot is perfectly located in the diagonal line, then the relative gene expression level for the representing gene exhibits no difference within HET and WT. **(F)** Comparison of expression of total RNA from MUT (y axis) vs. WT (x axis). Each dot in both axes represents relative RNA expression levels for an individual gene in MUT vs. WT respectively. **(G)** Comparison of expression of total RNA from MUT (y axis) vs. HET (x axis). Each dot in both axes represents relative RNA expression levels for an individual gene in MUT vs. HET respectively. Pitx2 expression levels were indicated by arrow. Pitx2 was strongly down regulated in the Pitx2 mutants. Comparison of expression of total RNA of genes from Table 1 of HET (y axis) vs. WT (x axis) **(H)**, MUT (y axis) vs. WT (x axis) **(I)**, MUT (y axis) vs. HET (x axis) **(J)**.

Chapter 2-Figure 3

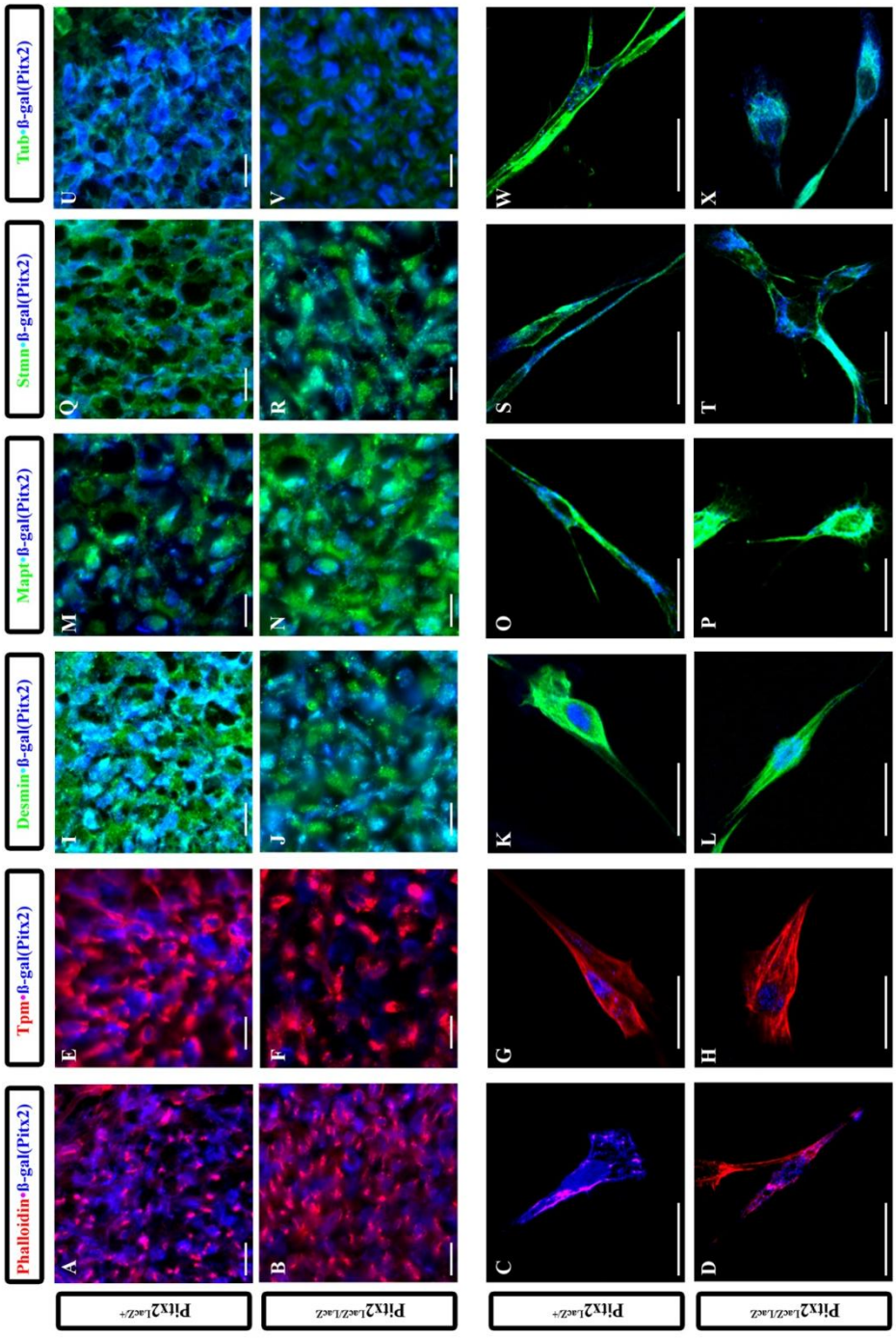

Figure 3. Increased Actin Bundling and Presence of Tau and Stathmin in Pitx2 Mutant Myogenic Cells. Immunostaining for Phalloidin (F-Actin) and beta-Gal(Pitx2) **(A-D)**, tropomyosin and beta-Gal(Pitx2) **(E-H)** desmin (Intermediate Filament) and beta-Gal(Pitx2) **(I-L)** on $Pitx2^{LacZ/+}$, Mapt (Tau) and beta-Gal(Pitx2) **(M-P)**, stathmin (stmn) and beta-Gal(Pitx2) **(Q-T)**, and tubulin (tub) and beta-Gal(Pitx2) **(U-X)** on $Pitx2^{LacZ/+}$. The F-actin, tropomyosin and desmin labeled fibers in cells in the MUT forelimbs were not aligned and cluster together as in the HET. MUT myogenic cells failed to develop protrusions, connect and align to each other. Mapt and stmn were highly expressed in forelimb tissue and myogenic primary cultured cells. Mapt, stmn and tub expression levels were increased in both tissue and primary myogenic cells cultures. Arrows denote points of interest between genotypes. White bar denotes 50 micrometer.

Chapter 2-Figure 4

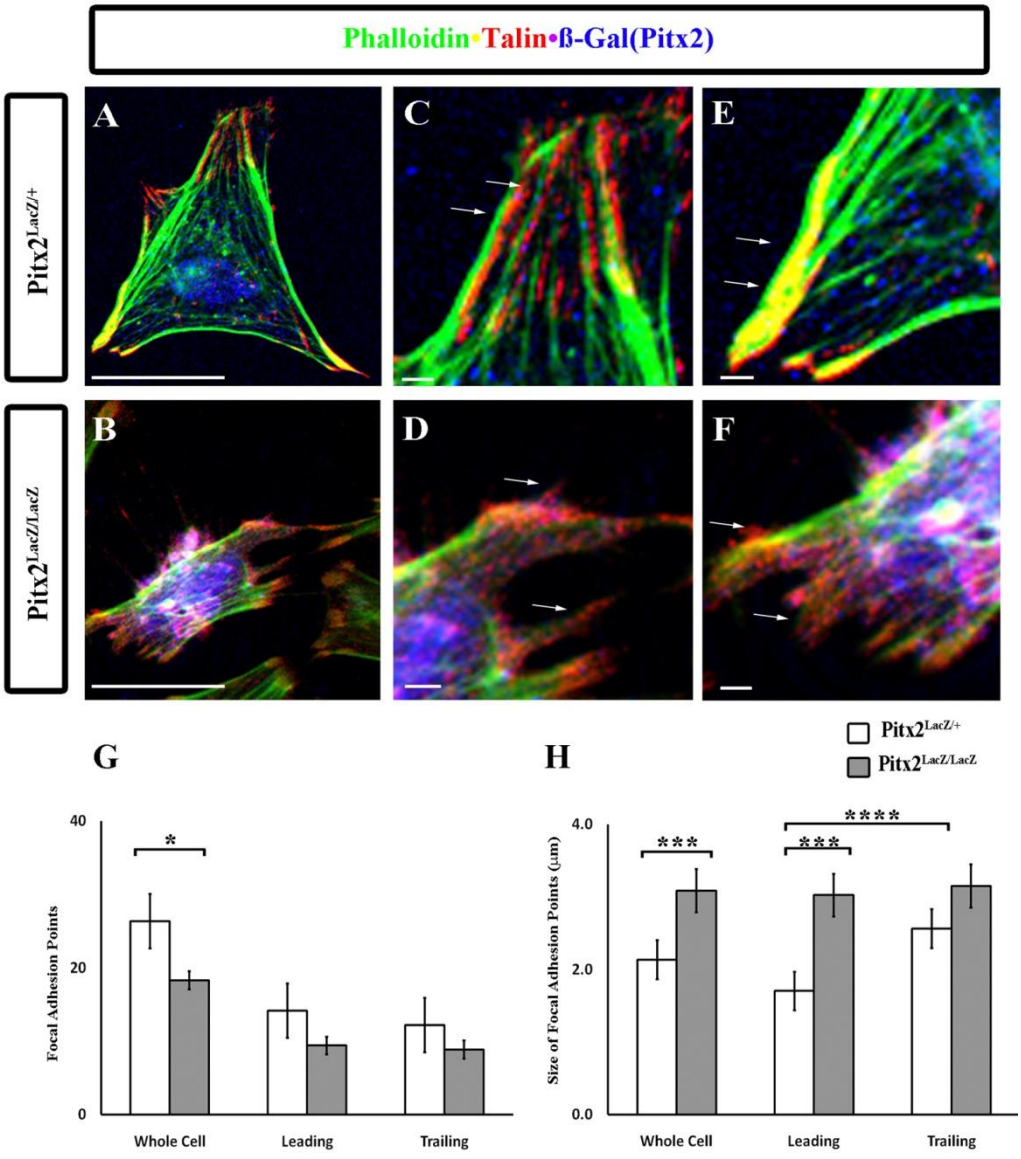

Figure 4. Altered Focal Adhesion in Pitx2 Mutant Myogenic Cells. Muscle progenitor cells were isolated from E12.5 forelimb tissue of $Pitx2^{LacZ/+}$ **(A, C, E)** and $Pitx2^{LacZ/LacZ}$ **(B, D, F)** mice. Cells were stained with alexa 488 phalloidin, (F-actin), talin (focal adhesions) and beta-Gal(Pitx2) **(A-F)**. **(G)** Myogenic cells had a mean ± standard error of the mean (SEM) of 26 ± 4 (total = 475) for HET and 18 ± 1 (total = 330) for MUT of focal adhesions per cell (n = 18). This difference in mean focal adhesion number was determined statistically significant using a two-tailed unpaired t-test (p = 0.0464). The distribution of the number focal adhesions between the leading and trailing edges of the muscle progenitor cells was not affected; the leading edges had an mean ± SEM of 14 ± 2 (total = 255) for HET and 9 ± 1 (total = 170) for MUT cells, while at the trailing edges had means ± SEM of 12 ± 2 (total = 220) for HET and 9 ± 1 (total = 160) for MUT cells. Neither of the differences of focal adhesion number at leading or trailing edges between HET and MUT cells were determined statistically significant using two tailed unpaired t-test (p = 0.05 and p = 0.0848, respectively). While differences between the leading and trailing edges within HET or MUT cells were also determined not statistically significant using two tailed paired t-test (p = 0.219 and p = 0.355). **(H)** The size of focal adhesions had an mean size ± SEM of 2.14 ± 0.27 micrometer in HET and 3.09 ± 0.3 micrometer in MUT cells. This difference in focal adhesion size was determined to be very statically significant using two-tailed unpaired t-test (p = 0.0013). The mean size ± SEM of focal adhesions at the leading edge was 1.70 ± 0.24 micrometer for HET and 3.03 ± 0.3 micrometer for MUT, while at the trailing edge the mean size ± SEM was 2.57 ± 0.26 micrometer for HET and 3.15 ± 0.3 micrometer for MUT. The mean focal adhesion size at the leading edge between HET and MUT cells were determined to be very statistically significantly different using unpaired two tailed t-test (p-value = 0.0016). When comparing leading and trailing focal adhesion size within HET cells there is a statistically significant difference in mean size two-tailed paired t-test (p-value = 0.001). Comparing mean focal adhesion size between leading and trailing edges within MUT cells showed no statistically significant difference using two tailed paired t-test (p = 0.1325). White bar denotes 50 micrometer.

Chapter 2-Figure 5

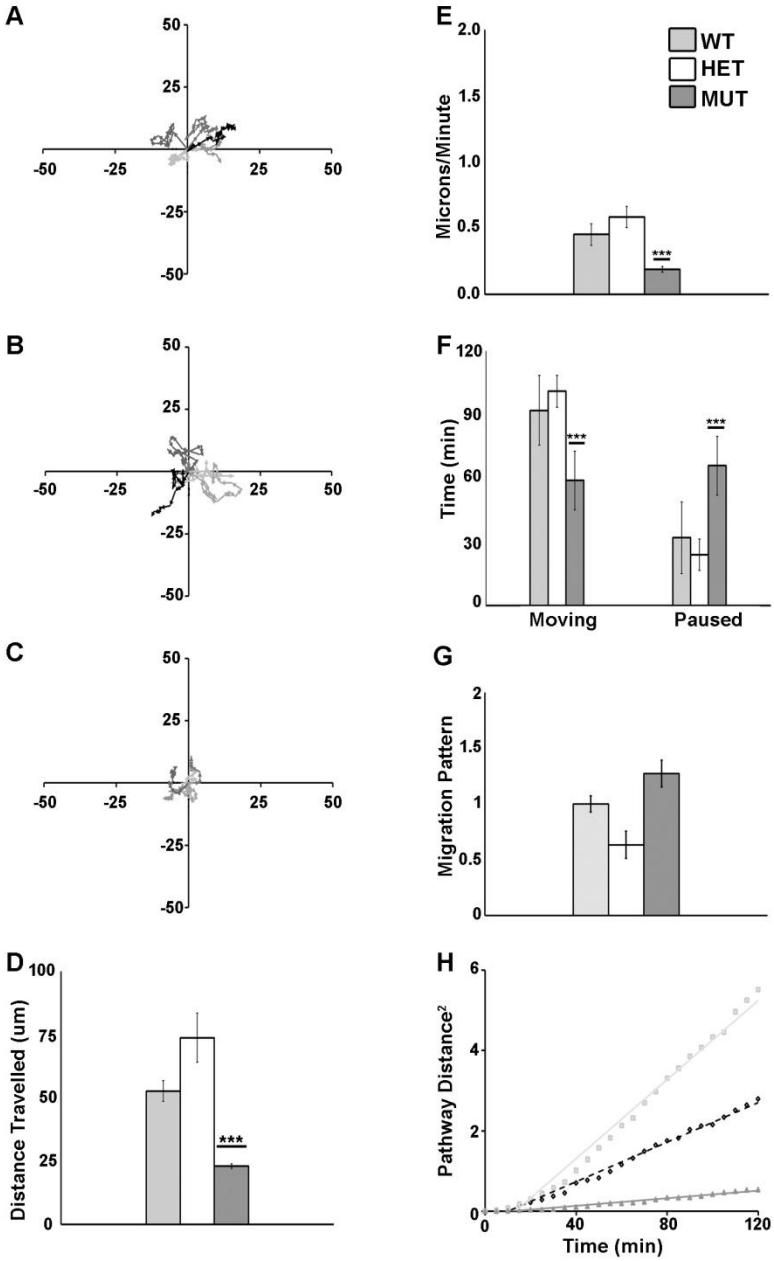

Figure 5. Motility Defects in Lbx1^{+} Myogenic Cells in Pitx2 Mutants. Live cell tracking assay of migratory muscle progenitors (n=5) isolated from forelimb tissue of E12.5 Lbx1$^{EGFP/+}$|Pitx2$^{+/+}$ (WT), Lbx1$^{EGFP/+}$|Pitx2$^{LacZ/+}$ (HET), or Lbx1$^{EGFP/+}$|Pitx2$^{LacZ/LacZ}$ (MUT) embryos. Migration pathway of migratory muscle progenitors over a 2 hour period for WT **(A)**, HET **(B)**, MUT **(C)**. **(D)** Mean total distance travelled of WT (53 ± 4 micrometer), HET (74 ± 10 micrometer), and MUT (23 ± 1 micrometer). **(E)** Mean velocity of movement of WT (0.5 ± 0.1 micrometer/min), HET (0.6 ± 0.1 micrometer/min) and MUT (0.2 ± 0.02 micrometer/min). **(F)** Mean time spent moving vs. paused for WT moving (92 ± 16.4 min) and paused (32 ± 16.8 min), HET moving (101 ± 7.4 min) and paused (24 ± 7.4 min) and MUT moving (59 ± 14 min) and paused (66 ± 14 min). Using Dunnett's ANOVA test setting WT as control, the MUT MMPs were found to be significantly different in distance travelled, velocity, and time moving vs. paused. Following Dunnett's ANOVA an unpaired T-test between WT and MT determined significance values for distance traveled (p=0.0001), velocity (p=0.0001), time moving (p=0.0089) and time paused (p=0.0082). **(G)** Quantitation of persistent migratory directionality. Relative ratios of direct distance from start point to end point (D) divided by the total pathway distance traveled (T), ratios expressed as relative to WT (value set = 1.0). The MMPs from HET had a ratio of 63% and MUT MMPs had a ratio of 127%. **(H)** The mean square displacement of total pathway distance traveled (T^2) measured every 20 min. The x-intercept HET (diamonds, black dotted line) and WT (light grey squares, solid light grey line) cells were as close to the origin as the intercept for MUT (dark grey triangles, solid dark grey line), indicating that cells from all genotypes exhibit similar migration behaviors.

Chapter 2-Figure 6

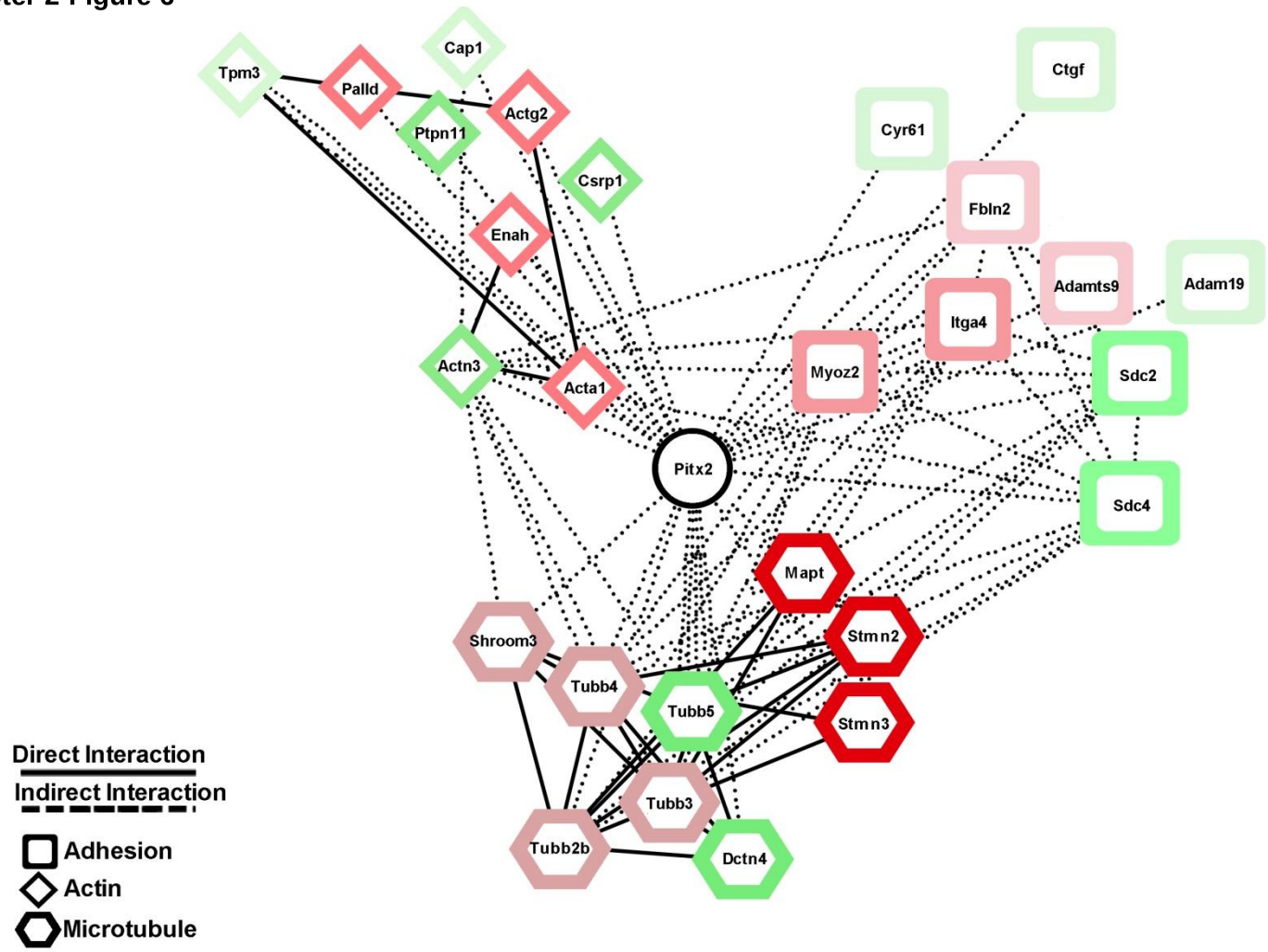

Figure 6. Pitx2-Mediated Myogenic Cell Gene Network During Filling Limb Muscle Anlagen. The network displays ten genes with the greatest fold change from each of the three groups; actin (diamonds), microtubule (octagons) and adhesion (squares) related genes. Color intensity is representative of reported fold change based on their gene expression analysis (Table 1), with darker color representing larger fold change. Connections between the nodes are displayed as solid lines for direct interactions and dashed lines for possible interactions.

Table 2.1

Pitx2 Target Genes In Forelimb Migratory Muscle Progenitor Cell Lineage

Name	Transcript	Gene	WT	HET	MUT	Δ Fold	Function	Bibliography
Actin Related Genes								
[1,2]Actin alpha 1	NM_009606	**Acta1**	1449±107	1544±349	2486±230	1.8	monomer	[66]
[2]Enabled homolog (*Drosophila*)	NM_001008493	**Enah**	133±8	153±1	194±111	1.5	organization	[67]
[2]Actin γ2	NM_009610	**Actg2**	96±23	113±14	129±27	1.3	monomer	[68]
[1,2]Palladin	NM_001166108	**Palld**	294±21	352±23	376±113	1.3	organization	[69]
[2]Actinin alpha 3	NM_01104	**Actn3**	1123±256	1017±88	650±17	-1.7	binding	[70]
[1]Cysteine and glycine-rich protein 1	NM_001193570	**Csrp1**	819±174	820±52	526±94	-1.6	dynamics	[71]
Protein tyrosine phosphatase	NM_001109992	**Ptpn11**	119±7	106±16	87±16	-1.4	dynamics	[72]
Tropomyosin 3	NM_001043351	**Tpm3**	192±43	196±18	155±29	-1.2	dynamics	[73]
Adenylate cyclase-associated protein 1	NM_001105530	**Cap1**	1253±274	1257±293	1031±338	-1.2	stability	[74]

1 Indicates one of the three array sets was inconsistent with the other two, expression means and range was calculated using only the two consistent arrays.
2 Member of the adhesome

Table 2.1 (Continued)

Pitx2 Target Genes In Forelimb Migratory Muscle Progenitor Cell Lineage

Name	Transcript	Gene	WT	HET	MUT	Δ Fold	Function	Bibliography
Microtubule Related Genes								
[1]Microtubule-associated protein tau	NM_001123066	**Mapt**	44 ± 3	51 ± 13	265 ± 144	5.8	dynamics	[75]
[1]Stathmin-like 2	NM_007029	**Stmn2**	32 ± 14	26 ± 2	131 ± 32	4.0	dynamics	[76]
[1]Stathmin-like 3	NM_009133	**Stmn3**	71 ± 2	62 ± 21	236 ± 106	3.3	dynamics	[76]
Shroom family member 3	NM_001077595	**Shroom3**	396 ± 54	438 ± 39	501 ± 61	1.3	dynamics	[77]
[2]Tubulin beta 4	NM_009451	**Tubb4**	130 ± 56	141 ± 84	165 ± 29	1.3	monomer	[78]
[1,2]Tubulin beta 3	NM_023279.2	**Tubb3**	170 ± 61	113 ± 11	216 ± 93	1.3	monomer	[79]
[1,2]Tubulin beta 2b	NM_23716	**Tubb2b**	2216 ± 312	2504 ± 198	2766 ± 426	1.3	monomer	[80]
[1,2]Tubulin beta 5	NM_011655	**Tubb5**	2079 ± 91	1670 ± 66	1460 ± 45	-1.4	monomer	[78]
Dynactin 4	NM_026302	**Dctn4**	129 ± 13	122 ± 31	94 ± 45	-1.4	dynamics	[81]

1 Indicates one of the three array sets was inconsistent with the other two, expression means and range was calculated using only the two consistent arrays.
2 Member of the adhesome

Table 2.1 (Continued)

Pitx2 Target Genes In Forelimb Migratory Muscle Progenitor Cell Lineage

Name	Transcript	Gene	WT	HET	MUT	Δ Fold	Function	Bibliography
Adhesion Related Genes								
[1]Myozenin 2	NM_021503	**Myoz2**	189 ± 11	211 ± 35	319 ± 69	1.7	adhesion	[82]
[1,2]Integrin alpha 4	NM_010576	**Itga4**	1985 ± 261	2180 ± 427	2920 ± 663	1.5	adhesion	[83]
[1,2]A disintegrin-like and metallopeptidase with thrombospondin type 1 motif 9	NM_175314	**Adamts9**	169 ± 92	167 ± 32	239 ± 63	1.4	adhesion	[84]
[1]Cysteine rich protein 61	NM_010516	**Cyr61**	521 ± 22	542 ± 6	732 ± 183	1.4	adhesion	[85]
[1]Fibulin 2	NM_001081437	**Fbln2**	372 ± 167	357 ± 23	467 ± 16	1.4	adhesion	[86]
SPARC related modular Ca-binding 1	NM_001146217	**Smoc1**	261 ± 27	282 ± 40	347 ± 40	1.3	adhesion	[87]
[1]Spectrin beta 2	NM_009260	**Spnb2**	123 ± 1	147 ± 11	162 ± 67	1.3	adhesion	[88]
[1]FAT tumor suppressor homolog 3	NM_001080814	**Fat3**	441 ± 55	466 ± 8	578 ± 72	1.3	adhesion	[89]
[2]Ring finger protein 165	NM_001164504.1	**Rnf165**	124 ± 20	152 ± 42	160 ± 16	1.3	adhesion	[90]

1 Indicates one of the three array sets was inconsistent with the other two, expression means and range was calculated using only the two consistent arrays.
2 Member of the adhesome

Table 2.1 (Continued)

Pitx2 Target Genes In Forelimb Migratory Muscle Progenitor Cell Lineage

Name	Transcript	Gene	WT	HET	MUT	Δ Fold	Function	Bibliography
Adhesion Related Genes								
[1,2]Syndecan 4	NM_011521	**Sdc4**	188 ± 15	200 ± 5	127 ± 29	-1.5	ECM reorganization	[91]
[1,2]Syndecan 2	NM_008304	**Sdc2**	360 ± 42	404 ± 61	251 ± 37	-1.4	ECM reorganization	[92]
[2]A disintegrin-like and metallopeptidase domain 19	NM_175506	**Adam19**	250 ± 24	222 ± 14	192 ± 0	-1.3	adhesion	[93]
[1]Connective tissue growth factor	NM_010217	**Ctgf**	158 ± 44	198 ± 87	104 ± 22	-1.3	adhesion	[94]
Sphingosine-1 phosphate phosphatase 1	NM_030750	**Sgpp1**	169 ± 43	145 ± 6	128 ± 33	-1.3	adhesion	[95]
[1]Junction adhesion molecule 3	NM_023277	**Jam3**	1258 ± 137	1197 ± 55	959 ± 38	-1.3	adhesion	[96]
Lim domain only 7	NM_201529	**Lmo7**	180 ± 96	158 ± 56	141 ± 57	-1.3	adhesion	[97]
[1]Periostin	NM_001198765	**Postn**	2110 ± 186	1722 ± 28	1625 ± 77	-1.3	adhesion	[98]
[2]Tetraspanin 33	NM_146173	**Tspan33**	367 ± 133	375 ± 30	300 ± 23	-1.2	adhesion	[99]

1 Indicates one of the three array sets was inconsistent with the other two, expression means and range was calculated using only the two consistent arrays.
2 Member of the adhesome

Table 2.1 (Continued)

Pitx2 Target Genes In Forelimb Migratory Muscle Progenitor Cell Lineage

Name	Transcript	Gene	WT	HET	MUT	Δ Fold	Function	Bibliography
Signaling Related Genes								
[1,2]Protein kinase, cAMP dependent regulatory, type II beta	NM_011158	**Prkar2b**	118 ± 9	137 ± 58	185 ± 15	1.6	cAMP regulation	[100]
1,23-phosphoinositide dependent protein kinase 1	NM_001080773	**Pdpk1**	632 ± 127	356 ± 34	293 ± 114	-2.2	protein kinase activity	[101]

1 Indicates one of the three array sets was inconsistent with the other two, expression means and range was calculated using only the two consistent arrays.
2 Member of the adhesome

Supplementary Information

Chapter 2-Supplementary Figure 1

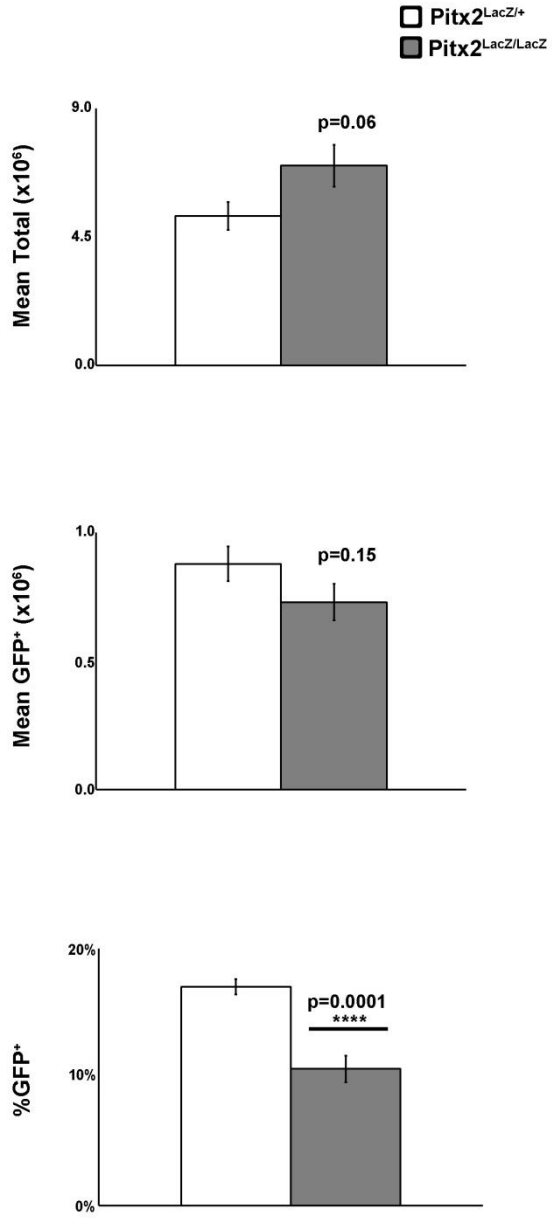

Supplementary Figure 1. Decrease in Number of EGFP^{+} cells in Pitx2 Mutant Forelimbs. Flow cytometry of dissociated forelimb tissue isolated from E12.5 Pax3$^{cre/+}$|ROSA^{EGFP}|Pitx2$^{LacZ/+}$ (HET, n = 8) and Pax3$^{cre/+}$|ROSA^{EGFP}|Pitx2$^{LacZ/LacZ}$ (MUT, n = 7) embryos **(A)** Mean (± SEM) number of cells (EGFP^{+} and EGPF^{-} cells combined) from HET tissue was 5,237,143 ± 482,445 cells and MUT tissue was 6,994,000 ± 731,302 cells. **(B)** Mean number of EGFP^{+} cells collected from HET tissue was 877,808 ± 67,469 cells and MUT tissue was 729,630 ± 70,855 cells at a purity of >90%. **(C)** Mean percent of EGFP^{+} cells present in HET forelimb tissue was 17 ± 0.6% and 11 ± 1% in MUT forelimb tissue. This reduced mean percent EGFP+ cells was determined to be significant using unpaired t-test, p = 0.0001.

Chapter 2-Supplementary Figure 2

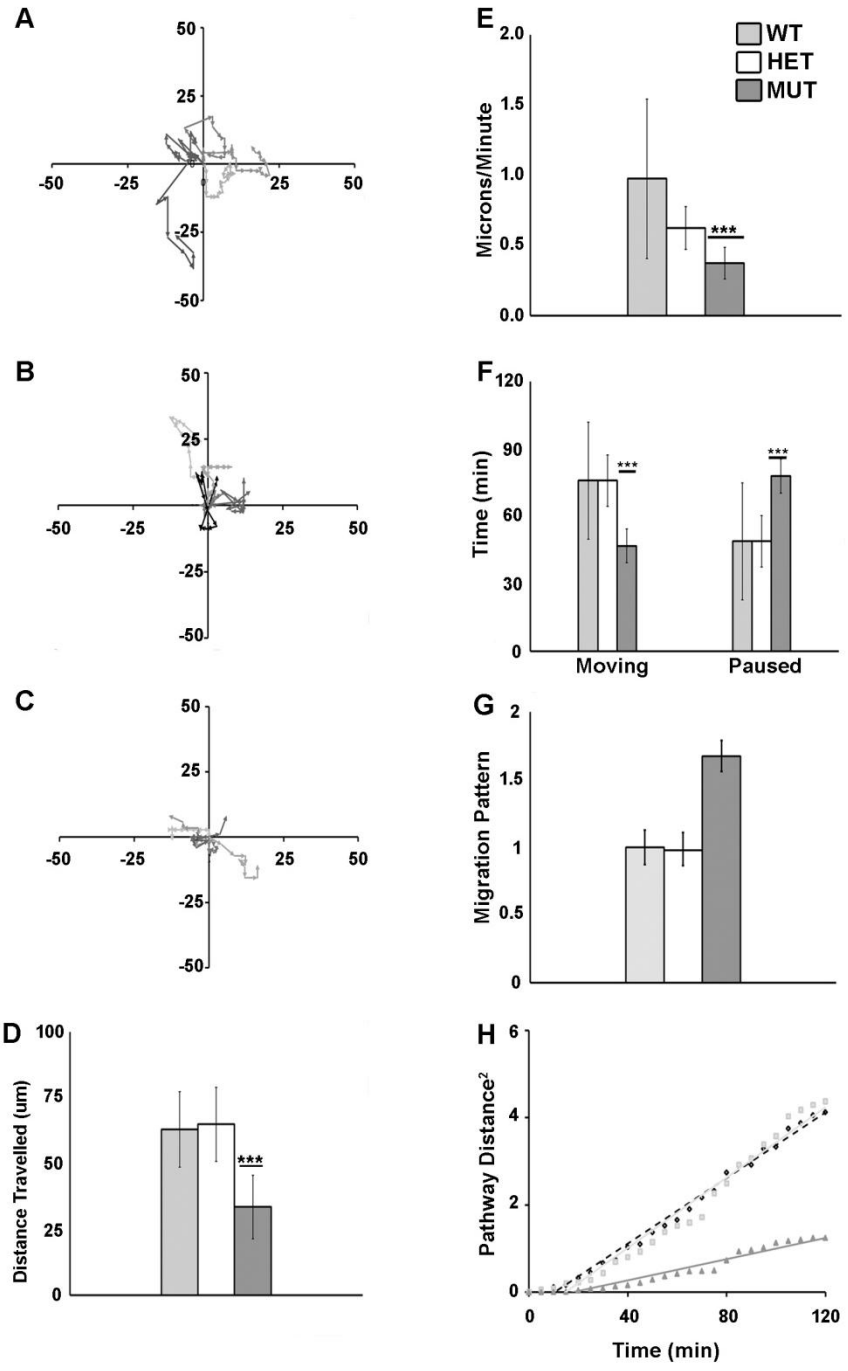

Supplementary Figure 2. Motility Defects in Pax3^{+} Myogenic Cells in Pitx2 Mutants. Live cell tracking assay of muscle progenitors (n=5) isolated from E12.5 forelimb tissue of Pax3$^{cre/+}$|ROSA^{EGFP}|Pitx2$^{+/+}$ (WT), Pax3$^{cre/+}$|ROSA^{EGFP}|Pitx2$^{LacZ/+}$ (HET), or Pax3$^{cre/+}$|ROSA^{EGFP}|Pitx2$^{LacZ/LacZ}$ (MUT) embryos. Migration pathways recorded for WT **(A)**, HET **(B)** and MUT **(C)**. **(D)** Mean total distance travelled of WT (63 ± 14 micrometer), HET (65 ± 14 micrometer) and MUT (34 ± 12 micrometer). **(E)** Mean velocity of movement of WT (1.0 ± 0.6 micrometer/min), HET (0.6 ± 0.2 micrometer/min) and MUT (0.4 ± 0.1 micrometer). **(F)** Mean time spent moving vs. paused for WT moving (76 ± 26 min) and paused (49 ± 26 min), HET moving (76 ± 26 min) and paused (49 ± 26 min) and MUT moving (47 ± 8 min) and paused (78 ± 8 min). Using Dunnett's ANOVA test setting WT as control, MUT MMPs were found to be significantly different in distance travelled, velocity, and time moving vs. paused**.** Following Dunnett's ANOVA an unpaired T-test between WT and MT determined significance values for distance traveled (p=0.008), velocity (p=0.0479), time moving (p=0.044) and time paused (p=0.044). **(G)** Quantitation of persistent migratory directionality. Relative ratios of D/T showed that HET cells had a ratio of 98% and MUT cells had a ratio of 167%. **(H)** The mean square displacement of total pathway distance traveled (T^2) measured every 20 min. The x-intercept for WT (diamonds, black dotted line) and HET (light grey squares, solid light grey line) cells were as close to the origin than the x-intercept for MUT (dark grey triangles, solid dark grey line) cells, indicating that cells from all genotypes exhibit similar migration behaviors.

Myoblast Fusion is Promoted by the Homeodomain Transcription Factor Pitx2

Chapter 3

Adam Campbell and Chrissa Kioussi

Formatted for submission to Developmental Biology

May 15, 2012

INTRODUCTION

The growth, repair and regeneration of muscle depend on a series of orderly cellular events comprising of proliferation, migration, committed differentiation, renewal and fusion of myoblasts. This process facilitates the withdrawal from the cell cycle, initiates the expression of myogenic specific genes, and the formation of multinucleated fibers. Myofibers increase in size through the subsequent fusion of myoblasts to the growing myofiber and start to express contractile proteins. Myofiber size and diameter has functional consequences in contractile strength of the adult tissue [1]. Myoblasts recognize and adhere to each other during myotube formation. Following recognition, the myoblasts align themselves into parallel arrays and fuse their plasma membranes to existing myotube or neighboring myoblast resulting in an elongated multinucleated cell.

The mechanisms involved in myoblast recognition, fusion, and myotube elongation are not completely understood. What has been elucidated is that when myoblasts are in close proximity cell-cell contacts made through transmembrane proteins (cadherins (N- and M-), integrins, IgG, etc.) activate intracellular signaling pathways. Signaling through these transmembrane proteins leads to the activation of beta-catenin and alpha-catenin which leads to cell cycle withdrawal, the expression of muscle specific proteins, and formation of actin cytoskeleton complexes at the membrane interfaces [2,3]. Simultaneously, they are activated and this leads to the activation of the GTPase, Cdc42, Rac1, and RhoA which in turn leads to the expression of muscle genes and accumulation of actin cytoskeleton complexes at the membrane interfaces [3,4,5,6,7]. The formation of the actin complexes at the sites of membrane interfaces provides mechanical force to facilitate union of the 2 membranes. Also,

at these membrane interface sites endocytic membrane recycling proteins, myoferlin and dysferilin, accumulate and align across the dual membrane within each cell. The endocytic vesicles then begin the dissolution of the dual membranes and allow for formation of a single continuous membrane [8,9].

The bicoid–related homeobox gene Pitx2 is expressed in the lateral plate mesoderm and in muscle anlagen in all stages of myogenic progression [10,11]. Pitx2 contributes to the establishment of network kernels that specify pre-myogenic progenitors for extraocular and mastication muscles [12]. Ablation of Pitx2 causes lethality in the mouse at E10.5-E14.5 with axial malformations, open body wall, heart defects, and arrest of organ development [13,14,15,16]. Pitx2 is positioned downstream of both Wnt and growth factor signaling pathways in skeletal myogenesis and promotes muscle progenitor proliferation by direct regulation of the expression of a number of cyclin-dependent kinases [17]. Analysis of $Lbx1^{EGFP}$ muscle progenitor cells isolated from forelimb tissue of $Pitx2^{LacZ/LacZ}$ mice at E12.5 has revealed that a small group of cytoskeletal, adhesion, and signaling genes are potential targets for regulation by Pitx2. Muscle progenitors of $Pitx2^{LacZ/LacZ}$ were smaller, more symmetrical, had increased actin bundling, and decreased motility preventing myogenic cells from filling limb bud anlagen [18].

In this study we address the role of Pitx2 in regulating myoblast fusion and its effects on the formation of multinucleated myotubes. Using information from microarray data $Lbx1^{EGFP}$ muscle precursors isolated from wild type and Pitx2 ablated mice, we identify several genes known to regulate myoblast recognition, adhesion and fusion. We over expressed Pitx2 in C2C12 cells as our model system to study myoblast behavior and observed that Pitx2 was capable to

decrease myoblast proliferation, promote migration, increase the number of nuclei in myofibers and enhance the alignment of myotubes into parallel arrays. These data identify Pitx2 as an important regulator for the formation and arrangement of myofibers important for skeletal muscle development, growth and regeneration.

MATERIALS AND METHODS

Cell Growth and Differentiation Conditions: C2C12 cells were maintained in growth media + 250 µg/ml G418 (DMEM/F12 [Gibco; Carlsbad, CA USA], 2.5 mM Glutamine [Hyclone; Rockford, IL USA], 10% FBS, 50 U/ml Pen/Strep [Cellgro; Manassas, VA USA], 0.25 µg/ml Fungizone [Invitrogen; Carlsbad, CA USA], and 250 µg/ml G418 [Invitrogen; Carlsbad, CA USA] in incubator 37 °C, 90% humidity, 5% CO2 and media was changed every 2-3 days. For differentiation, cells were grown to 90% confluence and media was changed to differentiation media + 250 µg/ml G418 (DMEM/F12 [Gibco; Carlsbad, CA USA], 2.5 mM Glutamine [Hyclone; Rockford, IL USA], 2% horse serum, 50 U/ml Pen/Strep [Cellgro; Manassas, VA USA], 0.25 µg/ml Fungizone [Invitrogen; Carlsbad, CA USA], and 250 µg/ml G418 [Invitrogen; Carlsbad, CA USA] and changed daily.

C2C12 Transfection: C2C12 cells were transfected using Neon transfection system [Invitrogen; Carlsbad, CA USA] according to manufacturer's protocol. Briefly, C2C12 cells were grown to 90% confluence in growth media and then trypsinized. Cells were centrifuged and washed several times with PBS (Ca^{2+}/Mg^{2+} Free). Cells were resuspended to a density of $1x10^7$ cells/ml with resuspension buffer and electroporated with 3 µg plasmid DNA using the following parameters: pulse voltage = 1650 v, pulse width = 10 ms, pulse number = 3. Cells were then seeded into 6-well tissue culture plates in growth media without antibiotics or G418 overnight in humidified incubator at 37 °C, 5% CO2. The subsequent day the media was changed growth media with antibiotics and G418.

Single Clone Selection: When transfected cells reached 90% confluence; single clones were generated using dilution method using a 96-well tissue culture plate. Cells were serial diluted 1:2 from 4000 cells/well to 1 cell/well. Cells were maintained in growth media in humidified incubator 37 °C, 5% CO2 changing media every 48 hrs. Cell growth in wells that were initially seeded with less than 4 cells was assumed to arise from single cells.

Cell Cycle Analysis: C2C12 cells were grown to 90% confluence, trypsinized, and centrifuged at 300 x g for 5 min. The supernatant was discarded and the cells were resuspended in PBS. Cells were centrifuged, supernatant was discarded and the pellet resuspended in 0.5 ml PBS + 0.1% Triton-X 100 in addition to 10 µl of RNAse A (10 µg/ml; [Invitrogen; Carlsbad, CA USA]) and 10 µl Propidium Iodide (PI; 1 mg/ml; [Sigma-Aldrich, St. Louis, MO USA]). Cells were incubated for 30 min at room temp prior to cell cycle using FC500 flow cytometer, analyzing $\geq$ 30,000 cells [Beckman Coulter; Brea, CA USA].

Cell Proliferation Analysis: Cell proliferation was measured using Click-it EdU Flow Cytometry Assay Kit [Invitrogen; Carlsbad, CA] using Alexa Fluor 647 azide [Invitrogen; Carlsbad, CA], according to manufacturer protocol. Cells were grown to 90% confluence in growth media, EdU was added to media (final concentration 10 µM) for 2 hrs. Cells were trypsinized and washed with 1% BSA in PBS solution. Cells were centrifuged and resuspended in Click-it fixative reagent, mixed and incubated at room temp for 15 min in the dark. Cells were washed with 1% BSA in PBS solution, centrifuged, resuspended in Click-it saponin-based permeabilization/wash reagent, and incubated at room temp for 15 min in the dark. During incubation Click-it reaction cocktail was prepared and 0.5 ml of cocktail was added to cells after incubation was completed. Cells were

incubated for 30 min at room temp in the dark. Cells were then washed with saponin-based permeabilization/wash reagent and resuspended in the same reagent to final volume of 0.5 ml. Cells were then analyzed using FC500 flow cytometer, analyzing $\geq$ 30,000 cells [Beckman Coulter; Brea, CA USA].

Scratch Assay: C2C12 cells were grown in growth media until 90% confluent in 6-well tissue culture plate. Cells were incubated in humidified incubator at 37 °C and 5% CO2. Wells were scratched with p100 pipette tip and media was changed to differentiation media to minimize the effects of proliferation. The cells were photographed every 24 hrs using Axiovert 40 CFL [Zeiss; Oberkochen Germany] microscope with Micropublisher model B [Q-imaging; Surrey, BC Canada] camera and Q-capture V2.66 software [Q-imaging; Surrey, BC Canada].

Immunocytochemistry: C2C12 cells were cultured in growth media on collagen coated coverslips until 90% confluent. The media was then changed to differentiation media and they were cultured for an additional 3 days to allow for formation of myotubes. Coverslips were then fixed in 4% paraformaldehyde for 5 min. Samples were washed 3 times with PBS and blocked for 1 hr at room temperature with 3SB blocking buffer (5% Fetal Calf Serum, 5% Goat Serum, 1% Calf Serum, 0.3% Boehringer Blocker, 0.1% Triton X-100, PBS). Primary antibody α-rat EGFP (homemade, 1:1500 dilution) was diluted in blocking buffer and added to samples, then samples were incubated overnight at 4° C. Samples were washed 3 times with PBST (PBS + 0.1% Triton X-100) for 10 min. Fluorescent conjugated secondary antibodies [1:500, Jackson Immuno.; West Grove, PA USA] and DAPI [1:5000, Invitrogen; Carlsbad, CA USA] were added and samples were incubated at room temperature for 2 hrs, followed by 3 times wash with PBST for 10 min. Samples were dehydrated and mounted with DPX

mounting media. Visualization for EdU+ was performed using Click-iT EdU AlexaFluor-647 Imaging Kits according to manufacturer protocols [Invitrogen; Cat# C10085; Carslbad, CA USA]. Single cells were imaged under Zeiss Confocal Microscope LSM 510 Meta [Zeiss; Oberkochen Germany] at 63x magnification.

Identification of Myoblast Fusion Genes: We analyzed microarrays from E12.5 mouse forelimb tissue enriched for $Lbx1^{EGFP}$ muscle progenitor cells published in Campbell et al., 2012 [in press, PLoS One]. The data discussed in this publication have been deposited in NCBI's Gene Expression Omnibus [19] and are accessible through GEO Series accession number GSE31945 (http://www.ncbi.nlm.nih.gov/geo/query/acc.cgi?acc=GSE31945).

RESULTS

Pitx2-dependent Myoblast G1 Cell Cycle Arrest

Ablation of Pitx2 in mice causes lethality at E10.5-E14.5 due to axial malformation, open body wall, heart defects, and arrest of organ development [13,14,16,20]. To study the role Pitx2 plays in myoblast fusion while avoiding embryo lethality we generated stable transfectants that express Pitx2-EGFP and control EGFP cells.

To determine if Pitx2 can regulate C2c12 cell cycle, cells were stained with PI. The distribution of cells analyzed found that (mean ± sem) in control cells were 71 ± 0.3% (G1), 14 ± 4% (G2), 16 ± 4% (S) between the different phases, while for Pitx2-overexpressing cells had a distribution of 76 ± 1% (G1), 19 ± 4% (G2), 7 ± 2% (S) cells in each phase. The 7% increase of the %cell in G1-phase was

determined to be statistically significant using unpaired t-test ($p = 0.017$) (Fig 1A). To determine if proliferation rates differed between the treatment groups, an EdU proliferation assay was performed on the cells. The percentage of EdU^+ cells was in CMV cells was 43 ± 0.2% and 36 ± 0.3% in CMV-Pitx2 cells. This approximate 14% increase in the uptake of EdU between CMV and CMV-Pitx2 cells was determined to be statistically signification using unpaired t-test ($p = 0.0085$) (Fig 1B). These data suggest that Pitx2 promotes myoblast G1 arrest by inhibiting their re-entry to the cell cycle to the cell cycle again and initiation of the differentiation process. The observed decrease in EdU incorporation in CMV-Pitx2 cells compared to CMV cells is consistent with withdrawal from the cell cycle and cell cycle arrest.

Pitx2-dependent Myoblast Migration and Myotube Formation

To determine if cellular motility was different between CMV and CMV-Pitx2 cells were performed a scratch assay (Fig 2). The cells were grown to 90% confluence in 6-well plates and a single scratch was made down the middle of the well with a p100 pipette tip. We observed that 2 days (D2) after the scratch was made CMV-Pitx2 cells had completely filled in the scratch, while CMV cells had taken until 3 days (not shown). Interestingly, 5 days (D5) after the scratch extensive myotubes had formed in the CMV-Pitx2 cells, while several myotubes were just beginning to appear in the CMV expressing cells.

To quantify the observed differences between stable transfected cells expressing CMV-EGFP and CMV-Pitx2-EGPF were grown on collagen coated coverslips for 3 and 6 days and the mean nuclei per myotube was determined (Fig 3A). The CMV-EGFP cells had become densely packed and few had undergone fusion

into myotubes with a mean (± sem) number of nuclei per myotube was 4 ± 0.2 while the CMV-Pitx2-EGFP cells had undergone extensive fusion into myotubes with a mean (± sem) nuclei per myotube of 6 ± 0.3. This increase in the number of nuclei per myotube was determined to be statistically significant using unpaired t-test ($p = 0.0001$) (Fig 3B). After 6 days the CMV-EGFP cells had fused into myotubes and was densely packed with nuclei, mean number of nuclei per myotube was 35 ± 4, with many mononucleated myoblasts surrounding the myotube. In the CMV-Pitx2-EGFP cells virtually all cells were fused into myotubes and aligned into parallel arrays with few mononucleated cells remaining. The mean nuclei per myotube as 25 ± 2 for CMV-Pitx2-EGFP cells and this difference was determined significant using unpaired t-test ($p=0.03$)(Fig 3C).

The results of this assay suggest that Pitx2 has a role in the efficient formation of multinucleated myotubes. The formation of multinucleated myotubes can either be the result of myoblasts migrating into close proximity, undergoing recognition, and fusing membranes to form a myotube. Myotubes can also grow through the migration of myogenic cells into close proximity to a previously existing myotube, undergoing recognition, and fusing membranes thus increasing the size and number of nuclei of the myotube. At this stage, it is unclear if Pitx2 is involved in one or both these scenarios.

Pitx2-dependent Repression of Myogenic Regulatory Factors in Myoblasts

To investigate if the there were differences in the expression of the myogenic regulatory factors (MRF) between CMV-EGFP and CMV-Pitx2-EGFP cells. Both cell types were grown on collagen coated coverslips and differentiated into

myotubes for 6 days. The cells were then stained for Myf5 and Myog to visualize if any differences in MRF expression (Fig 4). We observed that after 6 days of differentiation the CMV-EGFP cells had formed several myotubes and that many of the surrounding myoblasts were in juxtaposition with the myotubes. The nuclei for both the myotubes and myoblasts were stained positive in the CMV-EGFP cells. Interestingly, in the CMV-Pitx2-EGFP cells virtually all the cells had fused into myotubes and that all the myotubes were aligned into parallel arrays. Almost none of the cells in the CMV-Pitx2-EGFP cultures stained positive for Myf5 and a small number of nuclei were positive for Myog.

This data suggests that overexpression of Pitx2 down regulates the expression of MRFs (Myf5 and Myog) in differentiated myoblast and myotubes. The expression of Myf5 marks the initial onset of commitment to the myogenic program, whereas Myog expression is expressed in terminally differentiated myoblasts [21,22]. Pitx2 over-expression studies observed the down regulation of MRF expression in Sol8 myoblasts [23].

Myoblast Fusion Genes as Pitx2 Targets

To identify potential target genes involved in myoblast fusion we used Affymetrix mouse 430 arrays comparing $Lbx1^{EGFP}|Pitx2^{+/+}$ (WT), $Lbx1^{EGFP}|Pitx2^{Lacz/+}$ (HET) and $Lbx1^{EGFP}|Pitx2^{Lacz/LacZ}$ (MT) hypaxial muscle precursors isolated from E12.5 forelimb tissue. Analysis of these arrays focused on probe sets of genes known to play a role in myoblast recognition, alignment, and fusion. A small set of 8 genes, consisting of total of 12 probe sets was identified as having a fold change of greater than 1.2 fold cut off (Table 1).

The genes *Activated Leukocyte Cell Adhesion Molecule* (*Alcam*) and *Kin of IRRE like 3* (*Kirrel3* a.k.a. Nephrin 2) are both mammalian homologs of *Drosophila* membrane proteins *Kin of IRRE* (Kirre aka *dumbfounded*, *Duf*) and *Sticks and Stones* (Sns), respectively [24,25]. In *Drosophila* myogenesis, myoblast founder cells migrate and colonize areas where the presumptive muscle groups will form. These founder cells express the transmembrane protein Kirre/Duf). This process is followed by migration of fusion-competent myoblast (FCM), which express the transmembrane protein Sns [26] that interacts with Kirre/Duf initiating fusion of the two myoblasts. The expression of the cell surface protein encoded by Nephrin in skeletal muscle cells is generally low in adult tissue of mice and humans. During periods of myoblast fusion such as embryonic development or myofiber regeneration in response to injury/disease, Nephrin expression is upregulated. Myoblasts isolated from Nephrin^{KO} mice failed to form large myotubes and its expression is required for myoblasts to fuse to myotubes, but not vice versa [27]. Pitx2 acted as an inhibitor of Kirrel3 in migratory precursor cells (Table 1).

The gene *integrin alpha 4 subunit* (*Itga4* a.k.a VLA-4 receptor) encodes for a counter receptor for vascular cell adhesion molecule 1 (VCAM-1). During mouse development VLA-4 protein is first detected at E11 in areas were presumptive muscle groups will form, by E13 expression is significantly upregulated and restricted to the surface of primary myotubes. Conversely the expression of its ligand VCAM-1 is restricted to secondary myoblasts/myotubes in close proximity to primary myotubes starting at E16 and persisting until P2. Follow up studies using *in vitro* cultures of C2C12 cells and antibodies to block VLA-4 receptor and VCAM-1 inhibited the ability of these cells to form myotubes, and the myotubes

that did form appeared truncated [28]. Pitx2 acted as an inhibitor of Itga4 in migratory precursor cells (Table 1).

In our analysis we identified the myosin heavy chain isoform *Myh7* (a.k.a. *MYH-Beta/Slow*) as a potential target for Pitx2. The most abundant proteins expressed in striated muscle fibers are the myosin proteins. The myosin heavy chains (MHCs) and myosin light chains (MLCs) exist in several isoforms and are the product of three multigene families. The MHC family consists of several genes, each encoding for a specific isoform, that are sensitive to mechanical and hormonal stimuli which serve as “markers” for muscle plasticity and adaptive response to stimuli [29]. There are several MHC genes expressed in mammalian skeletal muscle which are detectable in developing mouse myotomes around E9.5. During limb muscle development the first wave of myoblast fusion gives rise to the primary myotubes in the anlagen. The subsequent secondary wave of myoblast fusion gives rise to the secondary myotubes which align themselves to the primary myotubes. The primary and secondary myotubes differ in MHC isoform expression prior to specification to slow/type I or fast/type II fibers [30]. In developing myofibers the expression of Myh7 is low and gradually reduced in fibers specified to become fast, while in slow fibers Myh7 expression resists and increases to become the predominate isoform [31].

We identified members of the IL-4 signaling pathway, *Bcl2-like11* (*Bcl2l11*) and *pyruvate dehydrogenase kinase isoenzyme 1* (*Pdk1*) as targets of Pitx2 repression. The IL-4 signaling pathway is interesting with respect to myofiber formation due to the finding that IL-4 is secreted from newly formed myotubes which acts on IL-4α receptors present on nearby myoblasts promoting their recruitment and fusion to the growing myotube in a pathway downstream of

Nuclear Factor of Activate T-cells calcineurin dependent 2 transcription factor (*NFATC2*) [32]. The NFAT protein family consists of three isoforms (NFATC1-3) expressed in skeletal muscle. Although their expression persists throughout all stages of myogenesis, the nuclear translocation in response to calcium is specific to each isoform at different stages of myofiber formation. The isoform NFATC3 translocates only in myoblasts, while NFATC1 and C2 translocate only in myotubes [33]. Studies of myotube formation using NFATC2$^{-/-}$ and IL-4$^{-/-}$ muscle cells show that myotubes form but are reduced in size and number of nuclei and addition of exogenous IL-4 rescues this phenotype, while addition of exogenous IL-4 to IL4α receptor$^{-/-}$ muscle cells does not [32].

The transmembrane *mannose receptor type c1* (*Mrc1*) gene was identified as having Pitx2 act as a potential activator. Studies with mannose receptor knockout myoblasts reveal that these myoblasts have reduced migration velocity and impaired fusion to myotubes [34]. Although, the function of mannose receptor in myoblast/myotube fusion remains unclear it is of note that mannose receptors are known to bind to glycosylated proteins and thus may act as myogenic cell recognition receptors and/or mediate cell-cell interactions.

The gene *prostaglandin I2* (a.k.a. *prostacyclin*) *synthase* (*Ptgis*) encodes the enzyme which synthesizes the soluble molecule prostacyclin (PGI2) [35]. Muscle cells synthesize and release prostaglandin I2 (PGI2) where it acts to negatively regulate myoblast migration and enhances initial fusion of myoblasts into myotubes through the PGI_2 receptor (IP) [36]. The anti-migratory effect PGI2 has on myoblasts and whether this directly or indirectly enhances fusion remains unclear.

DISCUSSION

Proper myofiber formation is dependent on a series of cellular events including myoblast fusion, migration and differentiation. Disruption of these processes in the myoblasts may inhibit the proper fusion of myoblasts into muscle fibers and compromise the structure and function of the growing muscle fiber. Here we identify several key genes for myoblast fusion as targets of the homeodomain transcription factor Pitx2.

In mammals skeletal muscle arises from the paraxial mesoderm, which segments into somites that flank the neural tube and notochord. The dorsal part of the somite will subdivide and give rise to the dermomyotome, while the ventral part will form the sclerotome. The dermomyotome is subdivided into the hypaxial dermomyotome, the source of the muscle progenitors that will form the muscles of the deep back, and the hypaxial dermomyotome, the source of muscle progenitor cells that will form the lateral trunk muscles. The induction of limb migratory muscle progenitor (MMP) cells begins when signaling molecules from the surface ectoderm and lateral plate mesoderm induce the expression of Lbx1 within Pax3 expressing cells along the ventrolateral lip of the dermomyotome at limb level.

Early in E9.0 cells from the limb level dermomyotomes will undergo an epithelial to mesenchyme (EMT) transition and migrate to areas where the presumptive muscle groups will form. At E10.5 and persists until E12.5 $Lbx1^{+}/Pax3^{+}$ muscle progenitor (MP) cells can be detected in the forelimb muscle anlagen. During this time the muscle masses enlarge and begin to position themselves with respect to the bone anlagen.

This enlargement of the muscle masses is due to the MP cells proliferating to increasing the number of myocytes and new myogenic cells migrating into the enlarging muscle mass. At this time the myogenic cells begin expression of the Muscle Regulatory Factors (MRFs) and undergo withdrawal from the cell cycle, where they either fuse together to form nascent multinucleated myotubes and/or mono-nucleated myoblasts fuse with pre-existing myotubes. Although muscle differentiation and cell cycle control has been studied extensively, the mechanism that governs transition from proliferative MP to terminally differentiated multinucleated myofiber remains unclear.

The differentiation of myogenic cells into skeletal muscle requires withdrawal from the cell cycle. The decision for myoblasts to either withdraw from the cell cycle or to undergo a new cycle of cellular division appears to be regulated at the G1/S-phase transition. At this checkpoint, D-type cyclins (D1-D3), bind to cdk4 or cdk6, and leads to phosphorylation of the retinoblastoma tumor suppressor protein (Rb). The phosphorylation of Rb inhibits its ability to repress the E2F transcription factors allowing for expression of genes required for S-phase entry [37]. Crosstalk between withdrawal from the cell cycle and expression of MRFs has been studied using cultured myoblasts. The expression of MyoD revealed that MyoD expression levels are highest in early G1-phase [38]. MyoD blocks progression into the S-phase through induction of p21, Rb, and cyclin D3 [39,40,41,42].

Pitx2 protein is expressed in myoblasts of the limb bud, co-localizing with the same expression pattern as *Pax3* and *MyoD* suggesting that it is involved in patterning of the muscle [43]. Originally the function of Pitx2 was thought to be involved in initiation and patterning of the muscle, ablation studies of Pitx2 show

gross anatomical deformities. The muscle groups in these mice appear to form with mild distortion or truncated muscles. It has been reported that Pitx2 is a target of the Wnt/Dvl2/beta-catenin pathway and operates to control proliferation by regulating expression of cyclin D1, cyclin D2, and c-Myc [17,44].

Muscle fiber growth occurs postnatally through the activation and subsequent fusion of previously quiescent myoblasts, satellite cells, to the mature myofiber [45,46] In response to muscle damage induced through exercise, injury, or inherited genetic diseases satellite cells become activated. These activated cells proliferate, with some withdrawing from the cell cycle and fusing to the damaged muscle fiber to repair the damage; while other cells return to the quiescent state and line the basal lamina of the fiber [47,48,49]. Interestingly, many of the genes that regulate myoblast fusion during development are also involved in postnatal myogenic cell fusion to mature muscle fibers.

The target genes identified by microarray analysis play pivotal roles in cell proliferation and differentiation. Integrins (*Itga4/VLA receptor*) are key players in cell fate determination. Integrins provide sites of cell-cell and cell-extracellular matrix (ECM) interactions [50]. Inside the cell these pointes of interactions provide sites for the recruitment of cytoskeletal adaptor proteins (paxillin, p130, guanine-nucleotide exchange factors (GEFs), etc.) and signaling enzymes (focal adhesion kinase (FAK), Src, Jnk, Rho-GTPases, etc. which trigger downstream pathways that control cell survival, growth, migration and differentiation [51,52]. We identified members of the IL-4 signaling pathway which appear to play a role in the activating the NFAT family of transcription factors, Which in turn translocates into the nucleus in response to calcium signaling to regulate target genes [32]. Also identified was prostaglandin synthase enzyme which produces a

signaling molecule that has been found to influence myoblast proliferation, differentiation and fusion of myoblast to myotubes *in vitro* through G-protein-coupled receptors to increase cAMP [32,53,54,55].

Our findings suggesting that Pitx2 may act to regulate these cell surface transmembrane proteins, which function to allow myogenic cells to recognize myoblast and myotubes. During development, proper expression of Pitx2 target genes in myogenic cells may allow for the proper migration, alignment and fusion which give rise to the formation of parallel arrays of myotube in order for proper myofibril assembly, promote muscle tissue growth and develop functional sarcomeres. In postnatal/adult muscle, Pitx2 target genes allow for proper migration and allow for efficient fusion of the myocyte, repairing damage to the muscle fibers. Understanding how Pitx2 regulates the myogenic program is important in understanding the pathology and provides novel therapeutic targets for the treatment of impaired muscle growth associated with aging, disease, atrophy and injury.

REFERENCES

1. Lieber RL, Ward SR (2011) Skeletal muscle design to meet functional demands. Philos Trans R Soc Lond B Biol Sci 366: 1466-1476.
2. Borghi N, James Nelson W (2009) Intercellular adhesion in morphogenesis: molecular and biophysical considerations. Curr Top Dev Biol 89: 1-32.
3. Disatnik MH, Rando TA (1999) Integrin-mediated muscle cell spreading. The role of protein kinase c in outside-in and inside-out signaling and evidence of integrin cross-talk. J Biol Chem 274: 32486-32492.
4. Guasconi V, Puri PL (2009) Chromatin: the interface between extrinsic cues and the epigenetic regulation of muscle regeneration. Trends Cell Biol 19: 286-294.
5. Charrasse S, Meriane M, Comunale F, Blangy A, Gauthier-Rouviere C (2002) N-cadherin-dependent cell-cell contact regulates Rho GTPases and beta-catenin localization in mouse C2C12 myoblasts. Journal of Cell Biology 158: 953-965.
6. Hynes RO (2002) Integrins: bidirectional, allosteric signaling machines. Cell 110: 673-687.
7. Arthur WT, Noren NK, Burridge K (2002) Regulation of Rho family GTPases by cell-cell and cell-matrix adhesion. Biol Res 35: 239-246.
8. Davis DB, Doherty KR, Delmonte AJ, McNally EM (2002) Calcium-sensitive phospholipid binding properties of normal and mutant ferlin C2 domains. J Biol Chem 277: 22883-22888.
9. Doherty KR, Cave A, Davis DB, Delmonte AJ, Posey A, et al. (2005) Normal myoblast fusion requires myoferlin. Development 132: 5565-5575.
10. Shih HP, Gross MK, Kioussi C (2007) Cranial muscle defects of Pitx2 mutants result from specification defects in the first branchial arch. Proc Natl Acad Sci U S A 104: 5907-5912.
11. Shih HP, Gross MK, Kioussi C (2007) Expression pattern of the homeodomain transcription factor Pitx2 during muscle development. Gene Expr Patterns 7: 441-451.
12. Shih HP, Gross MK, Kioussi C (2008) Muscle development: forming the head and trunk muscles. Acta Histochem 110: 97-108.
13. Lu MF, Pressman C, Dyer R, Johnson RL, Martin JF (1999) Function of Rieger syndrome gene in left-right asymmetry and craniofacial development. Nature 401: 276-278.
14. Lin CR, Kioussi C, O'Connell S, Briata P, Szeto D, et al. (1999) Pitx2 regulates lung asymmetry, cardiac positioning and pituitary and tooth morphogenesis. Nature 401: 279-282.
15. Gage PJ, Suh H, Camper SA (1999) Dosage requirement of Pitx2 for development of multiple organs. Development 126: 4643-4651.
16. Kitamura K, Miura H, Miyagawa-Tomita S, Yanazawa M, Katoh-Fukui Y, et al. (1999) Mouse Pitx2 deficiency leads to anomalies of the ventral body wall, heart, extra- and periocular mesoderm and right pulmonary isomerism. Development 126: 5749-5758.
17. Kioussi C, Briata P, Baek SH, Rose DW, Hamblet NS, et al. (2002) Identification of a Wnt/Dvl/beta-Catenin --> Pitx2 pathway mediating cell-type-specific proliferation during development. Cell 111: 673-685.
18. Campbell AL, Shih H-P, Xu J, Gross MK, Kioussi C (2012) Regulation of Motility of Myogenic Cells in Filling Limb Muscle Anlagen by Pitx2. PLoS One 7: e35822.

19. Edgar R, Domrachev M, Lash AE (2002) Gene Expression Omnibus: NCBI gene expression and hybridization array data repository. Nucleic Acids Res 30: 207-210.
20. Gage PJ, Suh H, Camper SA (1999) The bicoid-related Pitx gene family in development. Mamm Genome 10: 197-200.
21. Emerson CP (1990) Myogenesis and developmental control genes. Curr Opin Cell Biol 2: 1065-1075.
22. Wright WE, Sassoon DA, Lin VK (1989) Myogenin, a factor regulating myogenesis, has a domain homologous to MyoD. Cell 56: 607-617.
23. Lozano-Velasco E, Contreras A, Crist C, Hernandez-Torres F, Franco D, et al. (2011) Pitx2c modulates Pax3+/Pax7+ cell populations and regulates Pax3 expression by repressing miR27 expression during myogenesis. Dev Biol 357: 165-178.
24. Chen EH, Olson EN (2005) Unveiling the mechanisms of cell-cell fusion. Science 308: 369-373.
25. Abmayr SM, Balagopalan L, Galletta BJ, Hong SJ (2003) Cell and molecular biology of myoblast fusion. Int Rev Cytol 225: 33-89.
26. Bour BA, Chakravarti M, West JM, Abmayr SM (2000) Drosophila SNS, a member of the immunoglobulin superfamily that is essential for myoblast fusion. Genes Dev 14: 1498-1511.
27. Sohn RL, Huang P, Kawahara G, Mitchell M, Guyon J, et al. (2009) A role for nephrin, a renal protein, in vertebrate skeletal muscle cell fusion. Proc Natl Acad Sci U S A 106: 9274-9279.
28. Rosen GD, Sanes JR, LaChance R, Cunningham JM, Roman J, et al. (1992) Roles for the integrin VLA-4 and its counter receptor VCAM-1 in myogenesis. Cell 69: 1107-1119.
29. Haddad F, Qin AX, Bodell PW, Zhang LY, Guo H, et al. (2006) Regulation of antisense RNA expression during cardiac MHC gene switching in response to pressure overload. Am J Physiol Heart Circ Physiol 290: H2351-2361.
30. Resnicow DI, Deacon JC, Warrick HM, Spudich JA, Leinwand LA (2010) Functional diversity among a family of human skeletal muscle myosin motors. Proc Natl Acad Sci U S A 107: 1053-1058.
31. Weiss A, Leinwand LA (1996) The mammalian myosin heavy chain gene family. Annu Rev Cell Dev Biol 12: 417-439.
32. Horsley V, Jansen KM, Mills ST, Pavlath GK (2003) IL-4 acts as a myoblast recruitment factor during mammalian muscle growth. Cell 113: 483-494.
33. Abbott KL, Friday BB, Thaloor D, Murphy TJ, Pavlath GK (1998) Activation and cellular localization of the cyclosporine A-sensitive transcription factor NF-AT in skeletal muscle cells. Molecular Biology of the Cell 9: 2905-2916.
34. Jansen KM, Pavlath GK (2006) Mannose receptor regulates myoblast motility and muscle growth. Journal of Cell Biology 174: 403-413.
35. Yokoyama C, Yabuki T, Inoue H, Tone Y, Hara S, et al. (1996) Human gene encoding prostacyclin synthase (PTGIS): genomic organization, chromosomal localization, and promoter activity. Genomics 36: 296-304.
36. Bondesen BA, Jones KA, Glasgow WC, Pavlath GK (2007) Inhibition of myoblast migration by prostacyclin is associated with enhanced cell fusion. FASEB J 21: 3338-3345.
37. Novitch BG, Mulligan GJ, Jacks T, Lassar AB (1996) Skeletal muscle cells lacking the retinoblastoma protein display defects in muscle gene expression and accumulate in S and G2 phases of the cell cycle. Journal of Cell Biology 135: 441-456.

38. Kitzmann M, Carnac G, Vandromme M, Primig M, Lamb NJ, et al. (1998) The muscle regulatory factors MyoD and myf-5 undergo distinct cell cycle-specific expression in muscle cells. Journal of Cell Biology 142: 1447-1459.
39. Guo K, Wang J, Andres V, Smith RC, Walsh K (1995) MyoD-induced expression of p21 inhibits cyclin-dependent kinase activity upon myocyte terminal differentiation. Molecular and Cellular Biology 15: 3823-3829.
40. Halevy O, Novitch BG, Spicer DB, Skapek SX, Rhee J, et al. (1995) Correlation of terminal cell cycle arrest of skeletal muscle with induction of p21 by MyoD. Science 267: 1018-1021.
41. Martelli F, Cenciarelli C, Santarelli G, Polikar B, Felsani A, et al. (1994) MyoD induces retinoblastoma gene expression during myogenic differentiation. Oncogene 9: 3579-3590.
42. Cenciarelli C, De Santa F, Puri PL, Mattei E, Ricci L, et al. (1999) Critical role played by cyclin D3 in the MyoD-mediated arrest of cell cycle during myoblast differentiation. Molecular and Cellular Biology 19: 5203-5217.
43. Marcil A, Dumontier E, Chamberland M, Camper SA, Drouin J (2003) Pitx1 and Pitx2 are required for development of hindlimb buds. Development 130: 45-55.
44. Baek SH, Kioussi C, Briata P, Wang D, Nguyen HD, et al. (2003) Regulated subset of G1 growth-control genes in response to derepression by the Wnt pathway. Proc Natl Acad Sci U S A 100: 3245-3250.
45. Gros J, Manceau M, Thome V, Marcelle C (2005) A common somitic origin for embryonic muscle progenitors and satellite cells. Nature 435: 954-958.
46. Relaix F, Rocancourt D, Mansouri A, Buckingham M (2005) A Pax3/Pax7-dependent population of skeletal muscle progenitor cells. Nature 435: 948-953.
47. Campion DR (1984) The muscle satellite cell: a review. Int Rev Cytol 87: 225-251.
48. Grounds MD, White JD, Rosenthal N, Bogoyevitch MA (2002) The role of stem cells in skeletal and cardiac muscle repair. J Histochem Cytochem 50: 589-610.
49. Hawke TJ, Garry DJ (2001) Myogenic satellite cells: physiology to molecular biology. J Appl Physiol 91: 534-551.
50. Zaidel-Bar R, Milo R, Kam Z, Geiger B (2007) A paxillin tyrosine phosphorylation switch regulates the assembly and form of cell-matrix adhesions. J Cell Sci 120: 137-148.
51. Giancotti FG, Tarone G (2003) Positional control of cell fate through joint integrin/receptor protein kinase signaling. Annu Rev Cell Dev Biol 19: 173-206.
52. Lo SH (2006) Focal adhesions: what's new inside. Dev Biol 294: 280-291.
53. Otis JS, Burkholder TJ, Pavlath GK (2005) Stretch-induced myoblast proliferation is dependent on the COX2 pathway. Exp Cell Res 310: 417-425.
54. Vandenburgh HH, Shansky J, Solerssi R, Chromiak J (1995) Mechanical stimulation of skeletal muscle increases prostaglandin F2 alpha production, cyclooxygenase activity, and cell growth by a pertussis toxin sensitive mechanism. J Cell Physiol 163: 285-294.
55. Zalin RJ (1987) The role of hormones and prostanoids in the in vitro proliferation and differentiation of human myoblasts. Exp Cell Res 172: 265-281.

Chapter 3-Figure 1

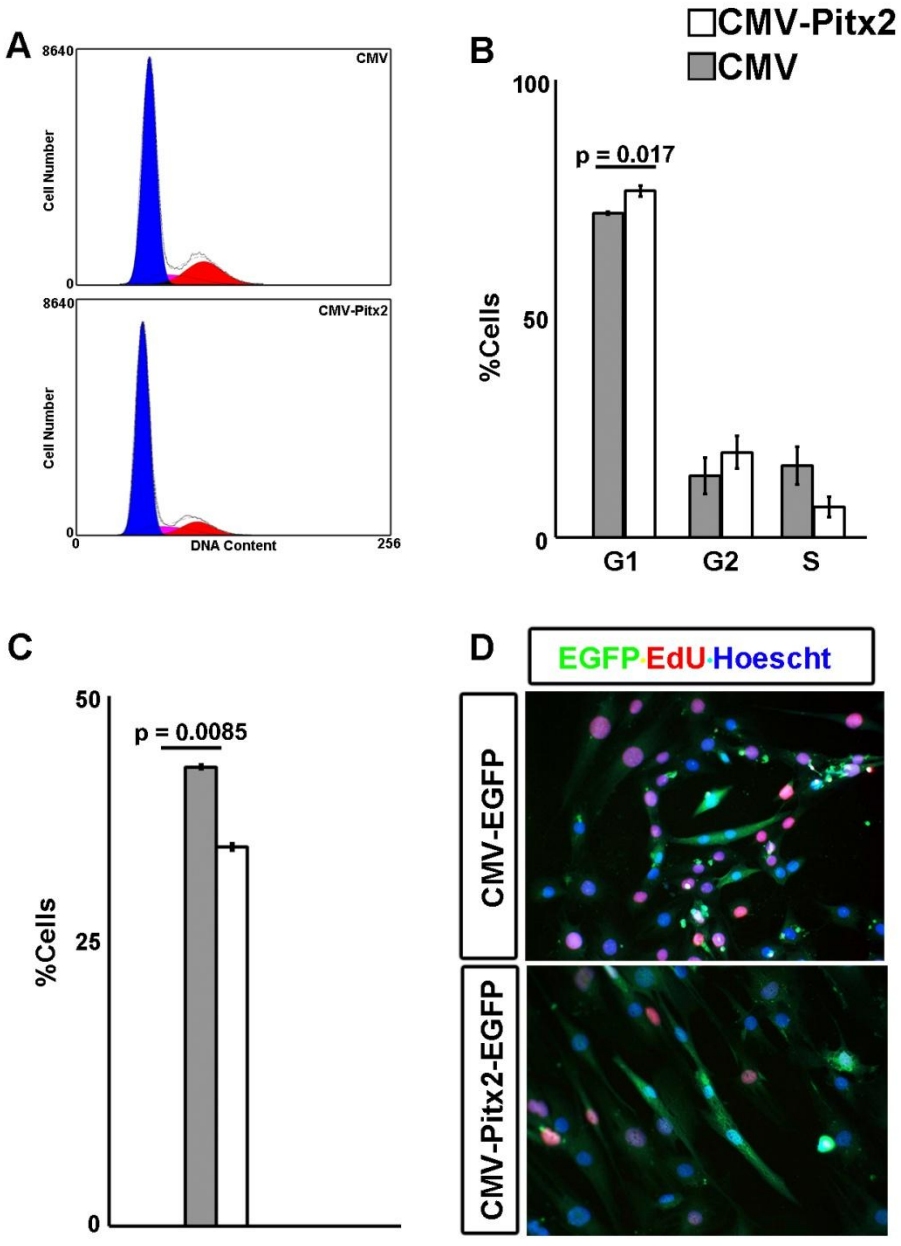

Fig 1. Pitx2 overexpression results in G1 arrest and inhibition of S-phase entry. (A) Cells stained with PI were analyzed. A mean ± standard error of mean (sem) value of 71 ± 0.3% (G1), 14 ± 4% (G2), 16 ± 4% (S) in CMV transfected cells, while 76 ± 1% (G1), 19 ± 4% (G2), 7 ± 2% (S) in CMV-Pitx2 transfected cells. The increased cell% of G1-phase in CMV-Pitx2 cells was determined to be statistically significant using unpaired t-test (p-value = 0.017). **(B)** Example histograms of PI cell cycle staining (**C)** EdU results of mean (± SEM) of transfected cells (n = 3), showing that 38 ± 0.3% were positive for CMV-Pitx2 transfected cells and 44 ± 0.2% were positive in CMV transfected cells. This difference in EDU+ cells between groups was determined statistically significant using unpaired t-test (p-value = 0.0085). (D) Immunocytochemistry triple staining for EGFP (vector expression), EdU (Proliferation marker), and Hoescht 33342 (Nuclear Stain) after 4 days in differentiation media.

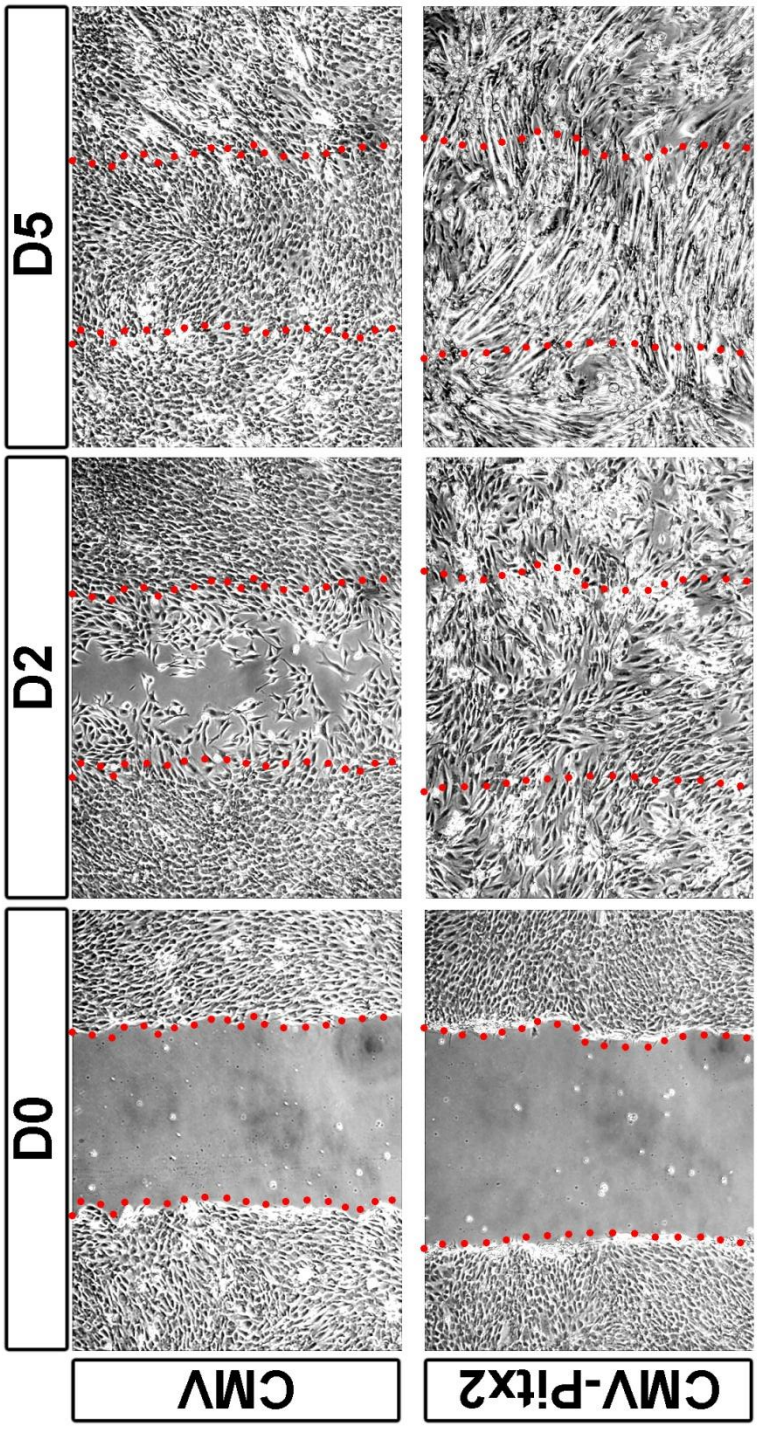

Chapter 3-Figure 1

Fig 2. Pitx2 facilitates migration. A wound was created using p100 pipette tip (red lines) and picture was taken (D0), after 48 hrs (D2) CMV-Pitx2 cells had filled the scratch. The CMV cells hadn't traversed the scratch until 3 days after the wound was created (Not shown). After 5 days (D5) CMV-Pitx2 cells had undergone extensive myotube formation, while few multinucleated fibers in CMV cells were observed.

Chapter 3-Figure 3

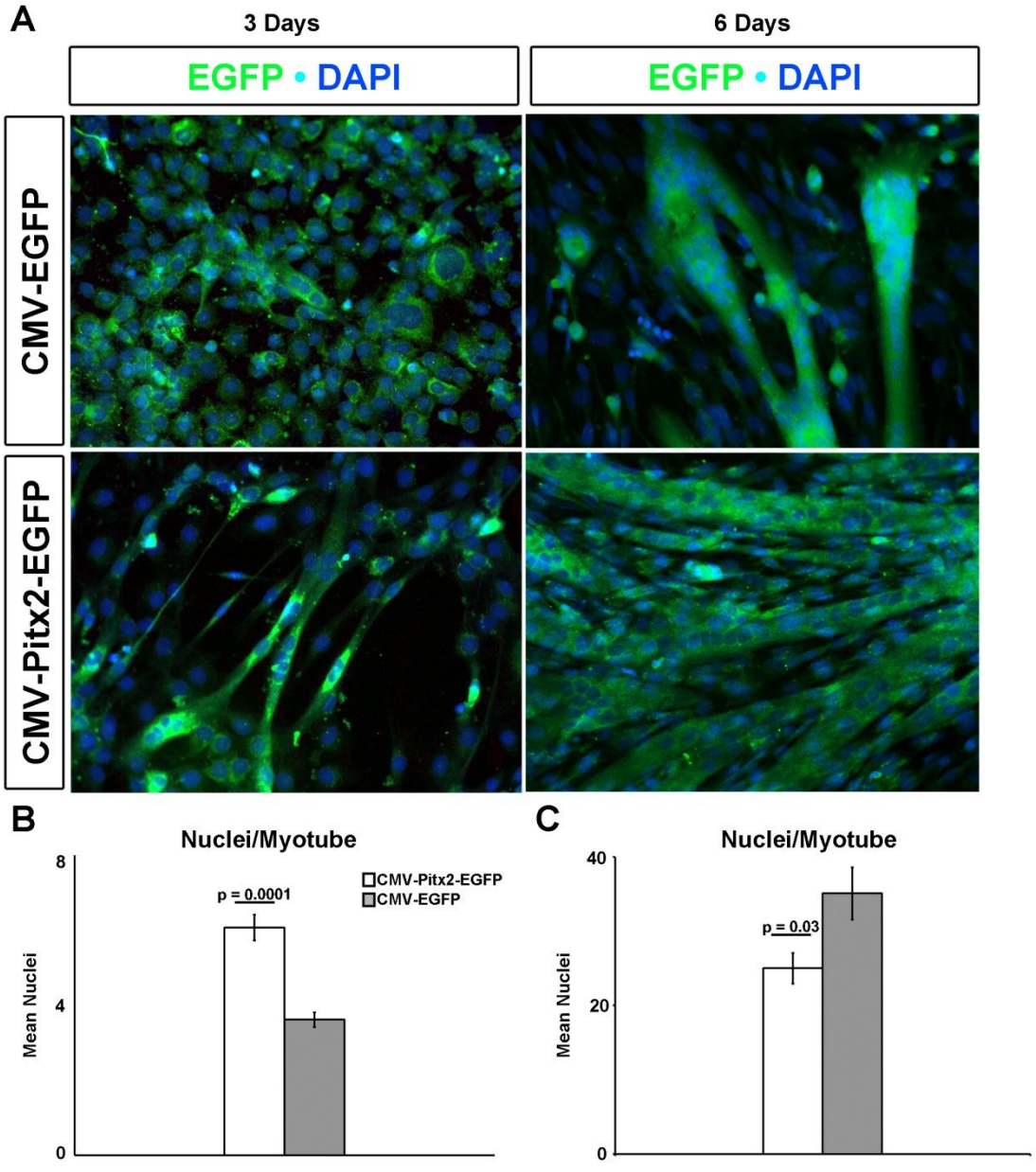

Figure 3. Pitx2 promotes multinucleated fiber formation. (A) Cells after 3 and 6 days in differentiation media. **(B)** Counting nuclei per myotube (n = 60) after 3 days in differentiation media revealed that CMV-EGFP myotubes had mean nuclei (± S.E.M) of 4 ± 0.2 and CMV-Pitx2-EGFP myotubes had 6 ± 0.3. This difference in mean nuclei per myotube was determined to be statistically significant using unpaired t-test (p = 0.0001). **(C)** Counting nuclei per myotube (n = 60) after 6 days differentiation revealed that CMV-EGFP myotubes had mean nuclei of 35 ± 4 and CMV-Pitx2-EGFP myotubes had mean nuclei of 25 ± 2 per myotube. These differences were signification using t-test (p = 0.03).

Chapter 3-Figure 4

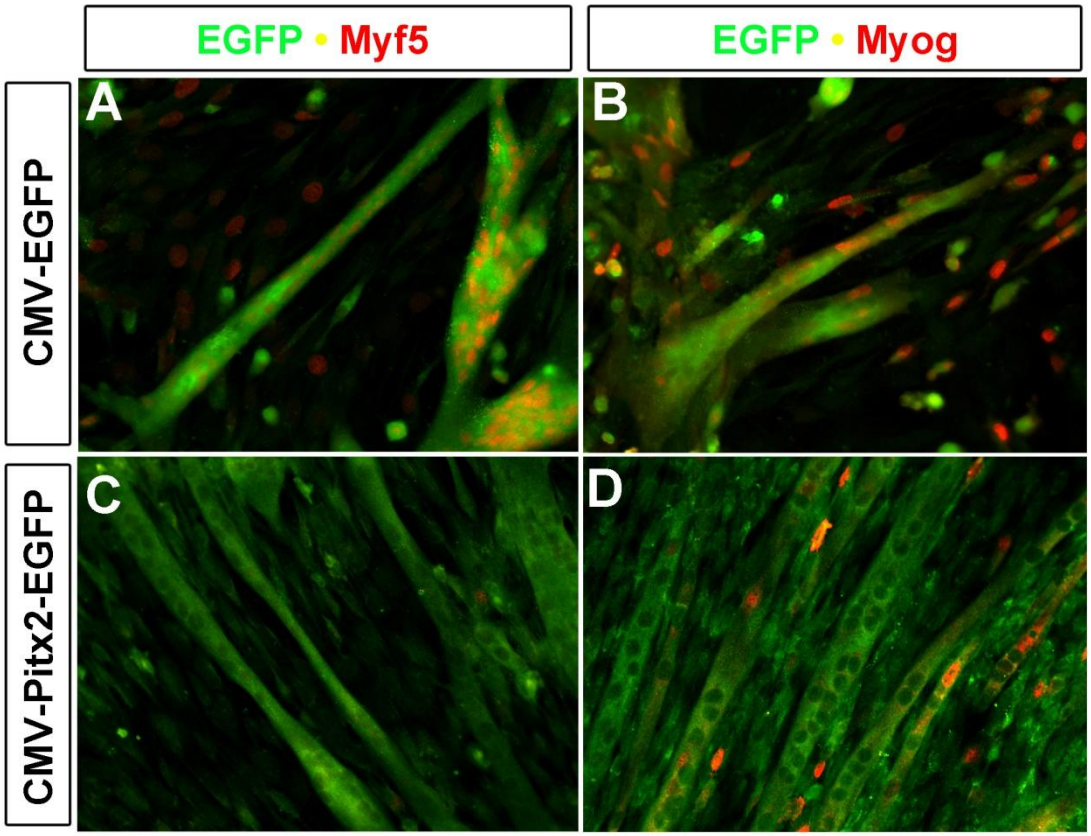

Figure 4. MRF expression in CMV-Pitx2 myotubes. (**A, B)** After 6 days in differentiation media CMV-EGFP cell have formed multinucleated myotubes with single myoblasts in juxtaposition to the myotube. Both myoblast and myotube nuclei stain positive for Myf5 **(A)** and Myog **(B)**. **(C, D)** CMV-Pitx2-EGFP cells differentiated under the same conditions have virtually all cells fused into multinucleated myotubes aligned in parallel arrays. Very few CMV-Pitx2-EGFP cells stained positive for Myf5 **(C)** although a small number nuclei can still be detected as positive for Myog **(D)**.

Table 3.1

Pitx2 Targets Myoblast Fusion Genes

Name	Transcript	Gene	WT	HET	MUT	Δ Fold	Function
Pitx2 Repressed							
Kin of IRRE like 3 (*Drosophila)*	NM_130867.3	Kirrel3	103±12	110±6	160±73	1.55	Myoblast Recognition
Integrin alpha 4	NM_010576	Itga4	1985±261	2180±427	2920±663	1.47	Myoblast Recognition
Activated leukocyte cell adhesion molecule	NM_009655.2	Alcam	198±135	292±44	283±99	1.42	Myoblast Recognition
Myosin heavy chain 7, cardiac, beta	NM_080728.2	Myh7	205±72	236±40	284±88	1.38	Myoblast Fusion
BCL2-like 111	NM_009754.3	Bcl2l11	209±15	177±18	266±67	1.27	IL-4 Signaling
Pyruvate dehydrogenase kinase, isoenzyme 1	NM_172665.4	Pdk1	360±89	314±76	436±112	1.21	IL-4 Signaling
Pitx2 Activated							
Mannose receptor, c-type 1	NM_008625.2	Mrc1	345±101	214±39	232±49	-1.49	Mannose Receptor
Prostaglandin I2 (prostacyclin) synthase	NM_008968.3	Ptgis	2122±201	1720±432	1521±58	-1.41	Prostacyclin Signaling

Limb Muscle Precursor Gene Networks

Chapter 4

Adam L Campbell, Diana Eng, Michael K Gross and Chrissa Kioussi

Gene
Submitted May 14, 2012

Abstract

The ventrolateral dermomyotome give rise to all muscles of the limbs through the delamination and migration of cells into the limb buds. These cells proliferate and form myoblasts, withdraw from the cell cycle and become terminally differentiated. The myogenic lineage colonizes pre-patterned regions to form muscle anlagen as muscle fibers are assembled. The regulatory mechanisms that control the later steps of this myogenic program are not well understood. The homeodomain transcription factor *Pitx2* is expressed specifically in the muscle lineage from the migration of precursors to adult muscle. Ablation of *Pitx2* results in distortion, rather than loss, of limb muscle anlagen, suggesting that its function becomes critical during the colonization of, and/or fiber assembly in, the anlagen. Gene expression arrays were used to identify changes in gene expression of flow-sorted migratory muscle precursors, labeled by $Lbx1^{EGFP}$, which resulted from the loss of *Pitx2*. Target genes of *Pitx2* were clustered using the "David Bioinformatics Functional Annotation Tool" to bin genes according to their gene ontology keyword enrichment. This provided a way to both narrow the target genes and identify potential gene families regulated by *Pitx2*. Representative target genes in the most enriched bins were analyzed for the presence and evolutionary conservation of Pitx2 consensus binding sequence, TAATCY, on the -20kb, intronic, and coding region sequences of the gene. Fifteen *Pitx2* target genes passed all the above requirements and were identified as having functions involving cytoskeleton organization, tissue specification, and transcription factors. Data from these studies suggest that *Pitx2* acts to regulate cell motility and expression of muscle specific genes in the muscle precursors during forelimb muscle development. This work provides a framework to develop the gene

network leading to skeletal muscle development, growth and regeneration.

Keywords

Homeobox; Pitx2; Development; Myoblast; Gene Expression Analysis; Bioinformatics

1. Introduction

The forelimb muscles originate from the hypaxial dermomyotome of the interlimb somites during embryonic development. Inductive cues from the lateral plate mesoderm and synergistically induce the expression of Lbx1 within the ventrolateral Pax3 expression domain of the dermomyotome [1]. These cells delaminate from the dermomyotome and migrate into the developing limb bud [2,3,4]. The dorsal and ventral muscle masses of mouse limb bud consist of $Lbx1^{+}/Pax3^{+}$ limb muscle progenitor (MP) cells at E10.5 and this gene expression persists until E12.5 [5]. At E11-E12.5 muscle masses enlarge, shape and position themselves with respect to bone anlagen. MP cells increase their numbers through proliferation, undergo withdrawal from the cell cycle and become terminally differentiated myocytes. Pax3 and Lbx1 have generally been placed at the beginning of myogenic progression and activation of the Muscle Regulatory Factors (MRFs) in the embryonic limb because they are expressed earlier and their mutation leads to a loss of migratory precursors before MRFs are normally expressed [5,6,7,8,9]. The myocytes fuse with each other to form multinucleated myotubes and muscle fibers. The precise regulatory mechanisms that control each step of the myogenic program are not well understood to date.

The bicoid–related homeobox gene *Pitx2* is expressed in the lateral plate mesoderm and in muscle anlagen in all stages of myogenic progression [10,11]. *Pitx2* contributes to the establishment of network kernels that specify pre-myogenic progenitors for extraocular and mastication muscles [12]. Ablation of *Pitx2* causes lethality in the mouse at E10.5-E14.5 with axial malformations, open body wall, heart defects, and arrest of organ development [13,14,15,16]. *Pitx2* is positioned downstream of both Wnt and growth factor signaling pathways

in skeletal myogenesis and promotes muscle progenitor proliferation by direct regulation of the expression of a number of cyclin-dependent kinases [17]. Analysis of $Lbx1^{EGFP}$ muscle progenitor cells isolated from forelimb tissue of $Pitx2^{LacZ/LacZ}$ mice at E12.5 has revealed that a small group of cytoskeletal, adhesion, and signaling genes are potential targets for regulation by *Pitx2*. Muscle progenitors of $Pitx2^{LacZ/LacZ}$ were smaller, more symmetrical, had increased actin bundling, and decreased motility preventing myogenic cells from filling limb bud anlagen [18].

In these studies we utilized gene expression data from microarray experiments in combination with online gene ontology databases and in house scripts to predict the presence of *Cis*-Regulatory Modules (CRM). The gene expression profile of $Lbx1^{+}$ muscle precursors isolated from forelimb tissue at E12.5 from Pitx2 WT, Het, and Mut mice was obtained using Affymetrix Mouse Genome 430 2.0 arrays, with RMA normalization and analyzed with SAMExcel [19,20]. This resulted in a total of 773 probe sets, representing 567 unique genes that were significantly differentially expressed. Genes were placed into a total of 175 bins based on putative functional annotations using DAVID Bioinformatics Functional Annotation Tool [21,22]. The first 10 bins had similar enrichment scores reported and were split with GOTERMs referring to cytoskeletal or transcription factor functions. These genes were analyzed for predicted Pitx2 binding sites within the genomic gene sequence and -20kb upstream region. The top 2 genes from each bin that contained Pitx2 binding site conserved in at least 4 species and gave us a representative pool of 20 genes. A predicted network model was constructed using BioTapestry version 5.0.2 to visually link Pitx2 with its target genes.

2. Material and methods

2.1 Mice

ICR Pitx2$^{LacZ/+}$ mouse embryos (HET) [14], Lbx1$^{EGFP/+}$ [5] were used. Pitx2$^{LacZ/+}$ mice were bred with Pitx2$^{LacZ/+}$, Lbx1$^{EGFP/+}$ and Pax3$^{Cre/+}$|Rosa$^{EGFP/+}$ to generate Lbx1$^{EGFP/+}$|Pitx2$^{LacZ/LacZ}$, Lbx1$^{EGFP/+}$|Pitx2$^{LacZ/+}$, Lbx1$^{EGFP/+}$|Pitx2$^{+/+}$, mice. Tail genomic DNA was extracted and used for PCR genotyping [5,14]. For cell flow sorting, embryos were rapidly genotyped under a fluorescent microscope to identify Lbx1 HET mice. Positive identification of Lbx1 HET embryos were followed up with X-gal staining to determine Pitx2 genotype.

2.2 RNA Preparation and Microarray Analysis

We analyzed microarrays from E12.5 mouse forelimb tissue enriched for Lbx1^{EGFP} muscle progenitor cells [18]. The data discussed in this publication have been deposited in NCBI's Gene Expression Omnibus [23] and are accessible through GEO Series accession number GSE31945 (http://www.ncbi.nlm.nih.gov/geo/query/acc.cgi?acc=GSE31945). The differentially expressed genes determined to be significantly altered above the 1.2 fold cutoff were analyzed with DAVID Bioinformatics Functional Annotation Tool [21,22]. The DAVID Functional Annotation Clustering application analyzed and sorted the genes into functional clusters that were individually searched for the presence of *Pitx2* binding sites.

2.3 Pitx2 Binding Site Analysis and BioTapestry

The genomic sequence with -20kb flanking sequence of each gene was downloaded from MGI's database to the mouse reference genome (NCBI v37, mm9). The data was then processed with a script generated in our lab,

binding_site_search.pl, to determine the location of Pitx2 binding sites, TAATCY, relative to the start of the gene and level of evolutionary conservation of the identified binding site by comparing the site to gene entry locations in the UCSC Genome browser [24]. Cytoscape v2.8.2 was utilized to compose visualizations of gene expression data and presence of binding sites [25]. BioTapestry v5.0.2 was utilized to compose the predicted gene network in the developing forelimb muscles [26].

3. Results and Discussion

3.1 Pitx2 Target Gene Functional Clusters in Forelimb

The DAVID Functional Annotation Clustering tool was applied to the genes identified as misregulated above the 1.2 fold cutoff. A total of 175 bins that covered 567 unique genes. The first 10 bins showed enrichment scores of 3 or greater (Table 1). Key gene ontology terms (GOTERMS) such as cell differentiation, cytoskeleton, transcription factor, etc. were ranked according to their frequency of occurrence in the Pitx2 target genes compared to their occurrence in the mouse genome. The Ptix2 target genes were arranged according to their putative function in the developing forelimb muscles. The top ten clusters enrichment score ranged from 4.9 to 3.0 with the top scoring clusters being genes involved in cell differentiation and morphogenesis, cytoskeleton binding, and sequence specific transcription factors (SSTFs) (Table 1). These genes represent the regulatory priorities of the cells at E12.5 of limb muscle development. These 10 categories can be divided into two main groups the structural genes (Bin 1, 2, 4, 8, 9, 10) and sequence specific transcription factors (SSTFs) (Bin 3, 5, 6, 7).

3.2 Evolutionarily Conserved Pitx2 Binding Sites

The identification of Pitx2 binding sites in the promoter, coding, and intronic regions of the target genes was accomplished through comparative genome analysis. We collected the -20kb region of the transcriptional start site along with the genomic sequence of each gene in bins 1 to 10 (Table 1). We searched for the presence of the TAATCY consensus sequence to confirm regulation by Pitx2. The average number of binding sites identified ranged from 17 to 6 per gene (Table 1). If genes were directly regulated by Pitx2 then the bin with the highest enrichment score should correlate to a higher number of Pitx2 binding sites. Our data show that the difference between the bins, either the average number of binding sites and enrichment scores has similar values compared to each other. This non-linear correlation between binding site and enrichment score may be due to indirect regulation through co-factor binding complexes. To address this possibility, we focused on those genes that are directly regulated by Pitx2 interaction with predicted binding sites. We chose to focus on the top 20 genes between all 10 functional bins because they contained a higher than average number of Pitx2 binding sites for further analysis of evolutionarily conserved binding sites. The use of a Perl script that was developed in our lab allowed us to align the output for each gene from the UCSC Genome Browser Assembly and identify the absolute location and species conservation of that site [27].

The Pitx2 binding sites on target genes were selected based on their conservation between a minimum of 4 species (mouse, human, plus 2 other) and a maximum of 8 (mouse, human, rat, orangutan, dog, horse, opossum, chicken). Within these genes, 5 genes were eliminated because of the presence of an

additional gene in the -20kb region. The top 15 genes all contained a number of Pitx2 binding sites conserved through the minimum number of species (Table 2). When the number of species was increased to the maximum of 8, the number of Pitx2 binding sites (Table 2, parentheses) reduced significantly to an average of 3 Pitx2 binding sites per gene (Fig 1, boxed regions). All of the Pitx2 binding sites conserved in all 8 species were located within intronic regions of the gene rather than the proximal promoter sequence (Fig 1).

3.3 Pitx2 Target Gene Function

The order of Pitx2 target genes based on the absolute fold change of gene expression from the microarray analysis was different than the order based on the number of conserved Pitx2 binding sites (Table 3). The genes with fold changes of 1.5 or greater were Doublecortin like kinase 1 (Dclk1), Met pro-oncogene (c-Met), Forkhead box P2 (Foxp2), and Down syndrome cell adhesion molecule like 1 (Dscaml1). The gene Dclk1 encodes for a protein that binds and regulates microtubule polymerization and dynamics [28]. The expression of Dclk1 is highly enriched in the developing brain; a low level of expression can be detected by northern blot in skeletal muscle of developing mice (E7-E11) [29]. Microtubule dynamics are important for migration of the cell as they provide stability to the cell body, allowing for actin cytoskeleton bundling to form protrusions of the cell membrane and allow the cell to elongate and form attachments to the extracellular matrix. Met encodes a tyrosine kinase receptor, is expressed in the lateral dermomyotome of all somites and is involved in the development of hypaxial musculature. Mice deficient for the Met receptor develop myogenic precursors but these precursors fail to delaminate from the

dermomyotome and migrate to eventually populate the limb bud [4]. The Foxp family members of SSTFs regulate gene expression in multiple developmental processes including lung, heart, and cerebral development. Foxp1/2/4 regulates smooth muscle differentiation and proliferation [30]. The Dscaml1 protein is a member of the Ig superfamily of cell adhesion molecules. Dscaml1 is highly expressed in the adult brain with lower levels during embryogenesis. Members of the Ig-superfamily are known to mediate cell adhesion and same cell-type recognition through homophilic interaction between neighboring cells. A similar mechanism for same cell sorting has been demonstrated for NCAM [31]. Dclk1 and Met were repressed by Pitx2 whereas Foxp2 and Dscaml1 were activated by Pitx2 in the $Lbx1^{+}$ migratory muscle precursors. All four genes are involved in regulating cell motility and expression of surface receptors to allow for homophilic cell recognition of the muscle precursors. We have shown that *Pitx2* regulates cytoskeletal, adhesion, and signaling genes in migratory muscle precursor cells [18]. Proper regulation of the cytoskeleton allows migratory cells to form protrusions in directions of positive signals order to explore the extracellular environment. This is followed by the formation of nascent adhesions to the extracellular matrix. Transmission of positive signals stabilizes these attachments allowing for anchoring of the cell body and providing traction points to allow the cell to propel itself forward. Once muscle cells reach their intended destination, cell-cell contacts also act to provide intracellular signaling cues that promote myogenic differentiation and fusion [32].

The next group of genes with a fold change between 1.4 and 1.3 were the Zinc finger homeobox 3 (Zfhx3), Midline 1 (Mid1), Transducin-like enhancer of split 4 (Tle4), Trichorhinophalangeal syndrome 1 (Trps1), Nuclear factor I/B (Nfib), Meis homeobox 2 (Meis2), and Protein kinase, cGMP-dependent, type 1 (Prkg1). The

SSTF Zfhx3 contains both a homeodomain and zinc finger motifs. Zfhx3-A isoform inhibits myogenic differentiation and expression of MRFs, while the B variant promotes myogenic differentiation and expression of MRFs [33]. Mid1 is an E3 ubiquitin ligase protein which targets the microtubule associated protein phosphatase 2A (PP2A-C) for degradation. Mutations in Mid1 result in reduced activity or loss of function and cause accumulation of PP2A-C, disrupting the downstream mTORC1 signaling which controls a number of cellular processes such as growth, autophagy, cell motility, cell cytoskeleton [34]. The transducin-like enhancer gene (Groucho-related genes or Grgs) encodes for a member of a closely related family of proteins that mediate Notch signaling through repression of the Hairy-related transcription factors (Hes genes) and the Lef/TCF transcription factors that mediate Wnt signaling. The isoform Tle4 is expressed in the posterior of the fore and hind limb buds [35]. The SSTF Trps1 recognizes GATA consensus to regulate transcription. Trps1 represses prostate-specific antigen (PSA), runt-related transcription factor 2 (Runx2), osteocalcin (Bglap), signal transducer and activator of transcription (Stat3), and parathyroid hormone related protein (Pthrp). Trps1 activates the expression of Wnt inhibitors *Wif1*, *Apcdd1*, and *Dkk4* during hair follicle development [36]. Trps1 null mice have shown that Trps1 acts downstream of BMP7 and functions in the development of bone, kidney, and hair follicles [37]. The SSTF Nfib is expressed in adipose tissue and brain in adult mice. Nfib induces differentiation through the induction of adipogenic transcription factors PPAR-gamma and C/EBP-alpha [38]. The SSTF Meis2 is expressed in the trunk of the embryo prior to limb bud induction (E9.0) and in the mesenchyme of the early limb bud (E10.0). As the limb elongates Meis2 becomes restricted to the proximal region of the limb bud (E11.0). This restriction of Meis2 to the proximal region of the limb is important,

since Meis2 represses Fgf8 at the apical ectodermal ridge and Shh, Tbx2, Bmp, and Hox genes in the mesenchyme of the limb bud. This restriction sets up zones to allow for proximal to distal patterning of the limb bud [39]. Prkg1 encodes for two isozymes, cGKI-alpha and cGKI-beta, which are expressed in smooth muscle, platelets, and purkinje cells, hippocampal neurons, and lateral amygdale. In the cardiovascular system small signaling molecules nitric oxide (NO) and naturitic peptides lead to the elevation of cGMP which in turn activates cGKI to interact with IRAG to reduce intracellular Ca^{2+} concentrations and activate myosin light chain phosphatase (MLC-P), leading to reduced contractility and vasodilatation. Signaling through NO/cGMP can induce cGKI-dependent switching between a proliferative/migratory cell and a differentiated contractile cell. Although the exact mechanisms are unclear, in response to smooth muscle injury vascular smooth muscle cells (VSMCs) de-differentiate by down regulating cGKI expression which in turn causes decreased expression of other smooth-muscle specific genes. Then the VSMCs migrate to the injured area, then re-differentiate by upregulation of cGKI and downstream target genes and switch to a contractile cell state to repair the damage [40]. The genes identified in this group collectively all share a similar function as regulating cell type specification and/or proliferation, primarily through the Wnt pathway. *Pitx2* is positioned downstream of both Wnt and growth factor signaling pathways in skeletal myogenesis and promotes muscle progenitor proliferation by direct regulation of the expression of a number of cyclin-dependent kinases [17].

The third group of genes with fold change of 1.2 was Palladin cytoskeleton associated protein (Palld), SRY-box containing gene 6 (Sox6), Ankyrin 2 (Ank2), and Zinc finger protein, multitype 2 (Zfpm2). Palladin is associated with actin stress fibers, focal adhesions, and Z-discs were it acts as a scaffolding protein to

allow for binding of other actin binding proteins and adhesion signaling proteins. Cells lacking Palladin have disrupted actin cytoskeleton and knockout of Palladin in mice shows embryonic lethality at E15.5. The exact mechanism of how Palladin knockout leads to embryonic lethality is unclear, but overexpression analysis of Palladin in cell culture revealed that Palladin is able to induce the expression of smooth muscle differentiation genes [41]. Sox6 is a member of the Sox SSTF family. Due to the lack of a regulatory domain, the Sox6 protein is completely dependent on cofactors to specify which genes to regulate. In developing skeletal muscle, activation of Sox6 expression leads to the inhibition of cardiac and embryonic muscle myosin isoforms, the inhibition of slow twitch fiber specification genes, the activation of fast twitch fiber specification genes [42]. The ankyrin-2 protein is an adaptor protein for stabilizing L-type calcium channel 1.3 ($Ca_v1.3$) to the surface of cardiac myocytes. Individuals with loss of function studies mutations of the ankryin-2 protein develop early onset atrial fibrillation (AF). In cell culture the loss of ankyrin-2 protein results in the reduction of $Ca_v1.3$ at the surface of atrial myocytes leading to shortened action potential duration (APD) a clinical sign of AF [43]. The zinc finger SSTF, multitype 2 encodes a GATA interacting protein called Friend of GATA 2 (Fog-2). The expression of Fog-2 is observed in the developing heart at E13.5-15.5 and in the adult expression is seen in heart, brain, testis, liver and lung. This pattern is very similar to the expression of GATA-4/-5/-6 suggesting they may serve as binding partners for Fog-2 to regulate target genes essential for cardiac development. Knockout mice for Fog-2 die at embryonic stage E12-15.5 due to abnormal coronary vessel and gonadal development [44]. The genes represented in this group encode for proteins required for proper expression of cell types specific genes required for organogenesis.

4. Conclusion

The studies used SAMExcel to analyze microarray data from migratory muscle precursors isolated from $Lbx1^{EGFP/+}|Pitx2^{LacZ/LacZ}$ (Mut), $Lbx1^{EGFP/+}|Pitx2^{LacZ/+}$ (Het) and $Lbx1^{EGFP/+}|Pitx2^{+/+}$ (WT) forelimb tissue for alterations in gene expression. Using the DAVID Functional Annotation Clustering Tool, we identified genes grouped according to enrichment of reported gene ontology keywords (GOTERMS). This provided a lead to identify *Pitx2* dependent cellular/biological processes in the developing forelimb muscles. Our studies suggest that *Pitx2* regulates genes involved in cytoskeletal organization and gene transcription, which are involved in cell motility, organogenesis, and myogenesis. *Pitx2* also regulates SSTFs and members of the Wnt signaling involved in tissue and cell lineage specification. These studies define *Pitx2* as an essential node in the transcriptional network required for skeletal muscle development of the forelimbs. Further studies to validate these findings in biological systems well be necessary to confirm this predicted network, with further studies at later stages to determine how the network state changes over time.

References

1. Tremblay P, Dietrich S, Mericskay M, Schubert FR, Li Z, et al. (1998) A crucial role for Pax3 in the development of the hypaxial musculature and the long-range migration of muscle precursors. Dev Biol 203: 49-61.
2. Hayashi K, Ozawa E (1995) Myogenic cell migration from somites is induced by tissue contact with medial region of the presumptive limb mesoderm in chick embryos. Development 121: 661-669.
3. Bladt F, Riethmacher D, Isenmann S, Aguzzi A, Birchmeier C (1995) Essential role for the c-met receptor in the migration of myogenic precursor cells into the limb bud. Nature 376: 768-771.
4. Dietrich S, Abou-Rebyeh F, Brohmann H, Bladt F, Sonnenberg-Riethmacher E, et al. (1999) The role of SF/HGF and c-Met in the development of skeletal muscle. Development 126: 1621-1629.
5. Gross MK, Moran-Rivard L, Velasquez T, Nakatsu MN, Jagla K, et al. (2000) Lbx1 is required for muscle precursor migration along a lateral pathway into the limb. Development 127: 413-424.
6. Goulding M, Lumsden A, Paquette AJ (1994) Regulation of Pax-3 expression in the dermomyotome and its role in muscle development. Development 120: 957-971.
7. Bober E, Franz T, Arnold HH, Gruss P, Tremblay P (1994) Pax-3 is required for the development of limb muscles: a possible role for the migration of dermomyotomal muscle progenitor cells. Development 120: 603-612.
8. Mennerich D, Schafer K, Braun T (1998) Pax-3 is necessary but not sufficient for lbx1 expression in myogenic precursor cells of the limb. Mech Dev 73: 147-158.
9. Schafer K, Braun T (1999) Early specification of limb muscle precursor cells by the homeobox gene Lbx1h. Nature Genetics 23: 213-216.
10. Shih HP, Gross MK, Kioussi C (2007) Cranial muscle defects of Pitx2 mutants result from specification defects in the first branchial arch. Proc Natl Acad Sci U S A 104: 5907-5912.
11. Shih HP, Gross MK, Kioussi C (2007) Expression pattern of the homeodomain transcription factor Pitx2 during muscle development. Gene Expr Patterns 7: 441-451.
12. Shih HP, Gross MK, Kioussi C (2008) Muscle development: forming the head and trunk muscles. Acta Histochem 110: 97-108.
13. Lu MF, Pressman C, Dyer R, Johnson RL, Martin JF (1999) Function of Rieger syndrome gene in left-right asymmetry and craniofacial development. Nature 401: 276-278.
14. Lin CR, Kioussi C, O'Connell S, Briata P, Szeto D, et al. (1999) Pitx2 regulates lung asymmetry, cardiac positioning and pituitary and tooth morphogenesis. Nature 401: 279-282.
15. Gage PJ, Suh H, Camper SA (1999) Dosage requirement of Pitx2 for development of multiple organs. Development 126: 4643-4651.
16. Kitamura K, Miura H, Miyagawa-Tomita S, Yanazawa M, Katoh-Fukui Y, et al. (1999) Mouse Pitx2 deficiency leads to anomalies of the ventral body wall, heart, extra- and periocular mesoderm and right pulmonary isomerism. Development 126: 5749-5758.
17. Kioussi C, Briata P, Baek SH, Rose DW, Hamblet NS, et al. (2002) Identification of a Wnt/Dvl/beta-Catenin --> Pitx2 pathway mediating cell-type-specific proliferation during development. Cell 111: 673-685.

18. Campbell AL, Shih H-P, Xu J, Gross MK, Kioussi C (2012) Regulation of Motility of Myogenic Cells in Filling Limb Muscle Anlagen by Pitx2. PLoS One 7: e35822.
19. Kioussi C, Gross MK (2008) How to build transcriptional network models of mammalian pattern formation. PLoS One 3: e2179.
20. Tusher VG, Tibshirani R, Chu G (2001) Significance analysis of microarrays applied to the ionizing radiation response. Proc Natl Acad Sci U S A 98: 5116-5121.
21. Dennis G, Jr., Sherman BT, Hosack DA, Yang J, Gao W, et al. (2003) DAVID: Database for Annotation, Visualization, and Integrated Discovery. Genome Biol 4: P3.
22. Huang da W, Sherman BT, Lempicki RA (2009) Systematic and integrative analysis of large gene lists using DAVID bioinformatics resources. Nat Protoc 4: 44-57.
23. Edgar R, Domrachev M, Lash AE (2002) Gene Expression Omnibus: NCBI gene expression and hybridization array data repository. Nucleic Acids Res 30: 207-210.
24. Eng D, Campbell A, Hilton T, Leid M, Gross MK, et al. (2010) Prediction of regulatory networks in mouse abdominal wall. Gene 469: 1-8.
25. Shannon P, Markiel A, Ozier O, Baliga NS, Wang JT, et al. (2003) Cytoscape: a software environment for integrated models of biomolecular interaction networks. Genome Res 13: 2498-2504.
26. Longabaugh WJ, Davidson EH, Bolouri H (2005) Computational representation of developmental genetic regulatory networks. Dev Biol 283: 1-16.
27. Kent WJ, Sugnet CW, Furey TS, Roskin KM, Pringle TH, et al. (2002) The human genome browser at UCSC. Genome Res 12: 996-1006.
28. Lin PT, Gleeson JG, Corbo JC, Flanagan L, Walsh CA (2000) DCAMKL1 encodes a protein kinase with homology to doublecortin that regulates microtubule polymerization. J Neurosci 20: 9152-9161.
29. Sossey-Alaoui K, Srivastava AK (1999) DCAMKL1, a brain-specific transmembrane protein on 13q12.3 that is similar to doublecortin (DCX). Genomics 56: 121-126.
30. Shu W, Lu MM, Zhang Y, Tucker PW, Zhou D, et al. (2007) Foxp2 and Foxp1 cooperatively regulate lung and esophagus development. Development 134: 1991-2000.
31. Agarwala KL, Ganesh S, Tsutsumi Y, Suzuki T, Amano K, et al. (2001) Cloning and functional characterization of DSCAML1, a novel DSCAM-like cell adhesion molecule that mediates homophilic intercellular adhesion. Biochem Biophys Res Commun 285: 760-772.
32. Abmayr SM, Balagopalan L, Galletta BJ, Hong SJ (2003) Cell and molecular biology of myoblast fusion. Int Rev Cytol 225: 33-89.
33. Berry FB, Miura Y, Mihara K, Kaspar P, Sakata N, et al. (2001) Positive and negative regulation of myogenic differentiation of C2C12 cells by isoforms of the multiple homeodomain zinc finger transcription factor ATBF1. J Biol Chem 276: 25057-25065.
34. Liu E, Knutzen CA, Krauss S, Schweiger S, Chiang GG (2011) Control of mTORC1 signaling by the Opitz syndrome protein MID1. Proc Natl Acad Sci U S A 108: 8680-8685.
35. Van Hateren N, Belsham A, Randall V, Borycki AG (2005) Expression of avian Groucho-related genes (Grgs) during embryonic development. Gene Expr Patterns 5: 817-823.
36. Fantauzzo KA, Christiano AM (2012) Trps1 activates a network of secreted Wnt inhibitors and transcription factors crucial to vibrissa follicle morphogenesis. Development 139: 203-214.

37. Gai Z, Gui T, Muragaki Y (2011) The function of TRPS1 in the development and differentiation of bone, kidney, and hair follicles. Histol Histopathol 26: 915-921.
38. Waki H, Nakamura M, Yamauchi T, Wakabayashi K, Yu J, et al. (2011) Global mapping of cell type-specific open chromatin by FAIRE-seq reveals the regulatory role of the NFI family in adipocyte differentiation. PLoS Genet 7: e1002311.
39. Capdevila J, Tsukui T, Rodriquez Esteban C, Zappavigna V, Izpisua Belmonte JC (1999) Control of vertebrate limb outgrowth by the proximal factor Meis2 and distal antagonism of BMPs by Gremlin. Mol Cell 4: 839-849.
40. Hofmann F, Bernhard D, Lukowski R, Weinmeister P (2009) cGMP regulated protein kinases (cGK). Handb Exp Pharmacol: 137-162.
41. Jin L, Gan Q, Zieba BJ, Goicoechea SM, Owens GK, et al. (2010) The actin associated protein palladin is important for the early smooth muscle cell differentiation. PLoS One 5: e12823.
42. An CI, Dong Y, Hagiwara N (2011) Genome-wide mapping of Sox6 binding sites in skeletal muscle reveals both direct and indirect regulation of muscle terminal differentiation by Sox6. BMC Dev Biol 11: 59.
43. Cunha SR, Hund TJ, Hashemi S, Voigt N, Li N, et al. (2011) Defects in ankyrin-based membrane protein targeting pathways underlie atrial fibrillation. Circulation 124: 1212-1222.
44. Cantor AB, Orkin SH (2005) Coregulation of GATA factors by the Friend of GATA (FOG) family of multitype zinc finger proteins. Semin Cell Dev Biol 16: 117-128.
45. Tevosian SG, Deconinck AE, Tanaka M, Schinke M, Litovsky SH, et al. (2000) FOG-2, a cofactor for GATA transcription factors, is essential for heart morphogenesis and development of coronary vessels from epicardium. Cell 101: 729-739.
46. Svensson EC, Huggins GS, Lin H, Clendenin C, Jiang F, et al. (2000) A syndrome of tricuspid atresia in mice with a targeted mutation of the gene encoding Fog-2. Nature Genetics 25: 353-356.
47. Salsi V, Vigano MA, Cocchiarella F, Mantovani R, Zappavigna V (2008) Hoxd13 binds in vivo and regulates the expression of genes acting in key pathways for early limb and skeletal patterning. Dev Biol 317: 497-507.
48. Kunath M, Ludecke HJ, Vortkamp A (2002) Expression of Trps1 during mouse embryonic development. Gene Expr Patterns 2: 119-122.
49. Fuerst PG, Bruce F, Tian M, Wei W, Elstrott J, et al. (2009) DSCAM and DSCAML1 function in self-avoidance in multiple cell types in the developing mouse retina. Neuron 64: 484-497.
50. Murai K, Vernon AE, Philpott A, Jones P (2007) Hes6 is required for MyoD induction during gastrulation. Dev Biol 312: 61-76.
51. Jin L, Yoshida T, Ho R, Owens GK, Somlyo AV (2009) The actin-associated protein Palladin is required for development of normal contractile properties of smooth muscle cells derived from embryoid bodies. J Biol Chem 284: 2121-2130.
52. Christ B, Brand-Saberi B (2002) Limb muscle development. Int J Dev Biol 46: 905-914.
53. Sureban SM, May R, Lightfoot SA, Hoskins AB, Lerner M, et al. (2011) DCAMKL-1 regulates epithelial-mesenchymal transition in human pancreatic cells through a miR-200a-dependent mechanism. Cancer Res 71: 2328-2338.

Chapter 4-Figure 1

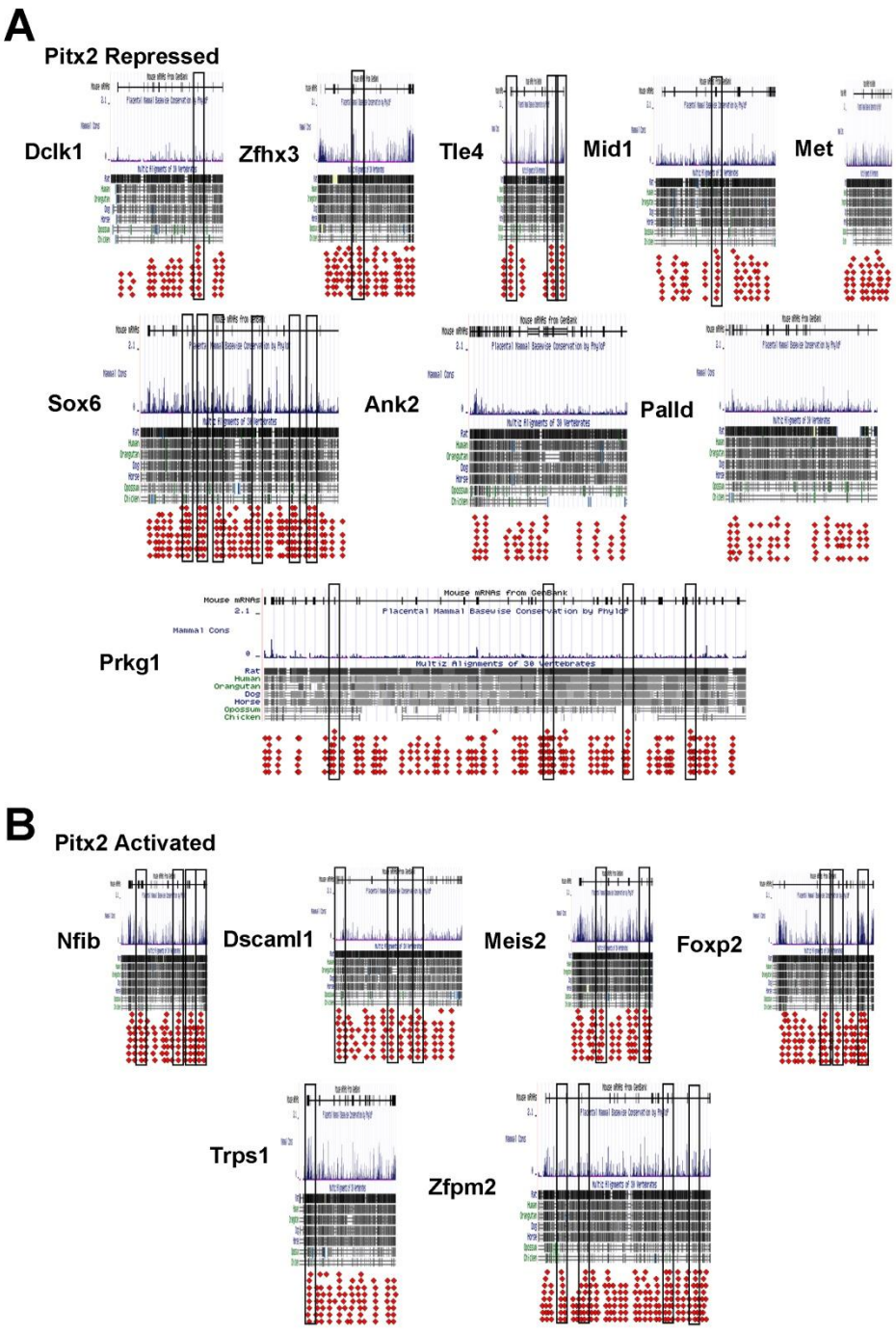

Fig 1. Evolutionary Conserved *Pitx2* Binding Sites. Comparative analysis of *Pitx2* consensus sequence binding sites in *Pitx2* target genes. Genomic plus 20kb upstream region of the transcriptional start site were mapped against the aligned sequences in the top 15 Pitx2 target genes. Columns of red dots indicate a predicted Pitx2 binding site and the number of species the motif was conserved in. Black boxes outline the binding sites that were found to be conserved in all 8 of the species.

Chapter 4-Figure 2

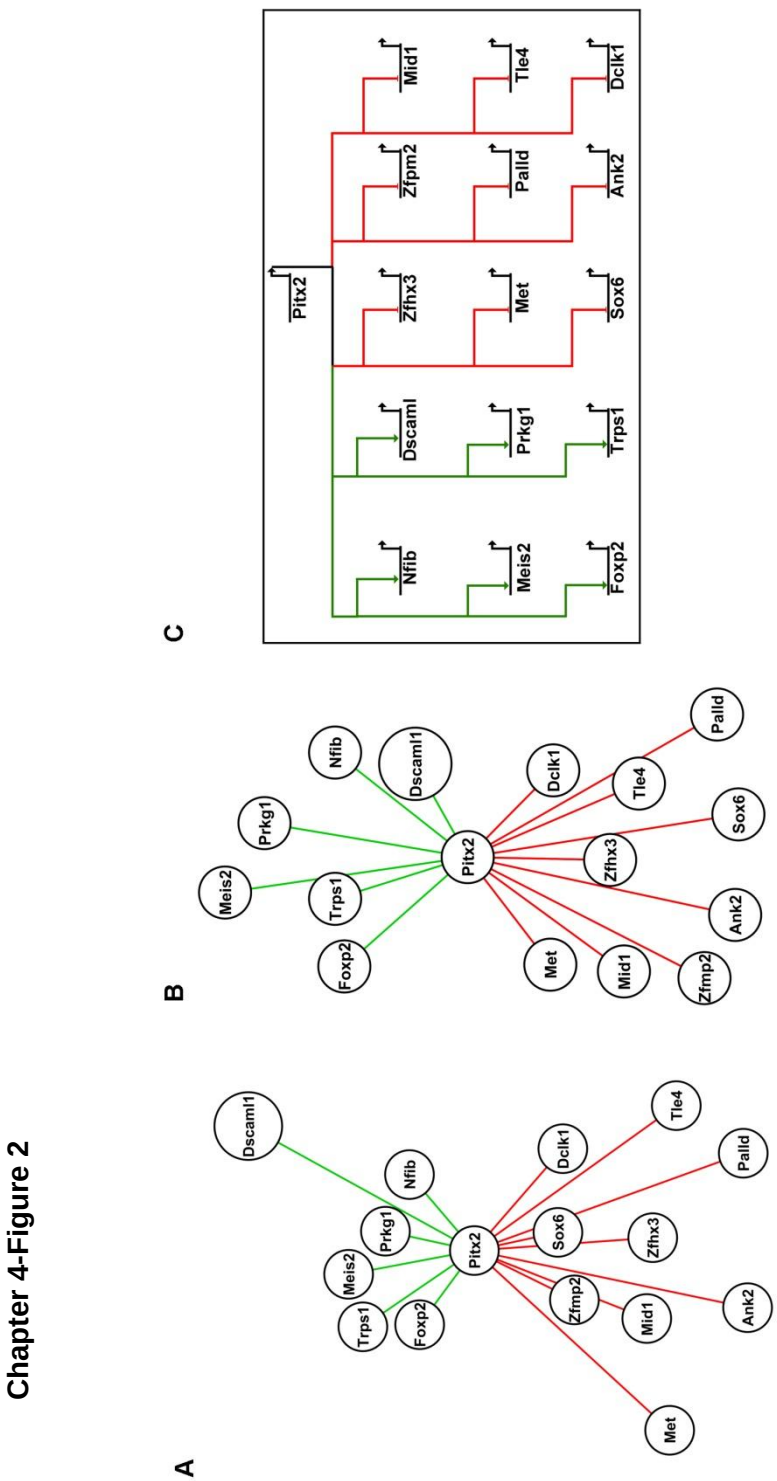

Fig 2. *Pitx2* Target Genes Visualized with Cytoscape. Individual target genes are represented by a white circle with *Pitx2* as the core regulator. Lines colored red represent targets of repression by *Pitx2* and lines colored green represent targets of activation by *Pitx2*. The distance of the gene from *Pitx2* represents the strength of their respective relationship. **(A)** Representation of target gene relationship based on the sum of evolutionary conserved binding sites from Table 2. Genes with greater number of binding sites are mapped closer to *Pitx2*; genes with fewer binding sites are further away. (B) Representation of target gene relationship based on the fold changes observed by microarray analysis. The greater the fold change the closer the gene is mapped to Pitx2, while smaller fold changes are mapped further away. It appears that *Pitx2* acts as a repressor for the majority of our target genes. (C) BioTapestry was used to generate a model of the Pitx2 regulatory network in the limb. Red links represent repressive interactions from *Pitx2*, while green links represent activation interaction with *Pitx2*.

Table 4.1

DAVID Functional Annotation Catagories of Pitx2 Target Genes in Forelimb Muscle Progenitor Cells

Annotation Bin	Enrichment Score	GOTERM	# of Genes	P-Value	Benjamini Corrected P-Value	Average # Pitx2 Binding Sites
1	4.9	Differentiation/Morphogenesis	26	1.7E-7	3.9E-4	13
2	4.2	Cytoskeleton Binding	37	1.5E-6	2.8E-4	7
3	4.2	Sequence Specific DNA Binding	47	2.1E-7	1.2E-4	13
4	4.0	Cytoskeleton Organization	31	2.2E-6	7.5E-4	6
5	3.6	Negative Regulation of Transcription	32	7.4E-5	8.0E-3	17
6	3.4	Transcription Factor Activity	58	3.8E-7	1.1E-4	13
7	3.4	Regulation of Transcription	46	4.4E-6	1.3E-3	15
8	3.2	Cytoskeleton	67	1.4E-5	4.8E-3	9
9	3.0	Cell Adhesion	21	3.3E-4	1.6E-2	16
10	3.0	Cell Motility	34	1.1E-6	1.4E-3	15

Table 4.2

Pitx2 Target Genes with Conserved Binding Sites

Gene	Gene Location	# of Pitx2 Binding Sites	Species	Function	Bibliography
Sox6 SRY-box containing gene 6	Chr7: 122,594,858-123,138,600	89 (6)	M, R, H, O, D, Ho, Op, Ch	Skeletal muscle differentiation	[42]
Zpm2 Zinc finger protein, multitype 2	Chr15: 40,466,588-40,936,138	85 (4)	M, R, H, O, D, Ho, Op, Ch	Cardiac development	[45,46]
Prkg1 Protein kinase, cGMP-dependent type 1	Chr19: 30,622,041-31,839,523	78 (4)	M, R, H, O, D, Ho, Op, Ch	Intracellular cGMP signaling	[40]
Nfib Nuclear factor 1/B	Chr4: 81,916,077-82,151,212	59 (4)	M, R, H, O, D, Ho, Op, Ch	Adipocyte differentiation	[38]
Foxp2 Forkhead box P2	Chr6: 155,115,506-15,391,977	53 (3)	M, R, H, O, D, Ho, Op, Ch	Smooth muscle differentiation	[30]
Zfhx3 Zinc finger homeobox 3	Chr8: 111,218,544-111,485,536	44 (1)	M, R, H, O, D, Ho, Op, Ch	Muscle differentiation	[33]
Mid1 Midline 1	ChrX: 166,103,179-166,428,729	42 (1)	M, R, H, O, D, Ho, Op, Ch	E3 ligase	[34]
Meis2 Meis homeobox 2	Chr2: 115,667,000-115,890,794	42 (2)	M, R, H, O, D, Ho, Op, Ch	Limb patterning	[39,47]
Trps1 Trichorhinophalangeal syndrome 1	Chr15: 50,466,305-50,721,587	41 (1)	M, R, H, O, D, Ho, Op, Ch	Cartilage, skeleton, lung, and trachea development	[37,48]
Dscaml1 Down syndrome cell adhesion molecule like 1	Chr9: 45,218,376-45,561,796	37 (3)	M, R, H, O, D, Ho, Op, Ch	Cell adhesion, Cell type self avoidance	[31,49]
Tle4 Transducin-like enhancer of split 4	Chr19: 14,502,562-14,672,473	33 (3)	M, R, H, O, D, Ho, Op, Ch	Mesoderm specification	[35,50]
Palld Palladin, cytoskeletal associated protein	Chr8: 63,972,041-64,381,487	29 (0)	M, R, H, O, D, Ho, Op	Cytoskeleton associated protein, Muscle differentiation	[41,51]
Met Met proto-oncogene	Chr6: 17,393,957-17,523,980	29 (0)	M, R, H, O, D, Ho, Op	Limb muscle development	[52]
Ank2 Ankyrin 2	Chr3: 126,630,030-127,111,949	28 (0)	M, R, H, O, D, Ho, Op	Ca^{2+} channel membrane targeting and stability	[43]
Dclk1 Doublecortin-like kinase 1	Chr3: 55,026,448-55,342,990	27 (1)	M, R, H, O, D, Ho, Op, Ch	Microtubule associated protein	[28,53]

M, mouse; R, rat; H, human; O, orangutans; D, dog; Ho, horse; Op, opossum; Ch, chicken

Table 4.3

Highly Regulated Pitx2 Target Genes in Muscle Precursor Cells

Gene	WT	HET	MUT	Δ Fold
Dclk1	150 ± 24	160 ± 3	217 ± 63	1.5
Met	1438 ± 273	1605 ± 79	2093 ± 119	1.5
Zfhx3	365 ± 12	531 ± 124	515 ± 101	1.4
Mid1	873 ± 83	947 ± 197	1132 ± 448	1.3
Tle4	146 ± 5	153 ± 28	188 ± 24	1.3
Palld	1033 ± 1	1045 ± 65	1240 ± 39	1.2
Sox6	147 ± 16	185 ± 47	171 ± 87	1.2
Ank2	238 ± 79	236 ± 40	253 ± 49	1.2
Zfpm2	187 ± 13	160 ± 22	222 ± 53	1.2
Prkg1	441 ± 36	425 ± 28	327 ± 13	-1.3
Meis2	873 ± 202	433 ± 182	689 ± 110	-1.3
Trps1	473 ± 101	418 ± 61	328 ± 115	-1.4
Nfib	758 ± 112	523 ± 60	553 ± 67	-1.4
Foxp2	225 ± 76	133 ± 33	147 ± 45	-1.5
Dscaml1	278 ± 10	269 ± 8	144 ± 9	-1.8

General Conclusion

Chapter 5

Adam L. Campbell

The muscular system represents the 70% of the body's weight and is composed by skeletal, cardiac and smooth muscles, which derive from different developmental fields. The head muscles fall into three categories the axial, laryngoglossal, branchial, and extraocular muscle (EOM) [1].

The axial muscles are the muscles of the neck that derive from the pre-otic somites, and allow for movement of the head. The larynglossal muscles are the muscles of larynx, mouth and tongue and derive from the pre-otic somites and branchial arch (BA) mesoderm..The branchial muscles are the muscles of the face/jaw and derive from the first 3 brachial arches [2]. The EOMs allow for movement of the eye and derive from the first BA mesoderm. In $Pitx2^{null}$ mice the muscles derived from the first brachial arch fail to initiate, resulting in absence of mastication muscles and EOMs in the developing embryo. The failure of initiation of these muscles is thought to be due to loss of expression of tissue specific transcription factors Tbx1, Tcf1, and Msc [3]. The mammalian heart develops from two distinct subpopulations of cells within the mesoderm also referred to as "cardiac fields". The first cardiac field arises from the cardiac crescent, and contributes cells that will form the left ventricle and atria. The second cardiac field derived from the 3^{rd} -6^{th} branchial arches and contributes cells to the cardiac outflow tract (OFT); right ventricle (RV) and atria [4]. The differentiation of mesodermal cells into a functioning heart is orchestrated through the extracellular signaling molecules, the bone morphogenic proteins (BMPs) and fibroblast growth factors (FGFs), that initiate the expression of tissue specific transcription factors. These transcription factors control cardiac progenitor cell proliferation, differentiation and migration through regulating the expression of target genes by binding at specific DNA sequences.

The skeletal muscles of the trunk derive from the somites, which arise from segmentation of the paraxial mesoderm during embryogenesis. The somites receive signals from the surrounding environment to differentiation and subdivide into the dermomyotome (dorsal) and sclerotome (ventral). The dermomyotome is further subdivided into the hypaxial dermomyotome, located along the dorsomedial side of the somite; and the epaxial dermomyotome, located along the ventrolateral side of the somite. The hypaxial dermomyotome gives rise to the cells that will elongate and form the muscles of the deep back, while the epaxial dermomyotome gives rise to the cells that will form the muscles of the limbs and abdominal body wall [5]. At limb level somites inductive cues from the lateral mesoderm and surface ectoderm synergistically induce the expression of tissue specific transcription factors which repress myogenesis, promote delamination and migration of the cells from the ventrolateral lip (VLL) of the somite and into the limb bud [6,7,8,9,10]. The dorsal and ventral muscle masses of E10.5 mouse limb buds consist of $Lbx1^{+}/Pax3^{+}$ limb muscle progenitor (MP) cells [11]. The MP cells proliferate, undergo withdrawal from the cell cycle and become terminally differentiated myocytes. These myocytes fuse with each other to form multinucleated myotubes and muscle fibers that provide skeletal muscle contractile function (Fig 1).

The abdominal wall begins as a thin layer lateral plate mesoderm derived cells inserted between the ectoderm and endoderm as a result of turning by the mouse embryo (E8.0). The cells along the ventrolateral lip of the abdominal somites positioned dorsally along the left and right sides of the embryo begin extend and proliferate ventrally (E9.5) toward the embryo's midline. Several days later (E12.5) these extensions meet along the ventral midline and fuse to close the body wall and enclose the internal organs. Failure of the body wall to close results in body wall defects such as gastroshisis, omphalocele, or susceptibility to abdominal injuries later in life [12].

Pitx2 is a bicoid-related homeobox gene expressed in the lateral plate mesoderm [13]. Point mutations in Pitx2 are associated with the autosomal dominant disorder, Axenfeld-Rieger syndrome, which is characterized with ocular abnormalities, dental hypoplasia, craniofacial dysmorphism, umbilical defects, and heart defects [14]. Ablation of Pitx2 causes embryonic lethality in mice (E10-E14.5), followed by axial turning defects, open body wall, heart septation defects, and arrest of organ development [15,16,17,18]. Pitx2 is a direct target of the Wnt/β-catenin pathway which results in the release of Pitx2 from associated corepressors and recruits coactivator complexes to regulate tissue specific target genes [13].

Pitx2 is first observed on the left side of the cardiac crescent and linear heart tube (E8.0) and later in the OFT and RV (E9-E14) [19]. Pitx2^{null} embryos fail to form a septated atrium, functional valves and OFT [13,16,17,18,20]. Pitx2 appears to act as part of a network kernel along with other transcription factors Isl1, Tbx1, and Nkx2.5 for the proper specification, migration, and proliferation of the second cardiac field cells to become atrial cells rather than ventricular cells [21,22].

In Pitx2^{null} mice the skeletal muscles of the forelimb are still formed, suggesting that Pitx2 is not needed for muscle initiation. The muscles that do form do not appear normal and are oddly distorted compared to control embryos. Identification of several cytoskeletal, adhesion, and fusion genes by microarray analysis along with cell motility assays suggest that Pitx2 may play a role in colonization and higher order assembly of muscle tissue [23].

Pitx2 is expressed in the cells that comprise the somatopleure at E8.5, which will eventually become the abdominal wall [24]. In developing abdominal wall tissue Pitx2 interacts with HDAC1, HDAC3, and N-CoR to target and regulate the expression of

target genes including members of the T-box transcription factor family [25,26]. The T-box transcription factors have been identified as being involved in organogenesis and body wall development [27,28,29]. In absence of Pitx2, the cells along the ventrolateral lip of the abdominal along the left side of the embryo fail to extend and proliferate ventrally at E9.5 toward the embryo's midline. The failure of the somitic cells to extend toward the midline results in the open body wall phenotype and exposure of the internal organs observed in $Pitx2^{null}$ mice.

Pitx2 is expressed in a variety of tissues during embryonic development. In the muscles derived from the 1^{st} BA mesoderm, EOM, and abdominal body wall of the embryo PItx2 appears to be essential to their development as ablation results in complete loss. In the forelimb muscles of $Pitx2^{null}$ mice we observe that specification and differentiation of is unaffected in absence of Pitx2, but cellular motility and proliferation were reduced in the migratory muscle progenitor (MMP) and muscle progenitor (MP) cells. Through microarray profiling many cytoskeletal, adhesion, myoblast recognition and myoblast fusion genes were identified as being misregulated in absence of Pitx2. This suggests that unlike other tissues where Pitx2 is essential for the tissue specific gene networks of initiation, in the forelimb muscles Pitx2 functions as a tissue specific network kernel to regulate colonization of the pre-patterned anlagen and assembly of higher order muscle tissue.

References

1. Noden DM, Francis-West P (2006) The differentiation and morphogenesis of craniofacial muscles. Dev Dyn 235: 1194-1218.
2. Noden DM, Trainor PA (2005) Relations and interactions between cranial mesoderm and neural crest populations. J Anat 207: 575-601.
3. Shih HP, Gross MK, Kioussi C (2007) Cranial muscle defects of Pitx2 mutants result from specification defects in the first branchial arch. Proc Natl Acad Sci U S A 104: 5907-5912.
4. Buckingham M, Meilhac S, Zaffran S (2005) Building the mammalian heart from two sources of myocardial cells. Nat Rev Genet 6: 826-835.
5. Christ B, Brand-Saberi B (2002) Limb muscle development. Int J Dev Biol 46: 905-914.
6. Tremblay P, Dietrich S, Mericskay M, Schubert FR, Li Z, et al. (1998) A crucial role for Pax3 in the development of the hypaxial musculature and the long-range migration of muscle precursors. Dev Biol 203: 49-61.
7. Venters SJ, Argent RE, Deegan FM, Perez-Baron G, Wong TS, et al. (2004) Precocious terminal differentiation of premigratory limb muscle precursor cells requires positive signalling. Dev Dyn 229: 591-599.
8. Bladt F, Riethmacher D, Isenmann S, Aguzzi A, Birchmeier C (1995) Essential role for the c-met receptor in the migration of myogenic precursor cells into the limb bud. Nature 376: 768-771.
9. Dietrich S, Abou-Rebyeh F, Brohmann H, Bladt F, Sonnenberg-Riethmacher E, et al. (1999) The role of SF/HGF and c-Met in the development of skeletal muscle. Development 126: 1621-1629.
10. Hayashi K, Ozawa E (1995) Myogenic cell migration from somites is induced by tissue contact with medial region of the presumptive limb mesoderm in chick embryos. Development 121: 661-669.
11. Gross MK, Moran-Rivard L, Velasquez T, Nakatsu MN, Jagla K, et al. (2000) Lbx1 is required for muscle precursor migration along a lateral pathway into the limb. Development 127: 413-424.
12. Brewer S, Williams T (2004) Loss of AP-2alpha impacts multiple aspects of ventral body wall development and closure. Dev Biol 267: 399-417.
13. Kioussi C, Briata P, Baek SH, Rose DW, Hamblet NS, et al. (2002) Identification of a Wnt/Dvl/beta-Catenin --> Pitx2 pathway mediating cell-type-specific proliferation during development. Cell 111: 673-685.
14. Semina EV, Reiter R, Leysens NJ, Alward WL, Small KW, et al. (1996) Cloning and characterization of a novel bicoid-related homeobox transcription factor gene, RIEG, involved in Rieger syndrome. Nature Genetics 14: 392-399.
15. Gage PJ, Suh H, Camper SA (1999) The bicoid-related Pitx gene family in development. Mamm Genome 10: 197-200.
16. Kitamura K, Miura H, Miyagawa-Tomita S, Yanazawa M, Katoh-Fukui Y, et al. (1999) Mouse Pitx2 deficiency leads to anomalies of the ventral body wall, heart, extra- and periocular mesoderm and right pulmonary isomerism. Development 126: 5749-5758.
17. Lin CR, Kioussi C, O'Connell S, Briata P, Szeto D, et al. (1999) Pitx2 regulates lung asymmetry, cardiac positioning and pituitary and tooth morphogenesis. Nature 401: 279-282.

18. Lu MF, Pressman C, Dyer R, Johnson RL, Martin JF (1999) Function of Rieger syndrome gene in left-right asymmetry and craniofacial development. Nature 401: 276-278.
19. Campion DR (1984) The muscle satellite cell: a review. Int Rev Cytol 87: 225-251.
20. Gage PJ, Suh H, Camper SA (1999) Dosage requirement of Pitx2 for development of multiple organs. Development 126: 4643-4651.
21. Galli D, Dominguez JN, Zaffran S, Munk A, Brown NA, et al. (2008) Atrial myocardium derives from the posterior region of the second heart field, which acquires left-right identity as Pitx2c is expressed. Development 135: 1157-1167.
22. Nowotschin S, Liao J, Gage PJ, Epstein JA, Campione M, et al. (2006) Tbx1 affects asymmetric cardiac morphogenesis by regulating Pitx2 in the secondary heart field. Development 133: 1565-1573.
23. Campbell AL, Shih H-P, Xu J, Gross MK, Kioussi C (2012) Regulation of Motility of Myogenic Cells in Filling Limb Muscle Anlagen by Pitx2. PLoS One 7: e35822.
24. Shih HP, Gross MK, Kioussi C (2008) Muscle development: forming the head and trunk muscles. Acta Histochem 110: 97-108.
25. Hilton T, Gross MK, Kioussi C (2010) Pitx2-dependent occupancy by histone deacetylases is associated with T-box gene regulation in mammalian abdominal tissue. J Biol Chem 285: 11129-11142.
26. Eng D, Campbell A, Hilton T, Leid M, Gross MK, et al. (2010) Prediction of regulatory networks in mouse abdominal wall. Gene 469: 1-8.
27. Naiche LA, Harrelson Z, Kelly RG, Papaioannou VE (2005) T-box genes in vertebrate development. Annu Rev Genet 39: 219-239.
28. Chapman DL, Garvey N, Hancock S, Alexiou M, Agulnik SI, et al. (1996) Expression of the T-box family genes, Tbx1-Tbx5, during early mouse development. Dev Dyn 206: 379-390.
29. Tada M, Smith JC (2001) T-targets: clues to understanding the functions of T-box proteins. Dev Growth Differ 43: 1-11.

Chapter 5-Figure 1

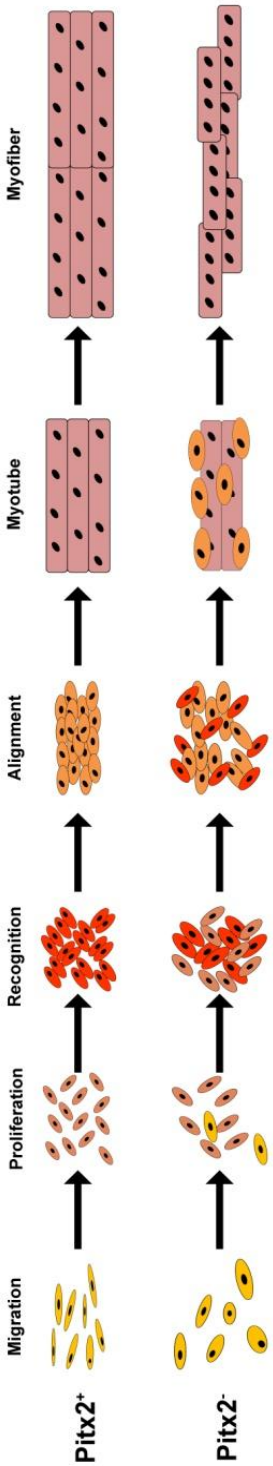

Figure 1. Ablation of Pitx2 Disrupts Timing of Muscle Precursors. Pitx2 is strongly expressed in the muscle precursor cells that fill the forelimb anlagen. Ablation of Pitx2 does not result in failure of muscles to form, but the muscles that do form are deformed and not well defined. The formation of muscles in the forelimb occurs over a limited window of opportunity as the forelimb itself grows and elongates. The muscle precursors must migrate in sufficient numbers to populate the muscle anlagen. Once there the cells increase their numbers through proliferation. At a certain population density the cells recognize each other through cell-cell contacts and begin to withdraw from the cell cycle and align into parallel arrays and subsequently fuse into a tightly bundled group of myofibers. The myogenic precursors from Pitx2 ablated mice undergo the same processes described above, but seem to do it at a slower pace. The muscle precursors have defects in migration and proliferation which would impair the ability to fill the anlagen and reach a critical mass necessary for growing myotubes and making a fully functional muscle.